

**University of Alberta**

**Development of Novel Stimuli-Responsive Drug Delivery  
Systems**

By

Nazila Safaei Nikouei

A thesis submitted to the Faculty of Graduate Studies and Research

in partial fulfillment of the requirements for the degree of

**Doctor of Philosophy**

in

**Pharmaceutical Sciences**

Faculty of Pharmacy and Pharmaceutical Sciences

© Nazila Safaei Nikouei

Spring 2014

Edmonton, Alberta

Permission is hereby granted to the University of Alberta Libraries to reproduce single copies of this thesis and to lend or sell such copies for private, scholarly or scientific research purposes only.

Where the thesis is converted to, or otherwise made available in digital form, the University of Alberta will advise potential users of the thesis of these terms.

The author reserves all other publication and other rights in association with the copyright in the thesis and, except as herein before provided, neither the thesis nor any substantial portion thereof may be printed or otherwise reproduced in any material form whatsoever without the author's prior written permission.

## ABSTRACT

In this thesis, novel pH and temperature responsive polymers based on triblock of poly(ethylene glycol) (PEG) and functionalized poly( $\epsilon$ -caprolacton) having different levels of carboxyl to benzyl carboxylate on the  $\alpha$ -carbon of caprolacton units (0:100, 30:70, 50:50, 100:0) were synthesized. The temperature and pH responsive self-assembly as well as sol-gel transition of prepared triblock copolymers was characterized by different methods including inverse flow method, dynamic mechanical analysis and differential scanning calorimetry. The mechanism of sol-gel transition and viscoelastic properties of the gels was also investigated by  $^1\text{H}$  NMR and dynamic mechanical analysis, respectively. Our results showed the presence of carboxylic group at 30 and 50 % substitution on the polymer backbone to introduce thermo/pH sensitivity to the polymeric solutions. The sol-gel transition temperature of these block copolymer solutions was around 30 °C at 7-15% w/w concentration. In the next step, the potential of developed hydrogels in stimulus and depot delivery of macromolecular drugs was investigated using a large molecular weight fluorescent probe, i.e., tetramethyl rhodamine-dextrose (TMR-D) at two molecular weights of 10 & 40 kDa, as a model. Loading of TMR-D do not affect the sol-gel transition of polymer solutions. The *in vitro* release of TMR-D was sustained by thermo-responsive gel only at 37° C and pH 7.4 or 9.0. Reducing the pH to 5.0 (at 37 ° C) or reducing the temperature to 25 ° C (at pH7.4) led to the disruption of gel structure and a consequent rapid release of TMR-D. In further studies, cyclosporine A (CyA) was loaded in the hydrogel to provide an alternative formulation for Restasis® eye drops for chronic dry eye disease. Release of

CyA was shown to be controlled by the hydrogel within a 7 day time frame at 37 °C and pH 7.4. We have also developed novel multifunctional polymeric micelles based on diblock copolymers of poly(ethylene oxide)-poly( $\alpha$ -carboxyl- $\epsilon$ -caprolactone) (PEO-PCCL) modified on their surface with GE11, a peptide targeting epidermal growth factor (EGFR). The complexation and pH responsive delivery of cisplatin as well as anti-cancer activity of polymeric micellar cisplatin with and without a tumor targeting peptide on its surface in EGFR<sup>+</sup> SKBR3 cells was then investigated. The results showed efficient complexation of cisplatin by the developed polymers and its enhanced release under mild acidic condition (pH=5.0) from polymeric micelles. Moreover, modification of polymeric micelles with GE11 enhanced the anti-cancer activity of cisplatin in SKBR3 cells.

In conclusion, our results showed novel di and tri block copolymers developed in this thesis are versatile materials with several potential applications in drug delivery. They can form temperature/pH responsive hydrogels with potential application for in situ and/or depot delivery of large molecular weight entities, and small molecular weight drugs. They can also form pH responsive nano-carriers that can provide acid triggered release of the incorporated anti-cancer drug in tumor for the purpose of targeted drug delivery.

## Acknowledgment

I would like to express my deepest gratitude to all of the following people.

- My supervisor Dr. Afsaneh Lavasanifar for giving me the opportunity to pursue my studies in her lab. Her encouragement, guidance and financial and academic support throughout the program enabled me to develop a deep understanding of the point of my research question.
- My supervisory committee members, Dr. Larry Unsworth and Dr. Raimer Loebenberg for their generous guidance and valuable comments and suggestions.
- My parents, Soraya and Freydon, for their love and support throughout my life, and for giving me strength to chase my dreams. My sisters, Niousha, and my lovely nephew and niece, Arshia and Amitis, deserve my wholehearted thanks as well who helped me with their love during the whole time.
- Ms. Elaine Moase for her help in the cell culture work, and some manuscript proofreading.
- Dr. Vishwa Somayaji for his help with the mass spectrometry and NMR.
- Mr. Jeff Turchinsky for helping us to order all the chemicals and supplies needed for my experiments.
- My previous and current lab mates for creating a wonderful work environment, and to my very best friends Mandana Assadi for her understanding and encouragement in my many moments of crisis.
- Mrs. Joyce Johnson for her help to facilitate all the administrative and paper work need during my studies.

Finally, I would like to thank all the funding agencies and institutes for their financial support.

- Faculty of Pharmacy and Pharmaceutical Sciences for the Shoppers Drug Mart Scholarship and the Teaching Assistantship.
- Graduate Student Association, University of Alberta for the professional development and travel grant.
- American Association of Pharmaceutical Sciences for the travel award.
- Cedarlane for the award of excellent of best poster at CSPS 2011

## Table of Contents

<b>Chapter 1</b> .....	<b>21</b>
<b>Introduction</b> .....	<b>21</b>
<b>1.1. Introduction</b> .....	<b>2</b>
<b>1.2. Amphiphilic block copolymers (ABC)s</b> .....	<b>4</b>
1.2.1 Definitions.....	4
1.2.2 Self-assembly of amphiphilic block copolymers .....	6
1.2.3 Most commonly used ABCs for drug delivery .....	7
1.2.4 Application of ABCs for drug delivery.....	10
<b>1.3 Characterization of in situ forming hydrogels</b> .....	<b>26</b>
1.3.1 Inverse flow method.....	26
1.3.2 Modulated Differential Scanning Calorimetry (MDSC) .....	26
1.3.3 Rheological Analysis .....	28
1.3.4 NMR investigation for transition temperature .....	29
1.3.5 Drug loading in hydrogels.....	30
1.3.6 Drug release .....	30
<b>1.4. Modes of drug release from hydrogels</b> .....	<b>31</b>
<b>1.5 Model drugs under current study</b> .....	<b>32</b>
1.5.1 Cyclosporine A.....	32
1.5.2 Cisplatin.....	35
<b>1.6. Thesis proposal</b> .....	<b>38</b>
1.6.1. Rationale .....	38
1.6.2. Hypothesis .....	40
1.6.3. Objective .....	41
1.6.4. Specific aims.....	41
<b>Chapter 2</b> .....	<b>53</b>
<b>Triblock copolymers based on poly(ethylene glycol) and functionalized poly(<math>\alpha</math>-caprolactone): Synthesis and characterization of their thermo/pH responsive assembly</b> .....	<b>53</b>
<b>1. Introduction</b> .....	<b>54</b>
<b>2. Materials and methods</b> .....	<b>55</b>
2.1. Materials.....	55
2.2. Synthesis of triblock copolymers.....	56
2.3 Characterization of prepared tri block copolymers .....	57
2.4. Characterization of the self-assembly of block copolymers.....	58
2.5 Assessing the effect of temperature on the self-assembly of triblock copolymers.....	59
2.6 Assessing the effect of pH on the self-assembly of triblock copolymers	59
2.7. Statistical Analysis.....	60
<b>3. Results</b> .....	<b>60</b>
3.1. Synthesis and characterization of triblock copolymers.....	60
3.2. CMC determination .....	66

3.3. Thermo-responsive size change of polymeric micelles .....	67
3.4. pH-sensitive assembly of block copolymers .....	69
<b>4. Discussion .....</b>	<b>71</b>
<b>5. Conclusions .....</b>	<b>79</b>
<b>Chapter 3 .....</b>	<b>82</b>
<b>Thermo-reversible Hydrogels based on Triblock Copolymers of PEG and functionalized Poly(<math>\epsilon</math>-caprolactone) .....</b>	<b>82</b>
<b>1. Introduction .....</b>	<b>83</b>
<b>2. Materials and methods .....</b>	<b>85</b>
2.1. Materials .....	85
2.2. Synthesis of triblock copolymers .....	85
2.3 Characterization of prepared triblock copolymers .....	86
2.4 Characterization of PCBCL-PEG-PCBCL Thermo-Responsive Sol-Gel Transition .....	87
2.5 $^1\text{H}$ NMR study .....	88
2.6 Statistical analysis .....	89
<b>3. Results and Discussion .....</b>	<b>89</b>
3.1. Synthesis and characterization of triblock copolymers .....	89
3.2 Characterization of the thermo-responsive phase transition of aqueous block copolymer solutions .....	95
3.3 $^1\text{H}$ NMR Study in $\text{D}_2\text{O}$ .....	103
<b>4. Conclusions .....</b>	<b>107</b>
<b>Chapter 4 .....</b>	<b>111</b>
<b>Characterization of pH dependent thermo-gelation and TMR-D delivery by triblock copolymers based on PEG and functionalized PCL .....</b>	<b>111</b>
<b>1. Introduction .....</b>	<b>112</b>
<b>2. Materials and methods .....</b>	<b>114</b>
2.1. Materials .....	114
2.2 Synthesis and characterization of triblock copolymer .....	114
2.3 Characterization of the sol-gel transition of PCBCL-PEG-PCBCL solutions .....	115
2.3.1. Inverse flow method .....	115
2.3.2. Dynamic Mechanical Analysis (DMA) .....	116
2.3.3 Modulated Differential Scanning Calorimetry (MDSC) .....	116
2.4. Characterization of tetramethylrhodamin-dextran (TMR-D) loaded hydrogels .....	116
2.5. In vitro release of TMR-D from hydrogels .....	117
2.3.6 Statistical analysis .....	117
<b>3. Results and discussions .....</b>	<b>118</b>
3.1 The effect of aqueous media (Tris buffer versus water) on the thermoreponsive sol-gel transition of PCBCL-PEG-PCBCL .....	118
3.2 The effect of pH on the thermo-responsive sol-gel transition of PCBCL- PEG-PCBCL .....	121

3.3. The effect of TMR-D loading on the thermo-responsive sol-gel transition of PCBCL-PEG-PCBCL .....	122
3.4 Temperature and pH responsive release of TMR-D from the prepared gels.....	124
<b>4. Conclusion.....</b>	<b>128</b>
<b>Chapter 5.....</b>	<b>132</b>
<b>Thremoresponsive PCBCL-PEG-PCBCL triblock copolymer for Cyclosporin A delivery .....</b>	<b>132</b>
<b>1. Introduction.....</b>	<b>133</b>
<b>2. Materials and methods.....</b>	<b>134</b>
2.1. Materials.....	134
2.2. Synthesis and characterization of triblock copolymer.....	135
2.3 In vitro degradation of the gel.....	135
2.4 In vitro cytotoxicity assay .....	136
2.5 Assessing the in vitro immunogenicity of polymer by studying the level of DC maturation and cytokine quantification .....	137
2.6 Drug loading.....	137
2.8 Characterization of thermo-responsive sol-gel transition for CyA loaded PCBCL-PEG-PCBCL.....	138
2.9 In vitro release study .....	139
2.11 Statistical analysis.....	139
<b>3. Results and Discussion .....</b>	<b>140</b>
3.1 Degradation study .....	140
3.2 In vitro cytotoxicity assay .....	141
3.6 In vitro immunogenicity .....	142
3.7 Loading CyA into hydrogel .....	144
3.8 Sol-gel transition of CyA loaded PCBCL-PEG-PCBCL.....	144
3.9 In vitro Release study .....	146
<b>4. Conclusion.....</b>	<b>147</b>
<b>Chapter 6.....</b>	<b>150</b>
<b>Development of multifunctional polymeric micelles for targeting of cisplatin to EGFR overexpressing tumors.....</b>	<b>150</b>
<b>1. Introduction.....</b>	<b>151</b>
<b>2. Materials &amp; Methods.....</b>	<b>153</b>
2.1 Materials .....	153
2.2 Synthesis of PEO-b-poly( $\alpha$ -carboxy- $\epsilon$ -caprolactone) ( PEO-b-PCCL) ...	153
2.3 Synthesis of acetal-PEO-b-PCCL .....	153
2.4 Characterization of prepared copolymer .....	154
2.5 Conjugation of GE11 to polymeric micelles .....	155
2.6 Preparation of cisplatin loaded micelles .....	155
2.7 In vitro release study .....	156
2.8 In vitro cytotoxicity study .....	156
<b>3. Results and Discussion .....</b>	<b>157</b>
<b>4. Conclusions .....</b>	<b>161</b>



<b>Chapter 7</b> .....	<b>163</b>
<b>General Discussion and Conclusion</b> .....	<b>163</b>
<b>1. Introduction</b> .....	<b>164</b>
<b>2. General Discussion</b> .....	<b>165</b>
<b>3. Future Direction</b> .....	<b>170</b>
<b>4. Conclusions</b> .....	<b>172</b>

## List of Tables

Table 2-1 Characteristics of the synthesized triblock copolymers .....	62
Table 2-2. Characterization of the self- assembly of different triblock copolymers under study .....	66
Table 3-1 Characteristic of synthesized triblock copolymers .....	93
Table 3-2 Transition temperature of 30 and 54 % reduced PCBCL-PEG-PCBCL copolymer at different concentrations in water measured by Dynamic Mechanical Analysis (n=3) .....	102
Table 3-3 Comparison of the sol-gel transition temperature for PCBCL-PEG-PCBCL aqueous samples prepared at 10 % w/w concentration measured by different methods.....	102
Table 4-1 Comparison between the sol-gel transition temperatures of PCBCL-PEG-PCBCL copolymer solutions in Tris buffer at different concentrations as defined by inverse flow method versus DMA.....	121
Table 4-2 Comparison between the sol-gel transition temperatures of PCBCL-PEG-PCBCL (10% w/w) loaded with TMR-D 10, or 40kDa using different methods of measurement.....	124
Table 5-1 loading efficiency of CyA into hydrogel .....	144
Table 5-2 Thermo responsive transition of CyA loaded hydrogel.....	145

## List of Figures

Figure 1-1- Judah Folkman is considered to be the first scientist introducing the concept of controlled drug release (Adapted from reference 2 with permission).	2
Figure 1-2 Early controlled release drug delivery systems introduced to pharmaceutical market (Adapted from reference 2 with permission) .....	3
Figure 1-3. Scheme of the structure of different amphiphilic block copolymers.....	5
Figure 1-4 General Chemical Structure of Pluronics® .....	8
Figure 1-5 Chemical structure of different polyesters.....	9
Figure 1-6. Schematic representation of EPR Effect (adapted from reference 71 with permission).....	12
Figure 1-7: Comparison of scanning electron micrograms of normal vessels (A and B) with tumor vessels in mice-bearing tumor after injection of water-soluble acrylic monomer. No polymer leakage is seen in normal vascular area (N), or in A and B. However, in the tumor vascular area (T), the extravasation of the polymer is seen. (Adapted from reference 72 with permission) .....	13
Figure 1-8: Chemical structure of GE11 .....	17
Figure 1-9 Schematic illustration of inter-micellar hydrophobic interaction leading to micellar association and gel formation as a result of an increase in temperature. ....	20
Figure 1-10 Structure of Cyclosporine A .....	33
Figure 1-11 Secretion of cytokines into tears can disturb the secretory-autonomic neural reflex loop (adopted from reference 136) .....	33
Figure 1-12 Aquation of cisplatin at low concentration of chloride.....	36
Figure 1-13. Current platinum-based anticancer drugs approved for human use .....	37
Figure 2-1 <sup>1</sup> H NMR spectrum of PCBCL-PEG-PCBCL block copolymers and peak assignments.....	62
Figure 2-2 MALDI-TOF mass spectra of a) PEG 1450 b) PBCL-PEG-PBCL c) PCBCL-PEG-PCBCL (27% debezylated) and d) PCCL-PEG-PCCL (100 % debezylated) triblock copolymers. The windows in 2B and 2D show an enlarged portion of the MALDI-TOF spectra of corresponding block copolymers as an example for the peak assignment in the MALDI-TOF spectra. The peak-to-peak increments of 248 and 158 in figure 2B and 2D correspond to the molecular weights of BCL and CCL units, respectively.....	65

Figure 2-3. Micellar size change of A) 0, B) 27, C) 50, D) 75, and E) 100% debenzylated block copolymers as a function of temperature assessed for a polymer aqueous solution at 1 mg/mL concentration at pH=4.5 (n=3).....	68
Figure 2-4. Micellar size change as a function of temperature for different concentrations of A) 27 % and B) 50 % debenzylated PCBCL- <i>b</i> -PEG- <i>b</i> -PCBCL aqueous solutions at pH 4.5 (n=3) .....	70
Figure 2-5. Micellar size change for block copolymers having different degrees of debenzylation. B) Changes in CMC values of block copolymers, as a function of pH at room temperature (n=3).....	71
Figure 2-6 The effect of pH on thermoresponsive changes in the size of micelles for A) 27%, B) 50 % and C) 75% debenzylated PCBCL- <i>b</i> -PEG- <i>b</i> -PCBCL block copolymers. Polymer concentration was 1 mg/mL (n=3).....	73
Figure 2-7 Proposed mechanisms for thermo-responsive aggregate size change for different block copolymer structures under study .....	77
Figure 3-1 A typical <sup>1</sup> H NMR spectrum of A) PBCL-PEG-PBCL; and B) PCBCL-PEG-PCBCL block copolymers (54% reduced) in CDCl <sub>3</sub> and peak assignments. C) <sup>13</sup> C NMR of PCBCL-PEG-PCBCL (54% reduced) in CDCl <sub>3</sub> and peak assignments .....	93
Figure 3-2 The effect of the duration of reaction on the percentage of PBCL reduction in triblock copolymers, using different amounts of catalyst (w/w % of used polymer) (n=3).....	94
Figure 3-3 Sol-gel phase transition diagrams of PCBCL-PEG-PCBCL 30, and 54% reduced block copolymer solution at 7, 10, and 15 % w/w concentration in distilled water.....	96
Figure 3-4 Modulated DSC thermograms of 30, and 54% reduced block copolymer solution in distilled water at 10% w/w concentration of copolymers .....	98
Figure 3-5 Changes in the storage modulus, <i>G'</i> , as a function of temperature for A) 30 %, and B) 54% reduced PCBCL-PEG-PCBCL block copolymer solutions in water at 7, 10, and 15% w/w as a function of raising temperature at 1°C min <sup>-1</sup> ; The graph shows the average of 3 measurement (n=3).....	100
Figure 3-6 Increases in storage modulus ( <i>G'</i> ) and loss modulus ( <i>G''</i> ) of A) 30%, and B) 54% reduced polymer (10% w/w) as a function of rising temperature at 1°C min <sup>-1</sup> . The graph represents the average of 3 measurement (n=3).....	101
Figure 3-7 Plot of viscosity as a function of time and temperature (3 heating/cooling cycles between 25, and 38 °C) for the 30% reduced PCBCL-PEG-PCBCL copolymer in distilled water at a concentration of 10% w/w (n=3).....	103
Figure 3-8 A) <sup>1</sup> H NMR spectra of 54% reduced PCBCL-PEG-PCBCL solution (10 mg/mL) in D <sub>2</sub> O at 23°C and 29°C B) The change in <sup>1</sup> H NMR ratio integration of phenyl protons, methylene protons of the benzyl carboxylate group on PCBCL,	

methylene protons of the PCBCL backbone, and PEG protons to the integration of dimethyl sulfone protons as a function of temperature .....	106
Figure 3-9 Schematic diagram for the sol-gel and gel-sol transition mechanisms of prepared triblock copolymers in aqueous solution as a function of increasing temperature. ....	107
Figure 4-1 Temperature dependent sol-gel transition of PCBCL-PEG-PCBCL 30% reduced polymer at different concentrations in Tris buffer versus water as defined by Inverse flow method. . Data in water is reproduced from Chapter 3, Figure 3.....	120
Figure 4-2 A) Increases in storage modulus ( $G'$ ) of PCBCL-PEG-PCBCL of different concentrations as a function of temperature. B) Increase in storage modulus ( $G'$ ) and loss modulus ( $G''$ ) of PCBCL-PEG-PCBCL polymer at 10 % concentration as a function of rising temperature at $1^{\circ}\text{C min}^{-1}$ ( $n=3$ ). ....	120
Figure 4-3 Changes in the storage modulus of PCBCL-PEG-PCBCL block copolymer solution in water versus Tris buffer (10 % w/w) as defined by DMA ( $n=3$ ).....	121
Figure 4-4 pH and temperature dependent sol-gel transition of PCBCL-PEG-PCBCL solution in Tris buffer (10 % w/w) as defined by inverse flow method	122
Figure 4-5 Changes in storage modulus as a function of temperature for PCBCL-PEG-PCBCL block copolymer solution in water (10% w/w) alone or loaded with TMR-D 10 or 40k Da ( $n=3$ ) .....	123
Figure 4-6 DSC thermogram of TMR-D loaded PCBCL-PEG-PCBCL solution in Tris buffer .....	123
Figure 4-7 Release profile of TMR-D 10 and 40 kDa, or pluronic 127 from PCBCL-PEG-PCBCL gels in Tris Buffer (pH 7.4) at $37^{\circ}\text{C}$ ( $n=3$ ). ....	126
Figure 4-8 Temperature dependent release profile of TMR-D A) 10kDa and B) 40kDa from prepared hydrogels in Tris buffer (pH=7.4) ( $n=3$ ).....	127
Figure 4-9 pH dependent release profile of TMR-D A) 10 and B) 40 kDa from the prepared hydrogel at $37^{\circ}\text{C}$ ( $n=3$ ).....	128
Figure 5-1 The change in A) medium pH; and B) size of polymeric micelle over time upon incubation in distilled water at $37^{\circ}\text{C}$ . Error bar is standard deviation of average size of micelle based on three measurements. ....	140
Figure 5-2 The change in degree of polymerization of PCBCL backbone as measured by $^1\text{H}$ NMR upon incubation in distilled water at $37^{\circ}\text{C}$ .....	141
Figure 5-3 Cytotoxicity of PCBCL-PEG-PCBCL against HUV-EC cell line after 72 h of incubation .....	142

Figure 5--4 The effect of PCBCL-PEG-PCBCL triblock copolymer on DC maturation measured as expression of of A) CD40; B) CD86 on DCs or C) secretion of IL-12 by DCs in comparison to LPS treated (positive control) or untreated DCs (negative control) (n=3).....	144
Figure 5-5 Modulated DSC thermograms of cyA loaded and unloaded block copolymer in distilled water at 10% w/w polymer concentration.....	146
Figure 5-6 Release profile of CsA from hydrogel or ethanolic solution.....	147
Figure 6-1 Scheme for the preparation of cisplatin loaded PEO-b-PCCL micelles .....	158
Figure 6-2 Effect of concentration of sodium bicarbonate/or molar ratio of cisplatin to polymer on loading efficiency .....	158
Figure 6-3 Release profile of cisplatin from PEO-PCCL micelle at two different pHs.....	160
Figure 6-4 IC <sub>50</sub> obtained by MTT Assay using SKBR3 cell line after 72 h incubation .....	161

## List of Schemes

Scheme 2-1 Synthesis of triblock copolymers .....61

Scheme 3-1 synthetic scheme for the preparation of PBCL-PEG-PBCL, and  
PCBCL-PEG-PCBCL triblock copolymers.....91

## List of abbreviations

ABCs	Amphiphilic Block Copolymers
ANOVA	Analysis of variance
BALB	Bagg Albino (inbred research mouse strain)
BCL	$\alpha$ -Benzylcarboxylate $\epsilon$ -caprolactone
BPEA	2-hydroxyacetaldehyde
Bu-Li	Butyl Lithium
CCL	Carboxylate $\epsilon$ -caprolactone
CDCL <sub>3</sub>	Deuterated chloroform
CDDP	Cis-Diamminedichloroplatinum (II)
$\epsilon$ -CL	Caprolactone
CGC	Critical gel Concentration
CMC	Critical micelle concentration
Cp	Heat Capacity
CyA	Cyclosporine A
Da	Dalton
DCTX	Docetaxel
DC	Dendritic cell
DHB	2,5 dihydroxybenzoic acid
DHT	Dihydrotestosterone
DLS	Dynamic light scattering
DMA	Dynamic Mechanical analysis
DMSO	Dimethyl sulfoxide
DNA	Deoxyribonucleic acid
DOX	Doxorubicin
DPPG	Dipalmitoyl phosphatidyl glycerol



DSC	Differential Scanning Calorimetry
ECGS	Endothelial cell growth supplement
EGF	Epidermal growth factor
EGFR	Epidermal growth factor receptors
ELISA	Enzyme-linked immunosorbent assay
EPR	Enhanced permeation and retention
FACS	Fluorescence activated cell sorter
FBS	Fetal bovine serum
FCS	Fetal calf serum
FDA	Food and drug administration
HbsAg	Surface antigen of the hepatitis B virus
$G'$	Storage Modulus
$G''$	Loss Modulus
G-CSF	Granulocyte colony-stimulating factor
GPC	Gel permeation chromatography
h	Hour
HCL	Hydrochloric acid
HEMA	Hydroxyethyl methacrylate
HLB	Hydrophilic/hydrophobic Balance
HPLC	High-performance liquid chromatography
HPMC	Hydroxypropyl methylcellulose
HUVEC	Human umbilical vein endothelial cells
IC <sub>50</sub>	Inhibitory Concentration for 50%
IL12	Interleukin 12
L	Litre
LCST	Lower Critical Solution Temperature

LC-MS	Liquid chromatography–mass spectrometry
LPS	Lipopolysaccharide
M	Molar
mAb	Monoclonal antibody
MALDI	Matrix-assisted laser desorption/ionization
MDR	Multidrug resistance
MDSC	Modulated Differential Scanning Calorimetry
mg	Milligram
MHC	Major histocompatibility complex
min	Minute
mL	Millilitre
$M_n$	Number average molecular weight
$M_w$	Weight average molecular weight
MTT	(3-(4,5-Dimethylthiazol-2-yl)-2,5-diphenyltetrazolium bromide
MW	Molecular weight
NaOH	Sodium hydroxide
NIS	Sodium iodine Symporter
nm	Nanometer
NMR	Nuclear magnetic resonance
Pa.s	Pascal.Second
PBCL	Poly( $\alpha$ -Benzylcarboxylate $\epsilon$ -caprolactone)
PBCL-PEO-b-PBCL	Poly( $\alpha$ -benzyl carboxylate- $\epsilon$ -caprolactone)-polyethylene oxide-block-poly( $\alpha$ -benzyl carboxylate- $\epsilon$ -caprolactone)
PBS	Phosphate buffer saline
PCBCL	Poly( $\alpha$ -Benzyl carboxylate-co- $\alpha$ -carboxyl- $\epsilon$ -caprolactone)

PCCL	Poly( $\alpha$ -carboxylate $\epsilon$ -caprolactone)
PCCL-PEO-b-PCCL	poly( $\alpha$ -carboxyl- $\epsilon$ -caprolactone)-polyethylene oxide-poly( $\alpha$ -carboxyl- $\epsilon$ -caprolactone)
PCL	Poly( $\epsilon$ -caprolactone)
Pd/C	Palladium, 10% on activated charcol
PDEAEMA	Poly(diethylaminiethyl methacrylate)
PDI	Poly dispersity index
PDLLA	Poly-DL-lactide
PEG	Polyethylene glycol
PEI	Polyethelenimine
PEO	Polyethylene oxide
PEO-b-PCL	Polyethylene oxide-block-poly( $\epsilon$ -caprolactone)
PGA	Polyglutamic acid
PGlu	Poly(glutamic acid)
PLA	Poly L-lactide
PLGA	poly(lactic-co-glycolic acid)
PLLA	Poly(L-lactic acid)
PNIPAm	Poly(N-isopropylacrylamide)
PMA	Poly(methacrylic acid)
ppm	Part Per Million
PPO	Poly(propylene oxide)
PTX	Paclitaxel
RES	Reticuloendothelial system
rHGH	Recombinant Human Growth Hormone
rpm	Round per minute
SD	Standard deviation
SDS	Sodium dodecyl sulfat

SMA	Poly(styrene-co-maleic anhydride)
SnCl <sub>2</sub>	Tin (II) Chloride
T	Absolute Temperature
THF	Tetrahydrofuran
TMR-D	Tetramethylrhodamine-dextran
TNF- $\alpha$	Tumor necrosis factor alpha
TOF	Time of flight
$\mu$ L	microlitre
$\mu$ M	micrometer
UCST	Upper Critical Solution Temperature
UV	Ultraviolet
VEGF	Vascular endothelial growth factor
Vis	Visible
W/W	Weight per weight

## Chapter 1

### **Introduction**

## 1.1. Introduction

The concept of controlled release of drugs was first established by Judah Folkman (Figure 1-1) in mid-1960s. While he was circulating rabbit blood in silicon rubber, he realized that exposing rubber to anesthetic gases made rabbits fall asleep. He then suggested implanting silicon rubber containing drug, could release drug in constant rate or Zero order [1]. Meanwhile, Ed Schmitt and “Roco” Polestina at Davis & Geck, Cyanamid Co. introduced poly(glycolic acid) as biodegradable suture in mid 1960s [2]. The first controlled drug delivery devices, i.e., Ocusert® (Zero ordered released device of pilocarpine in eye) and Progestesert® (intrauterine device (IUD) releasing progesterone in uterine cavity) manufactured by Alza, were introduced to pharmaceutical market in 1970s (Figure 1-2). Later on, in 1980 Norplant® a contraceptive implant containing levo-Norgestrel, was developed by the World Health Organization (WHO).

### *The Use of Silicone Rubber as a Carrier for Prolonged Drug Therapy*

JUDAH FOLKMAN, M.D., AND DAVID M. LONG, LCDR, MC, USNR, *National Naval Medical Center*



Folkman

**Figure 0-1- Judah Folkman is considered to be the first scientist introducing the concept of controlled drug release (Adapted from reference 2 with permission)**

Different materials and dosage forms have been introduced and used for controlled drug release afterwards (Figure 1-2). Among these dosage forms, hydrogels are of particular

interest, because of their biocompatibility and feasibility for pharmaceutical production. Hydrogels are three-dimension polymeric networks with high water content. Their high water content and viscoelastic nature make them biocompatible with living tissue. The first hydrogel was synthesized by Wichterle and Lim as soft contact lenses in 1960.

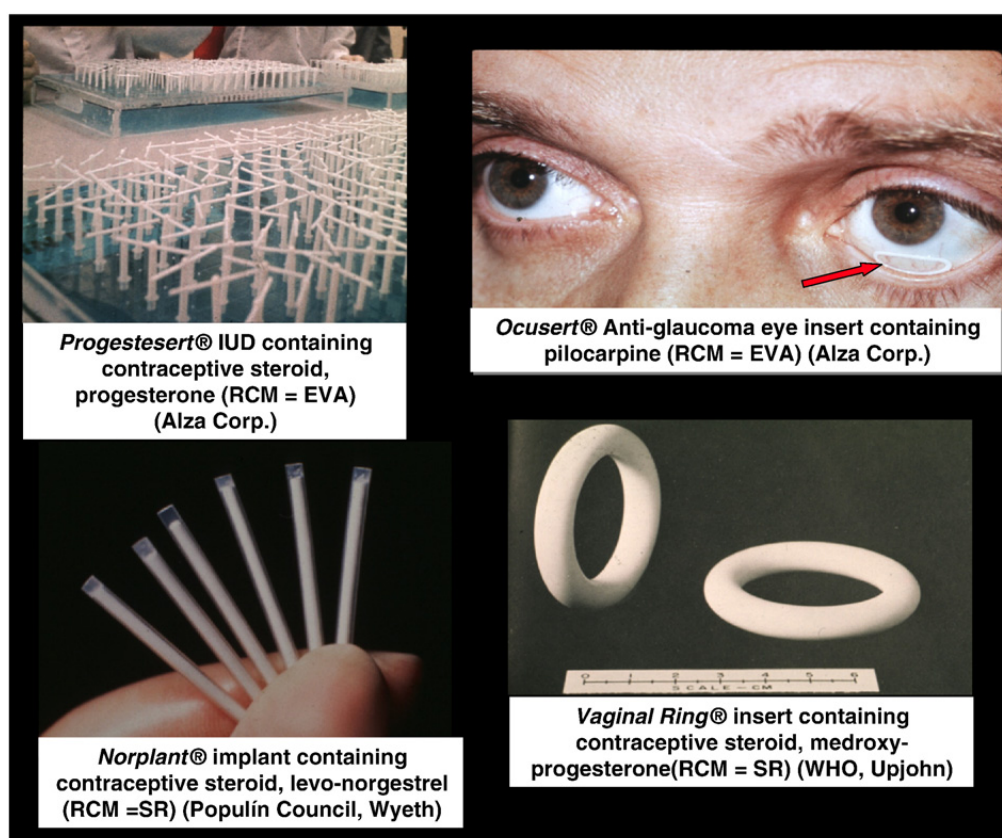


**Figure 0-2 Early controlled release drug delivery systems introduced to pharmaceutical market (Adapted from reference 2 with permission)**

Among different kinds of hydrogels, those that undergo gel formation in response to stimuli (e.g., temperature) may find many applications in smart delivery of drugs and living cells. Drug molecules and living cells can be simply mixed with polymers in aqueous media and then, by gel formation in response to stimuli, be incorporated in hydrogel network without using any organic solvent or cross-linker [3,4]. Thermoresponsive hydrogels that

become gel by increasing temperature can also be used for tissue engineering applications [5-7], formation of biosensors membranes [8], as bulking agent in chronic infarcted myocardium [9], and as post-surgical adhesion prevention [10]. Preparation of thermo-responsive hydrogels has been reported from homopolymers [11] as well as random and block copolymers [12-14].

Stimulus responsive nano-carriers have also attracted much interest in the field of targeted drug delivery [15-18]. In this case, development of nano-carriers that can hold into their therapeutic cargo in systemic circulation, but release the drug in response to internal or external stimuli is of great interest.

In this thesis, we report on the development of novel stimuli responsive delivery systems for potential application in depot or targeted drug delivery. In chapters 2-5, development of pH and temperature responsive hydrogels for potential application in controlled or sustained regional or mucosal drug delivery is described. In chapter 6), development of a pH responsive nano-carrier with potential application in targeting of cisplatin to solid tumors is described. Both delivery systems were fabricated from novel amphiphilic block copolymers (ABC)s based on poly(ethylene oxide) (PEO) and functionalized poly(caprolactone) (PCL).

## **1.2. Amphiphilic block copolymers (ABC)s**

### **1.2.1 Definitions**

Amphiphilic is a Greek word meaning, “loving both”, which describes the affinity toward any two incompatible solvents. In the world of pharmaceutical sciences, this dual affection is based on interest or disinterest to water. Amphiphilic materials have two parts:



hydrophilic (water loving) part, and hydrophobic (water repelling) part. The most common examples of low molecular weight amphiphilic molecules are surfactants (e.g. Cremophor EL, and polysorbates), and lipids (e.g. phospholipids, and cholesterol). Block copolymers are examples of amphiphilic macromolecules [19].

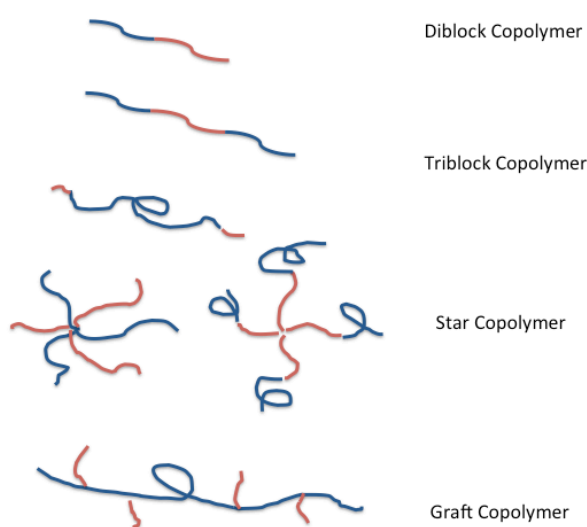


**Figure 0-3. Scheme of the structure of different amphiphilic block copolymers**

Amphiphilic block copolymers are synthesized through polymerization of more than one type of monomer in different blocks, so that the resultant copolymers have different regions with different affinity for aqueous solutions. The advantage of these polymers over low molecular weight amphiphilic molecules is the ability to change the hydrophilic lipophilic balance of the polymer through changing the structure of units, and/or the length of each block [19,20]. In the context of drug delivery, since block copolymers have higher molecule size, their self-assembled form is thermodynamically more stable and has higher residence time in biological system compared to self-assembled structures formed from surfactants or lipids [19, 21]. Amphiphilic block copolymers can be used to increase the solubility of poorly soluble drugs in aqueous media by physically encapsulating the

hydrophobic drug in the hydrophobic domain of their self-assembled structure [22]. Amphiphilic block copolymers can be formed as di-block, tri-block, star-shaped, and grafted copolymers (Figure 1-3) [19, 23, 24].

### 1.2.2 Self-assembly of amphiphilic block copolymers

When a hydrophobic molecule mixes with water it breaks the hydrogen bond network between water molecules. As a result, water molecules become ordered around hydrophobic molecule. This decreases the entropy ( $\Delta S$ ) of the system. According to Gibbs free energy Equation (1.1), this decrease in entropy will cause an increase in free energy.

$$\Delta G = \Delta H - T\Delta S \quad (\text{eq 1.1})$$

Decrease in entropy can be compensated through expulsion of hydrophobic molecules from water, leading to the separation of hydrophobic domain from water. Unlike pure hydrophobic molecules, amphiphilic block copolymers have at least one hydrophilic, and one hydrophobic region. At concentrations below critical micelle concentration (CMC), water molecules are highly ordered around the hydrophobic segment of polymer chains. This orderly arrangement of water molecules decreases the entropy and increases the free energy of the system. Water reduces the free energy by expelling block copolymers to the interface in order to reduce the contact of hydrophobic part with water. By increasing the concentration of polymer, at CMC, water interface is saturated with polymers as well as bulk phase. Further increase in concentration of block copolymer in water will lead to the aggregation of block copolymers preventing hydrophobic parts to interact with water. Formation of this hydrophilic shield minimizes free energy of system. Therefore, micellization process is an spontaneous process [25-27]. Micelle formation can happen at low concentration of block

copolymers (above CMC) by entropic driven force. At higher concentration of block copolymers, called critical gel concentration (CGC), interaction between micelles increases. Increasing of temperature can promote the dehydration of hydrophobic chains in micelles and lead to an increase in hydrophobic interaction between micelles and formation of polymeric micelle networks.

### **1.2.3 Most commonly used ABCs for drug delivery**

Over the past decades, there has been an increase in the use of ABCs for biomedical applications. This is mostly because of their unique structure. Block copolymers have the ability to combine properties of different macromolecules by building a polymer consisting of different blocks with different hydrophobic/hydrophilic nature. As a consequence, block copolymers can adapt a wide range of structures, and chemistry. In the following section, the most commonly used block copolymers in the biomedical field will be discussed in more detail. The most common hydrophilic block used in the structure of ABCs for biomedical applications, is poly(ethylene glycol) (PEG) or poly(ethylene oxide) (PEO). PEG is mostly used to define low molecular weight PEO. Poly(ethylene oxide) has a very polar nature. The solubility of PEO depends on temperature; therefore self-assembly of block copolymers containing PEO is influenced not only by the size of PEO, but also by temperature [28]. Unlike hydrophilic block, the choice of hydrophobic blocks used in the structure of block copolymers is diverse.

#### *i. Pluronic®*

Pluronics® (manufactured by BASF corporation) or Polaxamers (Manufactured by Imperial

Chemical Industries (ICI)) are tri-block copolymers consisting of PEO as the hydrophilic block, and poly(propylene oxide) (PPO) as their hydrophobic block (Figure 1-5). Pluronic® block copolymers have been used as pharmaceutical excipient for a long time [29]. They have been used to enhance the solubility of hydrophobic drugs like haloperidol [30], carboplatin [31], Indomethacin [32], and Diazepam [33]. Beside their ability to enhance solubility, Pluronics® can also form thermo-responsive gels. The thermo responsive behavior of Pluronic® block copolymers has been used to prepare topical controlled release dosage forms for vancomycin [32], pilocarpine [33], and sulfathiazide [34]. Pluronic® block copolymers have the ability to change the biological response of cells preventing drug efflux transporters, like P-glycoprotein (Pgp) [34-38] and other multidrug resistance (MDR) proteins [39,40].

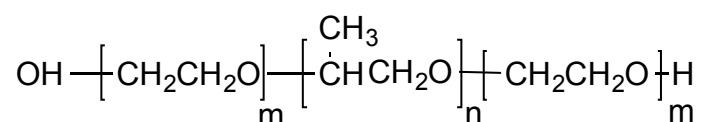
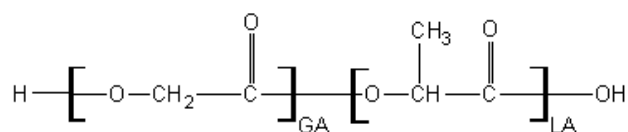


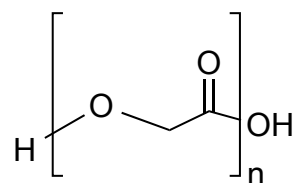
**Figure 0-4 General Chemical Structure of Pluronics®**

#### *ii. PEO-Polyesters*

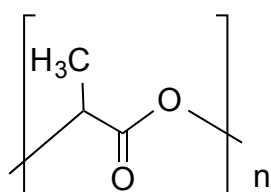
Polyester based block copolymers have been used safely as biodegradable sutures, [41] orthopedic fixation devices [42], and controlled drug delivery carriers. PEO-Polyesters are composed of biocompatible and biodegradable polyester hydrophobic blocks, and nontoxic hydrophilic PEO. Polylactides (PLA), polyglycolide (PGA), poly(lactide-co-glycolide) (PLG), and poly(ε-caprolactone) (PCL) are some example of polyesters (Figure 1-6).



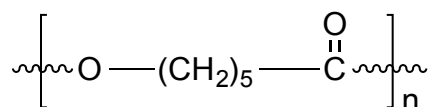
Poly(D,L-lactide-co-glycolide)



Poly(glycolide)



Poly(lactide)



Poly(caprolactone)

**Figure 0-5 Chemical structure of different polyesters**

Among polyesters family, PCL based block copolymers have attracted attention mainly because PCL is biodegradable, and at the same time it is miscible with a wide range of polymers. In addition, PCL has good permeability, and its mechanical properties are suitable for drug incorporation and delivery [43,44]. However, the high crystallinity of PCL reduces its compatibility with tissues and its hydrophobicity increases the chance for non-specific protein adsorption to PEG. Moreover, it has a slow degradation, which is a drawback for its application in human. Polymerization of PCL with other monomers, especially PEG is one way of solving these problems. PEG can cover the PCL block *in vivo*; therefore, decrease protein adsorption. The degree of crystallinity of PCL can be reduced by polymerization with PEG. This can in turn increase the degradation rate of PCL, as well [45].

Different drugs have been loaded in PEO-PCL block copolymers, and assessed for their encapsulation and release properties, These includes indomethacin [46],

dihydrotestosterone [47], cyclosporine A (CyA) [48], doxorubicin (DOX) [49], paclitaxel (PTX) [50], and curcumin [51]. In addition, PEO-PCL block copolymers have been used as scaffolds in tissue engineering [52]. Tri-block copolymers of PEG-PCL-PEG, or PCL-PEG-PCL have been used as in situ gel-forming controlled drug delivery systems [53-55].

The lack of functional groups on PCL has limited the flexibility of this polymer for adaptation to different applications. Attachment of functional group on PCL can modify drug-loading capacity of PEO-PCL micelles and/or introduce pH sensitivity to these carriers. Depending on the structure of functional group, the crystallinity of polymer can be changed, leading to changes in degradation rate of the polymer [56].

There are two main methods to introduce functional groups to aliphatic polyesters. Reaction of PCL by lithium amides is one approach. Poly(enolate)s resulted from the reaction of lithium amides with PCL is reactive towards a variety of electrophiles like benzaldehyde, carbon dioxide, acid chlorides, and benzyl carboxylate. However, degradation of polymer chain is common due to high affinity of enolate group to react with ester groups within the polymer chain [56-58]. Ring opening polymerization of functionalized caprolactone monomer is the other alternative. The substitution is usually introduced on the  $\alpha$  or  $\gamma$  carbon [57].

#### **1.2.4 Application of ABCs for drug delivery**

##### *i. Micellar nanocarriers for drug solubilization and sustained delivery*

Around 40% of active ingredients in use have poor solubility in water. The low aqueous solubility of hydrophobic drugs hinders their therapeutic use by decreasing their bioavailability, and makes it difficult to formulate them [59]. Block copolymers can change the solubility of hydrophobic molecules by providing hydrophobic reservoirs for drug

incorporation. Since the core section of micelles is incompatible with water the micelles can provide a good environment to dissolve drugs that are poorly soluble in water [60]. Depending on the structure of core-forming block and drug, covalent, van der Waals, and electrostatic interactions between the micellar core and the drug can be introduced [61-62]. Several poorly soluble drugs/small molecules including PTX, dihydrotestosterone (DHT), docetaxel (DCTX), CyA, cucurbitacin, and curcumin have been physically incorporated in polymeric micelles. For instance, the water solubility of DHT was increased 300 times when encapsulated into PEG-PCL micelles [47]. The calculated micelle-to-water partition coefficient for PTX and DCTX incorporated into poly(N-vinylpyrrolidone)-b-poly (D,L-lactide) micelles was  $5.07 \times 10^4$  and  $2.46 \times 10^4$ , respectively [63]. Ma et al. increased the solubility of curcumin  $5 \times 10^4$  times by encapsulation into PEO-PCL micelles [64]. The solubility of CyA increased 48 times after it was incorporated in PEO-PCL micelles [65]. The use of PEO-PCL micelles for cucurbitacin encapsulation, was shown to enhance cucurbitacin's solubility 13-fold [66]. The physical encapsulation of drugs within the micellar carrier usually occurs because of a hydrophobic interaction between the drug and the polymer. Therefore, the hydrophobicity of the micelle core and its compatibility with the drug play a key role in micellar capacity for drug solubilization.

The release of drugs from micelles can be controlled by different factors including the hydrophobicity of the micellar core, the nature of the polymer-drug interaction, and the crystallinity of the core-forming block. The diffusion of hydrophobic drugs from the micellar cores of higher hydrophobicity is expected to be slower [67,68]. Stronger interactions between the drug and the hydrophobic core can reduce the release rate of the drug from micelles [68]. Drug molecules diffuse faster through amorphous cores than semi-crystalline ones. In any case, micelle structure can be tailored to obtain sustained release profile for

drugs [2,69].

*ii. Micellar nanocarriers for passive, active and physical drug targeting*

Polymeric micelles can be designed for targeted delivery of drugs like anticancer agents. The preferred accumulation of micellar carriers in a tumor site is believed to be due to the enhanced permeation and retention (EPR) effect in solid tumors. When the size of solid tumors grow above a diameter of 0.8-1 mm, tumor cells will be deprived of nutrients and oxygen. In this case, they induce the growth of new blood vessels (angiogenesis) through the secretion of vascular endothelial growth factor (VEGF). The newly formed blood vessels (neo-vasculature) have an abnormal architecture. They have a large opening in endothelial cells allowing the leakage of large molecules to tumor interstitium [70]. Angiogenesis can occur in other conditions like inflammation and infarcts leading macromolecules to leakage into interstitial fluid, but the lymphatic system can recover the permeated macromolecules in those tissues. In contrast, lymphatic drainage does not work effectively in a tumor, causing macromolecules to accumulate in the interstitial fluids for days (Figure 1-7) [70-71].

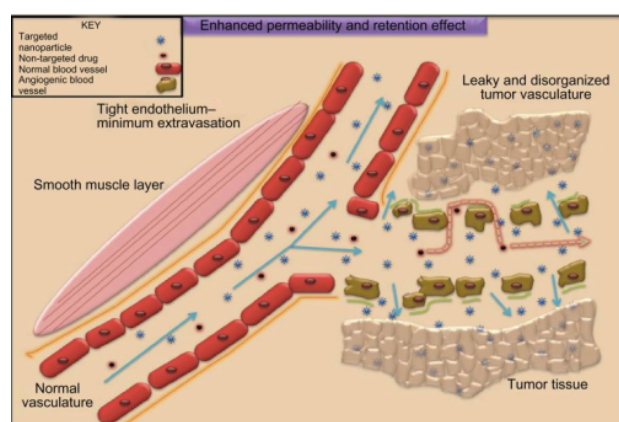


**Figure 0-6. Schematic representation of EPR Effect (adapted from reference 71 with permission)**



The EPR effect was first discovered by Hiroshi Maeda in 1984. While Maeda was working on styrene-maleic anhydride (SMA) conjugated to the anti-cancer peptide drug, neocarzinostatin (NCS), labeled with a dye, he realized that the dye had mostly accumulated in the tumor. So he concluded that the high-density vascular system in tumors must have high permeability [2]. The EPR effect became a landmark principle for passive targeting using nano-carriers including micelles, dendrimers, and liposomes to carry anti-cancer drugs to the tumor site later. Maeda et al. showed the EPR effect by injecting a water-soluble acrylic monomer into the blood vessels of mice with cancerous tissue. This monomer forms a polymeric resin in blood vessels. The cast of the polymeric resin was observed around cancerous blood vessels. Figure 1-8 shows the electronic scanning micrographs of normal versus cancerous vessels. The leakage of plastic resin to outside of vessels due to the EPR effect (Figure 1-8 C & D) is compared to no leakage in normal vessels (Figure 1-8 A & B) [72].

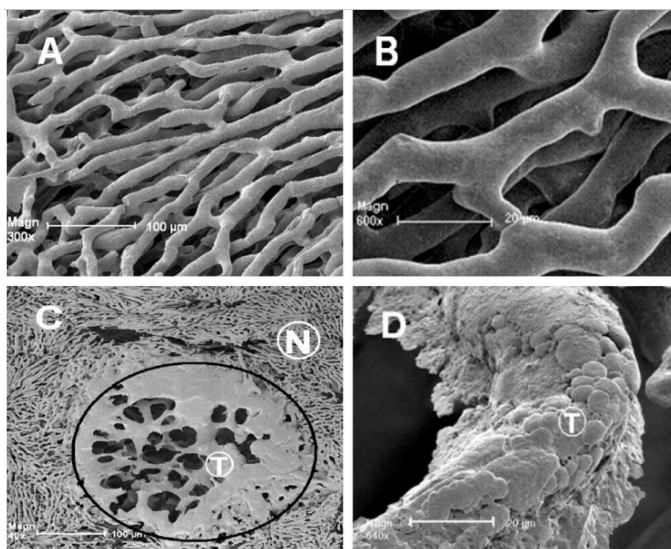


**Figure 0-7: Comparison of scanning electron micrograms of normal vessels (A and B) with tumor vessels in mice-bearing tumor after injection of water-soluble acrylic monomer. No polymer leakage is seen in normal vascular area (N), or in A and B. However, in the tumor vascular area (T), the extravasation of the polymer is seen. (Adapted from reference 72 with permission)**

Nanoparticles should be able to stay long enough in the blood circulation to have a chance for the EPR effect to impact tumor accumulation. Changing the size, and surface properties can modify the nanoparticles' circulating time in the blood. The kidney is an important organ: it purifies the blood by removing foreign materials. Any particle less than 10 nm in diameter will be removed by the kidney through the glomerular capillary wall (first pass renal filtering). Therefore, nanoparticles smaller than 10 nm will be removed, and won't have long circulation time. On the other hand, particles larger than 200 nm can be easily recognized by the reticular endothelial system (RES) and removed from circulation. The efficient size of particle for passive targeting is believed to be between 80 and 200 nm [73]. The size of a particle is inversely related to the tumor interstitial diffusion coefficient. Particles > 400 nm can't diffuse well within a tumor.

The size of micelles can be tailored by changing the polymer composition, molecular weight, and method of preparation [56-60]. Nanoparticles like micelles have a high surface area that causes high interaction with the environment. Therefore, their surfaces should have protection against phagocytic clearance by RES. The hydrophilic shell of a micelle can introduce stealth properties to the carrier and prevent rapid uptake of micelles by RES. Micelles can be structurally tailored for passive targeting.

Micelle selectivity for tumor cells can be enhanced by attaching targeting moieties to the surface of the cells. This is called active targeting. After accumulating in the tumor's interstitial fluid, targeting moieties can improve selective attachment of the carrier to tumor cells, and enhance intracellular drug delivery to tumor cells by endocytosis. Kabanov *et al.* were among the pioneers in reporting active targeted drug delivery by polymeric micelles. In 1989, Kabanov and his colleagues developed polymeric micelles for delivering haloperidol to the brain. Haloperidol was incorporated into Pluronic P85, and Pluronic analog of 2-

hydroxyacetaldehyde (BPEA), attached to murine polyclonal antibody(30).

There are different targeting moieties that can be attached to micelles. Monoclonal antibodies (mAbs) or their Fab fragments, folate, transferrin and peptides are among most common targeting moieties applied to polymeric micelles [73]. Micelle circulation time, cellular uptake, and extravasation can be affected by changing the targeting moiety, and their density on the micellar surface.

Antibodies can target specific antigens on cancer cells. They can interfere with ligand-receptor stimulation alone or along with an active anti-cancer agent. Epidermal growth factor receptor (EGFR) can bind to either epidermal growth factor or transforming growth factor- $\alpha$ . Binding to either of these ligands can lead to rapid proliferation of cancer cells. EGFR is over-expressed on most cancer cells, and; therefore, interfering in receptor-ligand stimulation by antibodies can be used for cancer therapy. Vega *et al.* conjugated antibody C225 against epidermal growth factor receptors to poly(L-glutamic acid)-co-polyethylene glycol (PG-PEG) conjugated with DOX (C225-PEG-PG-Dox). Antibody C225 can compete with natural ligand of EGFR in binding to receptor. The internalization of C225-PEG-PG-Dox into human vulvar squamous carcinoma A431 cells that overexpress epidermal growth factor receptors happened within five minutes compared to unimmunized micelles [74].

There are some limitations in using antibodies for active drug targeting. First, the synthesis of antibodies is expensive and the procedure is complicated. Second, the antibodies are usually humanized antibodies driven from mice, and there is a possibility for the antibodies to cause an immune response [73].

Folate receptors are overexpressed on a variety of cancer cells including uterine sarcomas, ovarian, brain and kidney. Folate has an important role in the synthesis of nucleotide bases in human; therefore, it is essential for cell proliferation [75]. Upon

interaction with its receptor, folate internalized conjugated drugs. This may be followed by a drug release from the conjugate within the cell [73]. Yoo and Park developed a diblock copolymer micelle of poly(D,L-lactic-co-glycolic acid)(PLGA) and PEG with DOX conjugated to the PLGA block, and folate attached to the PEG segment. They showed that active targeting can increase the uptake by target cells *in vitro*. However, the *in vivo* distribution to the heart showed a reduced trend, which was not significantly different from the unmodified micellar DOX [76].

Transferrin is the natural ligand for transferrin receptors, which help the cell to uptake iron. Transferrin receptors are overexpressed on various cancer cells, and can be targeted by transferrin-conjugated nanoparticle. After attaching to its receptor, transferrin internalizes nanoparticle by endocytosis process [73]. Shaoo *et al.* prepared a PTX loaded nanoparticle by copolymerization with PLGA, and poly(vinyl alcohol) (PVA). Transferrin was then conjugated to nanoparticles. The cellular uptake of nanoparticle modified with transferrin by prostate cancer cell line PC3 was three times higher than those without transferrin [77].

Peptides are another class of targeting moieties, which have been used widely for tumor-targeted therapy. Their synthesis is less expensive and less complicated compared to antibodies. GE11 (Figure1-9) is a synthetic peptide ligand for the Epidermal Growth Factor Receptor (EGFR), which can compete with the EGF, the natural ligand of EGFR. Epidermal growth factor positive signaling is responsible for cell proliferation stimulation, prevention of apoptosis, and induction of angiogenesis [69,78]. Therefore, EGF is not a proper targeting ligand for EGFR.

EGFR is overexpressed on a variety of cancer cells, and can be targeted for anti-cancer drug delivery. Song *et al.* attached GE11 to a liposomal nanoparticle loaded with DOX. They assessed binding and distribution toward EGFR expressed on cancer cells by

fluorescence imaging techniques. They found that both GE11-conjugated and non-conjugated liposomes accumulated in tumor, but the liposomes conjugated with GE11 had higher accumulation, and they remained in the tumor longer than the unconjugated liposomes [79]. Klutz *et al.* developed polyplexes based on polyethylenimine (LPEI), and PEG-loaded with sodium iodide symporter (NIS), and attached GE11 as a targeting ligand on the polyplexes. NIS is a transmembrane glycoprotein that mediates iodine uptake into cells. Klutz *et al.* compared iodine uptake by hepatocellular carcinoma after consuming polyplexes with or without GE11. Polyplexes conjugated to GE11 increased iodine uptake 22 times higher than those without GE11 [80]. Vega *et al.* used physical targeting for the efficient internalizing of DOX by conjugating of DOX to PEO-b-P(L-glutamic acid) [84].

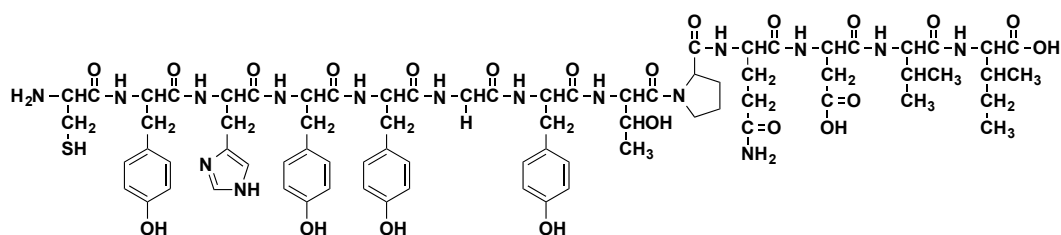


**Figure 0-8: Chemical structure of GE11**

Although active targeting enhances drug delivery inside cancer cells, in some cases even though micelles are actively entered into cells, the drug cannot release efficiently from the micelles. In order to solve this problem, physical targeting is used. In this approach stimuli-sensitive structural components will be added to the nanoparticles' construct. For instance this structural component could be sensitive to the acidic pH releasing the incorporated drug in the acidic environment of the tumor or within the acidic intracellular compartments [18,81]. The low pressure of oxygen in the tumor mass can affect the metabolic profile of the tumor cell, leading to an increase in lactic acid. Therefore, the pH in

the extracellular tissue of cancer cells is lower than normal: about 6.0. Polymeric micelles can accumulate in tumor interstitial tissue as a result of the EPR effect, but success in cancer therapy depends on the proper release of the anticancer drug in the site of action. pH sensitive polymeric micelles can release drug molecules in either tumor interstitial fluids or in lysosomes (pH between 4.5-5) [82]. Seong Lee *et al.* developed adriamycin loaded in micelles composed of poly(L-histidine)-PEG which was mixed with poly(L-lactic acid) (PLLA) -PEG block copolymers with or without folate conjugation as a targeted moiety which is an example of physically targeted polymeric micelles. Seong lee *et al.* showed that the release of adriamycin from polymeric micelles increased by decreasing the pH [83].

#### *ii. Stimulus responsive hydrogels based on ABCs*

Hydrogels are three-dimensional hydrophilic polymeric networks that can take up to 99% w/w water. They become insoluble in water by chemical or physical crosslinking. Hydrophilic polymers without cross-linking are soluble in water, and are called hydrosol [85]. Upon crosslinking of hydrophilic polymers, the polymeric chains become immobile due to the formation of cross-links. It is necessary to form networks to keep the polymer from dissolving in water, however hydrogels can absorb water up to 90-99% w/w due to the existence of hydrophilic groups in the network [86]. Chemical cross-linking occurs when covalent bond between polymeric chains; therefore, hydrogels with chemical cross-linked networks have permanent properties. Chemical cross-linking can be achieved using aldehyde-containing cross-linkers for water-soluble polymers with hydroxyl groups, or by using carboxylic acid-containing cross-linkers that condense polymers with hydroxyl, or amine groups. In addition radical polymerization using cross-linking agent can be conducted to obtain chemical cross-linked hydrogels. Physically cross-linked hydrogel, on the other hand,

are formed by a physical interaction such as ionic or hydrophobic interactions between polymer chains. Such polymers can reversibly shift between hydrosol and hydrogel by changes in inter-chain physical interactions [87].

In recent years, stimuli-responsive hydrogels have been used for different applications including drug delivery, tissue engineering, and biological sensors. Stimuli-responsive hydrogels can undergo change in their solubility in response to different stimuli like pH, temperature, light, electric or magnetic field, as well as biological or chemical analyst. As a result, these smart hydrogels can sense environmental changes, and respond to them. Stimuli-responsive hydrogels can be designed for pulsed or self-regulated drug delivery [82]. Among different stimuli, more research has been dedicated to pH, and temperature sensitive hydrogels since these two stimuli can differ naturally in different physiological conditions in the body.

#### *a) Thermo-responsive Hydrogels*

Thermo-responsive hydrogels are among the most common stimuli-sensitive hydrogels used for drug delivery. The common characteristic of thermo-responsive polymers is the existence of a hydrophobic group in a polymer chain. These polymers will undergo a sudden change in their solubility in water above a certain temperature. This temperature is called the critical solution temperature. If polymers become soluble as their temperature increases, they are considered to have an upper critical solution temperature (UCST), but if they become insoluble as their temperature increases, they are considered to have a lower critical solution temperature (LCST). Hydrogels made from polymers with LCST properties will shrink upon heating, which is known as inverse temperature dependence, and it is governed by hydrophobic interaction, and free energy of mixing [82,88].

When an ABC having LCST property is added to water, at a concentration higher than its CMC, it self-assembles to micelles. At low temperatures water molecules orderly orient around polymeric micelles making hydrogen bonds with polar segments of polymers. As the temperature increases, the hydrogen bonds are broken, and the production value of entropy multiplied by the absolute temperature will be higher than the enthalpy of the hydrogen bonds between water, and the polar segments of the polymers [89]. Therefore, the free energy of the polymeric micelle association ( $\Delta G = \Delta H - T\Delta S$ ) is negative. If the concentration of the polymer in water is high enough, this negative free energy leads to the association of micelles in water (Figure 1-9) [90]. This tendency of micelles or non-polar substance to aggregate in aqueous solutions is called hydrophobic effect.

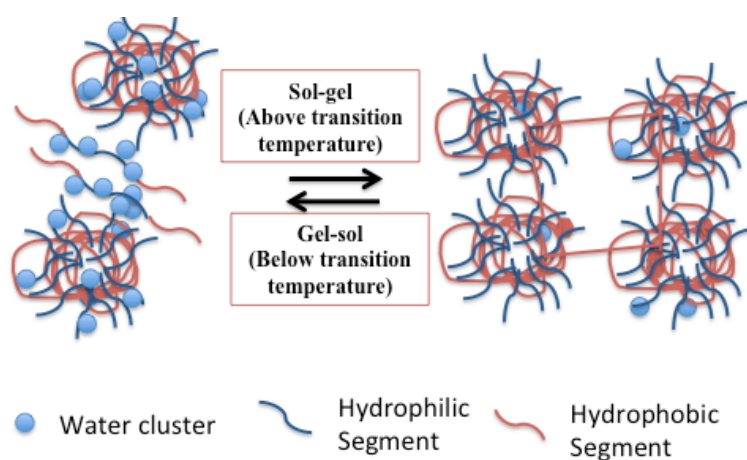


**Figure 0-9 Schematic illustration of inter-micellar hydrophobic interaction leading to micellar association and gel formation as a result of an increase in temperature.**

The minimum concentration at which a gel can form from a polymer in a water solution is called critical gelation concentration (GCG). Above LCST of polymer at concentration above CGC gel formation will occur by the hydrophobic effect.



Poly(N-isopropylacrylamide) (PNIPAm) is a well-known thermo-responsive polymer which has been studied for modulated drug delivery since 1990. NIPAm has LCST around 32°C. Among other commonly used thermo-responsive polymers, PEG-based ABCs including PEO-PPO-PEO triblock copolymers (known as Pluronics®), and PLGA–PEG–PLGA triblock copolymers (known as ReGel™) have been widely investigated for controlled drug delivery.

Pluronics® have been used widely in the pharmaceutical industry. Pluronic F127 displays sol-gel transition around body temperature (37°C) at concentrations higher than 20% (w/w) [88]. Schmolka *et al.* reported this copolymer for the treatment of burns [91]. The aqueous solution of this copolymer can undergo a sol-gel transition after parental injection [88]. Katakam *et al.* investigated the *in vitro*, and *in vivo* subcutaneous, or intramuscular injection of recombinant human growth hormone (rhGH) from Poloxamer 407 (Pluronic® F-127) gel. Their results showed an *in vitro* Zero-order release of rhGH for 60-72 h, and first order *in vivo* release for one week after intramuscular, or subcutaneous injections in rats [92]. Prolonged release of vancomycin loaded Pluronic® F127 was observed by Veyries *et al.* after local injection in rats to treat infections [93]. Pluronics® have also been used as thermally gelling liquid suppositories for improving the bioavailability of propranolol in rats [94]. In addition, Pluronics® have been investigated for drug delivery through vaginal [95] and ophthalmic [96] routes. However, their gel doesn't show strong mechanical properties, and they are non-biodegradable. Moreover, they have a short residence time at the site of injection [85].

ReGel™, on the other hand, is a biodegradable ABC. The aqueous solution of ReGel™ forms a gel at concentrations between 5 to 30% w/w. ReGel™ has been studied widely for parental drug delivery since 1999. OncoGel™ is paclitaxel loaded ReGel™ for

the intra-tumor injection of paclitaxel. It provides a paclitaxel-sustained release over four to six weeks [97]. Choi *et al.* investigated controlled release of insulin from ReGel™. They observed a sustained, two-week release of insulin after subcutaneous injection [98]. Protein delivery (e.g., pGH, G-CSF, insulin, rHbsAg) through ReGel™ was also accessed, and results showed a sustained release over 10 to 14 days [99]. The only drawback of ReGel™ is a high concentration of polymers needed for obtaining thermo-responsive behavior [97,100]. Moreover, the PLGA block degradation in copolymers produces lactic acid and glycolic acid. The resultant acidic condition can promote degrade the block copolymers [13].

Block copolymers consisting of PEG and PCL [53,101,102] have been widely studied for drug delivery or tissue engineering applications [101,103,104]. The sol-gel transition of these block copolymers has been studied by several groups. Bae *et al.* suggested that the sol-gel transition of PCL-PEG-PCL block copolymers can be prompted by micellar aggregation [105,106]. At a temperature much lower than the sol-gel transition temperature, small micelles flow freely in the aqueous medium. The micelle size increased slightly as the temperature increased, but the micelles remained in the sol state. With further increase in temperature to around the sol-gel transition temperature, the micelle size increased rapidly, leading to a sol-gel transition [107].

As mentioned earlier thermo-responsive polymers especially those having sol-gel transition temperatures around the body temperature, i.e., 37°C or lower, have potential in different biomedical fields. Biomolecules can be easily mixed with polymer solution, without requiring any organic solvent or special procedures. Therefore, biomolecules with different structures can be incorporated into such hydrogels. The three-dimensional configuration of hydrogels, resembles the real scenario. Since cell morphology, and gene expression can be different from two-dimensional environment, hydrogels can provide a biologically friendly

resembling the real life situation for cell implantation. Moreover, since the hydrogels are liquid at the time of injection, and form a gel *in vivo*, they can transfer a drug to the site of action in a less invasive way than implants [108]. In addition, injected solution can easily obtain the shape of a cavity before forming a gel [109].

Thermo-responsive hydrogels have also been used recently to prevent post-surgical adhesion [10]. In this regard, poly(caprolactone-co-lactic acid)-poly(ethylene glycol)-poly(caprolactone-co-lactic acid) (PCLA-PEG-PCLA) can form a physical barrier upon injection by undergoing a sol-gel transformation, and protect peritoneum from adhesion [86,110].

#### *b) pH-sensitive hydrogels*

pH can change in different parts of the body. For example through the gastrointestinal tract, pH changes from 1-3 in the stomach to up to 7-7.5 in colon. Moreover, pH can be changed due to disease or other conditions. For instance, pH in chronic wounds is around 5.4-7.4. Tumor interstitial fluids have an acidic pH (around 6.0 to 6.5) [111]. Therefore, the variation in pH can be used as a trigger for pH-sensitive hydrogels to modulate drug delivery.

pH-sensitive hydrogels are usually composed of polymers with acidic (e.g. carboxylic and sulfonic acids) or basic (e.g. ammonium salts) functional group. Poly(acrylamide) (PAAm), poly(acrylic acid) (PAA), poly(methacrylic acid) (PMA), and poly(diethylaminoethyl methacrylate) (PDEAEMA) are some examples of pH-sensitive polymers. The ionization state of these polymers varies around their  $pK_a$  resulting in changes in their solubility in water. Polymers bearing acidic groups will release protons above their  $pK_a$  and; therefore, become more hydrophilic, while polymers having alkaline groups are ionized at a pH below their  $pK_a$  [86]. Moreover, the existence of fixed charges in the polymer

structure causes networks to swell due to the electrostatic repulsion, and osmotic pressure exerted by the counter-ions neutralizing the fixed ions [112,113].

Peppas *et al.* proposed a mechanism for swelling, and de-swelling of poly(methacrylic acid) (PMA) grafted with PEG hydrogels. They suggested that at a low pH, carboxylic acid could form a complex with the oxygen of the PEG segment through hydrogen bonding leading to the de-swelling of the hydrogel. However; at a higher pH the ionization of carboxylic acid breaks the hydrogen bonds, and causes decomplexation, which leads to the swelling of the hydrogel [114]. This kind of complexation mechanism can be applied to other polymers consisting of two segments, which can interact through pH-sensitive hydrogen bonding [115].

One of the applications of pH sensitive polymers is in cancer targeting as explained in the previous sections. pH sensitive polymers can also be used as biosensors. An example system is glucose-responsive hydrogels for modulated-insulin release. Traitel *et al.* used poly(2-hydroxyethyl methacrylate-co-N,N-dimethylaminoethyl methacrylate) (poly(HEMA-co-DMAEMA)) as hydrogels for entrapping glucose oxidase, catalase, and insulin. At high concentration of glucose, it diffused into hydrogel, and converted to gluconic acid by glucose oxidase. The resulting acidic condition caused the pH-sensitive hydrogel to swell and release the insulin [116].

### *c) Temperature and pH sensitive hydrogels*

Stimuli responsive polymers, which are able to respond simultaneously and independently to two stimuli, are called dual stimuli responsive polymers. Temperature and pH are two important biological stimuli, which have been used for designing modulated drug release from stimuli sensitive polymeric carriers.

pH sensitive moieties usually contain acidic or basic groups. Introducing pH sensitive moieties keeps hydrogel in liquid state at a pH higher or lower than the physiological pH. Ideally for application in drug delivery, the sol becomes a gel at pH 7.4 [10,117]. One of the drawbacks of thermo-responsive polymers for injectable implants is their broad sol-gel transition temperature range. pH sensitive moieties used are usually deionized at pH 7.4, leading to an increase in hydrophobicity at this pH promoting inter-polymer or inter-micelle interaction and the formation of physically cross-linked hydrogel networks. Therefore, introducing pH sensitive moieties to a temperature responsive polymers may, in fact, narrow down the sol-gel transition temperature range and make the transition narrower. On the other hand, hydrogels made of a thermo-responsive polymer may become a gel in the needle during injection. Introducing pH sensitive entities to such polymers can prevent this problem. Moreover, drug molecules with charge can form ionic complex with acidic or basic functional groups of pH sensitive polymers. This can increase their loading capacity and modify their release properties[108].

pH and thermo-responsive polymers can be prepared in different ways. One way would be by copolymerization of different segments that introduce pH and temperature sensitivity. For example poly(N-isopropylacrylamide-co-acrylic acid), and poly(N-isopropylacrylamide-co-propylacrylic acid) copolymers were designed to combine sections with pH and temperature responsiveness [118]. Another approach would be by derivitization of thermo-responsive polymers with pH sensitive moieties. Oligosulfamethazine–poly(lactide-co-caprolactone)–PEG–poly(lactide-co-caprolactone)–oligosulfa-methazine (OSM–PCLA–PEG–PCLA–OSM) is one example of a pH/thermo-responsive polymer prepared through derivitization of PCLA-PEG-PCLA.

### **1.3 Characterization of in situ forming hydrogels**

The determination of the sol-gel transition temperature of polymer solutions, the kinetics of gel formation, the mechanical strength of the in situ forming gel, the loading capacity, and the mechanism of drug release from hydrogels are important properties that should be investigated to develop a reliable drug delivery system. The following sections briefly describe methods used to investigate such properties.

#### **1.3.1 Inverse flow method**

The inverse flow method, or tube inverting method is a traditional way to determine the sol-gel transition of lyophilic polymer solutions. In this method, vials containing polymer aqueous solutions are immersed in a water bath. The water bath temperature is allowed to increase gradually from room temperature. The phase transition (flow/no flow) is assessed by inverting the incubated tube vertically to allow a visual assessment of the aqueous polymer sample. The copolymer solution is considered to be a gel when the solution does not flow for one minute upon inversion of vial. The incubation temperature, at which this phenomenon is observed, is recorded as the transition temperature.

#### **1.3.2 Modulated Differential Scanning Calorimetry (MDSC)**

Differential Scanning Calorimetry (DSC) is a thermal analysis method for measuring changes in the physical properties of materials as a function of temperature against time. DSC analyzes the thermal behavior of samples by estimating the difference in the heat that flows out or into samples compared to references in exothermic or endothermic transitions, respectively. DSC has been used commonly for characterizing pharmaceuticals, polymers, nanoparticles, hydrogels, and food due to the ease of sample preparation. DSC can be used

for solids, liquids, powders, and films. In addition, analyzing samples usually doesn't take too much time, and it can measure transitions in a wide temperature range. However, DSC has limitations; for transitions occurring in close temperature, DSC is not able to separate peaks, and overlap happens. Moreover, in order to increase sensitivity for elucidating low energy transitions, the sample size or heating rate should increase which leads to a reduction in resolution. DSC applies a linear heating rate to the sample; therefore, it is able to measure the sum of heat flow, and cannot provide a quantitative analysis of each transition.

Modulated Differential Scanning Calorimetry (MDSC, on the other hand, can apply linear, and sinusoidal (modulated) heating rates simultaneously in samples. Equation 1.2 describes how both DSC, and MDSC calculate the total heat flow (dH/dt).

$$dH/dt = C_p dT/dt + f(T,t) \quad (\text{eq 1.2.})$$

Where  $C_p$  is the heat capacity of the sample, and  $dT/dt$  is the rate of changes in temperature.  $T$  is the absolute temperature and  $f(T,t)$  is a function of time and temperature expressing the calorimetric response of the chemical or physical reaction, which is controlled kinetically[121].

According to the equation, the total heat flow consists of two components. Reversing heat flow component responds to changes in the heat capacity of the sample, and heating rate ( $dT/dt$ ). The kinetic or non-reversing component of total the heat flow is independent of the rate of the temperature change, and only depends on the absolute temperature and time. In conventional DSC the only way to calculate  $C_p$  is to run the same sample twice at two different heating rates, whereas in MDSC,  $C_p$  can be estimated along with the total heat flow due to applying modulated heating rate[122,123].

One of the applications of MDSC is to determine the sol-gel transition temperature of thermo-responsive hydrogels. By heating a solution of thermo-responsive polymers in water,

the hydrogen bond between the polar group of polymers and water molecules will break, leading to an increase in hydrophobicity of polymer. This can lead to transition of polymer solution to gel at the polymer concentrations above CGC through hydrophobic interactions between polymer chains or micelles. MDSC elucidates this transition by endothermic peaks in thermo-gram [124].

### 1.3.3 Rheological Analysis

Rheology explains how the deformation or flow of matters relates to applied force, and time. According to Hooke's law of elastic deformation, which was proposed in 1678, if a constant pushing force  $F$  is applied to upper part of a cube, it will deform in a way that the upper part will move while lower part is fixed [125]. Shear strain defines this deformation, and can be calculated by dividing the length of the upper part's movement by the distance of the upper part to the lower part. The equation is dimensionless since it is a ratio of two lengths. Shear stress can be calculated from the ratio of force ( $F$ ) to the area of applied force ( $A$ ), and its unit is  $N/m^2$  or Pascal. For materials with pure elasticity, according to Hooke's law, shear stress is proportional to shear strain, and the proportionality constant ( $G$ ) is described as shear modulus. If the stress is removed, the deformation will stop and the material goes back to its original position, or shape. Therefore, deformation is recoverable.

On the other hand, for fluids if stress is applied liquid will deform continuously, and the rate of deformation increases constantly. If the stress is removed, the liquids will not go back to their original shape. In other word, liquids irreversibly deform. According to the Newtonian law for liquids, stress is proportional to the rate of strain, which can be obtained from the ratio of shear strain to the duration of applied force. The proportionality constant is called viscosity and its units are Pascal-second (Pa.s) [125,126].



Newtonian and Hooke's law are linear relationships; however, for most materials stress and shear strain or shear rate do not have a linear relationship. Therefore, an accurate determination of the shear rate of these materials needs especial equipment that is able to apply shearing with small gaps. Moreover, in order to separate elastic properties from viscous properties of viscoelastic material an oscillatory rheometer should be used [127]. In an oscillatory rheometer, a sinusoidal oscillation of strain is applied on a sample. If the sample is pure elastic, the detected stress will be in the same phase as the strain, but if the sample is pure liquid, the obtained stress will be 90° out of the phase. For viscoelastic materials, there is always a phase difference ( $\delta$ ) between 0 to 90°. The software for the device can then calculate the elastic property (storage modulus), and viscous property (loss modulus) of the materials since  $\tan \delta$  is a ratio of the loss modulus to the storage modulus [127].

Thermo-reversible polymers can form physically cross-linked network in water as a function of an increase in temperature. The mechanical strength of hydrogel depends on the degree of cross-linking. In thermo-responsive hydrogels, this degree of cross-linking is not fixed and will change as a function of temperature. At low temperatures, thermo-reversible hydrogels are at a sol state. Therefore, at low temperature, the loss modulus is higher than the storage modulus. As the temperature increases, the storage modulus increases. At the gel state the storage modulus is higher than the loss modulus indicating that the hydrogel is more solid. Using an oscillatory rheometer at different temperatures can elucidate storage, and the loss modulus. The transition temperature of hydrogels can be obtained by plotting the storage, and loss modulus against the temperature [128].

#### **1.3.4 NMR investigation for transition temperature**

For an isotropic liquid, NMR signals appear sharp. The rapid collision and reorientation of molecules in isotropic fluids, causes averaging chemical shifts, and dipolar coupling. However, in semisolids systems like gels, dipolar coupling cannot be averaged, since the motion of molecules is restricted. Therefore, usually signals in the NMR spectrum broaden or disappear [129]. Thus, NMR spectroscopy can be used to investigate the phase transition of aqueous thermo-responsive polymers.

However, amphiphilic block copolymers, self-assemble to micelle-like structures above CMC in aqueous media. In this case, NMR peaks related to the hydrophobic portion of the block copolymer will appear broadened because of the localization in the viscous environment of the micellar core, where the mobility of the chemical groups are restricted. An increase in temperature in this case may lead to the mobilization of a core-forming block followed by a block copolymer bridging between individual micelles, shedding light over the mechanism of gel formulation.

### **1.3.5 Drug loading in hydrogels**

There are two main methods of drug loading in hydrogels: post-loading, and in situ loading. In the post-loading approach, the drug will be absorbed into the hydrogel after the hydrogel has formed; drug molecules solutions are incubated with pre-formed hydrogel for a specific time. The drug's uptake by hydrogel is mainly governed by diffusion. In situ loading method is achieved by mixing drug molecules and polymer solution. Therefore, drug loading and hydrogel formation will be done simultaneously. The loading efficiency mainly depends on the density of cross-links in the hydrogels networks [130].

### **1.3.6 Drug release**

Hydrogels have been extensively used to provide the sustained release of drugs. Different mechanism of drug release can be achieved by modifying the chemical structure of hydrogels and their degree of cross-linking in order to obtain the desired mode of drug release [131]. This issue will be addressed in more detail in the following section.

#### **1.4. Modes of drug release from hydrogels**

Three models of drug release have been described for hydrogels:

##### *a) Diffusion controlled release*

Diffusion is the most common model used to describe drug release from hydrogels. Drug release from hydrogels is predicted according to Fick's law in this model of release. In hydrogel systems the diffusion coefficient will be affected by the drug's size and nature, hydrogel's pore size and water content, and the polymer structure. For porous hydrogels whose pores are larger than drug molecule itself, diffusion coefficient will be characterized by the hydrogel's porosity and tortuosity, in addition to the diffusion coefficient of the drug molecule in solvent filled in pores. On the other hand, in hydrogels whose pores are smaller than or comparable to those of the drug molecules, diffusion coefficient will be reduced. In these conditions drug diffusion pathways will increase due to steric obstruction caused by cross-links. Moreover, the diffusion coefficient may remain constant or change during the release period [131,132].

##### *b) Swelling controlled release*

In swelling controlled release systems, the rate of drug release is characterized by the rate of hydrogel swelling. In this case, the transfer from the polymer's glassy to rubbery state

improves the drug transfer through hydrogels. Hydroxypropyl methylcellulose (HPMC) is an example of a swelling controlled systems [132].

### *c) Chemically controlled release*

In chemically controlled release systems, the drug release is determined by either a pure kinetic controlled release or a combination of kinetic release and diffusion. Kinetic controlled release is used to describe conjugated drug release as a result of the degradation of a cleavable spacer to a polymeric hydrogel network or a hydrogel degraded by surface erosion. Surface erosion happens in hydrogel systems when the enzyme penetration rate into the hydrogel is slower than the enzymatic degradation on the surface. In both cases diffusion doesn't play a major role in the drug release. A combination of kinetic and diffusion controlled release, on the other hand, is used to characterize hydrogel systems with bulk erosion. In these systems, the diffusion coefficient is time dependent, and not constant [132].

## **1.5 Model drugs under current study**

### **1.5.1 Cyclosporine A**

Cyclosporine A (Figure 1-10) is a cyclic endecapeptide made of 11 amino acids. Its molecular weight is 1202 g/mol and its molecular formula is  $C_{62}H_{111}N_{11}O_{12}$ . It is unionized at physiological pH, and its solubility in water at room temperature is 27.67  $\mu\text{g/mL}$ .

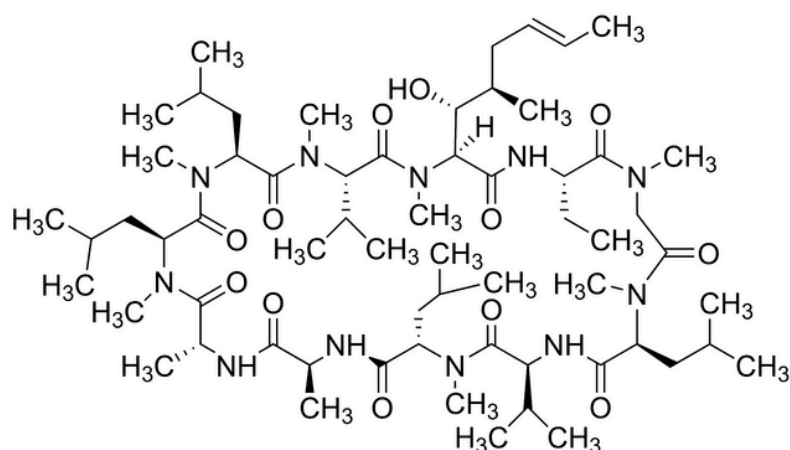


**Figure 0-10 Structure of Cyclosporine A**

Cyclosporine A is a potent immunosuppressive agent used to prevent organs` rejection after transplantation. Cyclosporine A is also used to treat autoimmune diseases including rheumatoid arthritis, and psoriasis [135,136]. Moreover, its anti-inflammatory effect has been used to treat many ophthalmic disorders including dry eye syndrome, uveitis, and peripheral ulcerative keratitis [137]. In such disease conditions, T-cell activation causes cytokines to secret, which can then cause inflammation on the ocular surface. Inflammation of the ocular surface in decreases the eye surface`s sensitivity, leading to dysfunction of the sensory autonomic neural reflex loop, leading to a decrease in tear secretion from the lacrimal glands (Figure 1-11) [136].

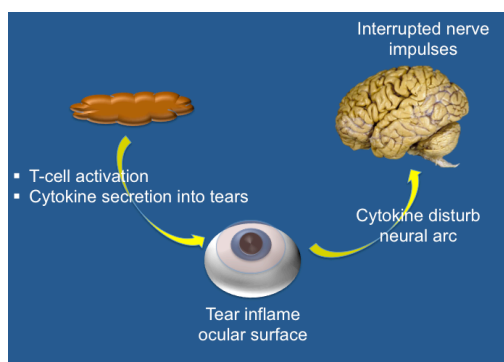


**Figure 0-11 Secretion of cytokines into tears can disturb the secretory-autonomic neural reflex loop (adopted from reference 136)**

*i. Commercial formulations of CyA*

Cyclosporine A is available as soft gelatin capsules and an oral solution by Novartis Pharma (Neoral®, Sandimmune®) for oral use. In addition to the oral route, cyclosporine can be administered by intravenous (IV) injection in form of a Sandimmune® Injection. Cyclosporine is also available for ophthalmic administration in Restasis® by Allergan [138].

*ii. Hydrogel loaded CyA*

Although eye drops are one of the most convenient methods of drug administration for patients, the bioavailability of such drugs is low through this route of administration. Almost 95% of a drug administered through this route will be wasted, since it may be absorbed by the conjunctiva or drained by the tear duct. Using a thermo-responsive hydrogels that forms a gel in contact with cornea, will increase the bioavailability by increasing residence time of the drug in the eye [139].

The release of CyA loaded in contact lenses has been investigated in order to overcome the low bioavailability of CyA using eye drops. Kapoor *et al.* developed nanostructured poly(2-hydroxyethyl methacrylate) (p-HEMA) hydrogels containing microemulsions or micelles of Brij 97 ( $C_{18}H_{35}(OCH_2CH_2)_{10}$ ) and assessed the release of CyA. The *in vitro* release study showed a sustained release of CyA for 20 days [140]. Peng *et al.* studied CyA release from ACUVUE® and extended wear silicone hydrogel (SiH) lenses. Cyclosporine was loaded into the contact lenses by soaking the lenses in a CyA solution. The release studies show one day, and two weeks release from ACUVUE® and SiH lenses, respectively [137]. Thermo-responsive hydrogels that form a gel in contact with the cornea, are expected to increase the bioavailability of CyA by increasing the residence time of the drug

in the eye [139] while improving patient compliance by reducing the frequency of drug administration. The transparent hydrogel may also make the eye vision less blurry compared to the micro emulsion formulation and provide a protective barrier for the eye at the same time.

### 1.5.2 Cisplatin

In 1845, an Italian chemist, Michele Peyrone synthesized cisplatin for the first time and called it Peyrone's chloride. However, it wasn't until 120 years later, in 1965, that Barnett Rosenberg discovered cisplatin's anticancer activity. Rosenberg was investigating the effect of electrical current on cell division using *Escherichia coli* (E. coli) in an ammonium chloride buffer. He realized that E. coli cells became long and filamentous; instead of retaining their original sausage shape. Rosenberg then realized that this phenomenon prevented cell division, which did not occur because of the electrical current, but because of the platinum electrodes produced hydrated platinum [141,142].

Cis-Diamminedichloroplatinum (II) (CDDP) known as cisplatin is a platinum-based chemotherapy drug. Cisplatin is made of a platinum (II) atom, which is planar-squared with two chlorides and two ammonia molecules in the cis position. Chloride is a leaving group in cisplatin structure, which can be replaced, by a variety of groups. The replacement of chloride depends on the chloride concentration in the solution. If the chloride concentration is low in aqueous solutions, water molecules can replace the chloride group, forming the monohydrated complex (Monoaqua) (Figure 1-12). The aquation of cisplatin molecules is essential for cisplatin's anticancer activity. Water molecules in monoaqua can be easily replaced by the base on the DNA, and the other chloride ligand can react with another base on the DNA, leading to cross-linking of DNA or cisplatin-DNA adducts [143,144]. Cross-linking of DNA with cisplatin prevents DNA from replication and transcription and

eventually causes apoptosis to the cell. In plasma the aquation of cisplatin doesn't happen because the concentration of chloride is high. However, once cisplatin enters into cells, it can be aquated due to the low concentration of chloride. Cisplatin can enter cells through either passive diffusion, or by copper transporter proteins, or organic cation transporters [145].

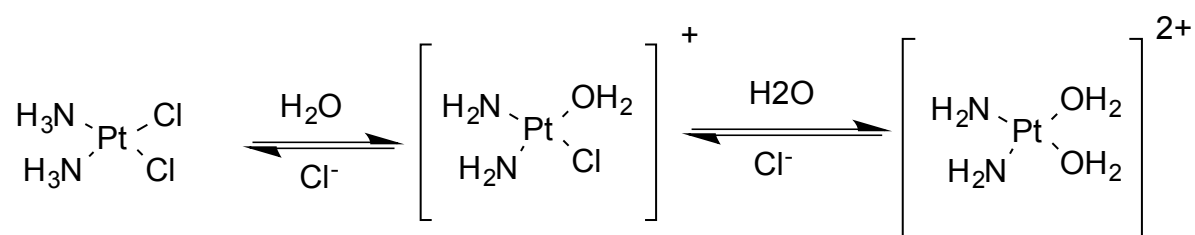


**Figure 0-12 Aquation of cisplatin at low concentration of chloride**

Cisplatin is used to treat different kinds of cancers including testicular, ovarian, bladder, head and neck, and lung. However, its use is limited due to drug resistance and systemic toxicity. The most common systemic toxicities associated with cisplatin are nephrotoxicity, neurotoxicity, and ototoxicity. Moreover, resistance to the drug can occur through three different mechanisms: drug efflux; detoxification of cisplatin through increased glutathione or thiol level in cells; and development of tolerance to DNA damage, by preventing apoptosis cascade [146].

There are two ways to decrease cisplatin systemic toxicity and/ or defeat a cell's resistance mechanism: modify the complex structure in a way that the complex binds to DNA in different mode or accumulate cisplatin at the tumor site using passive, or active targeting [147].

Currently there are five platinum-based anticancer drugs approved for use in humans. These drugs have either lower systemic toxicity or the potential to overcome resistance mechanisms (Figure 1-13). Carboplatin is a platinum-derivative drug, which is approved for



human use all over the world. This medication has less systemic toxicity. Carboplatin has a bis-carboxylates ligand instead of chloride. The ligand aquates very slowly. Since the platinum-based drug's toxicity depends on leaving groups' liability to be aquated, carboplatin is less toxic than cisplatin. Oxaliplatin is another platinum derivative, which is able to overcome cell resistance by binding to DNA by forming a different adduct. Nedaplatin is another analog of a platinum drug. It has 10 times less nephrotoxicity than cisplatin. Nedaplatin is approved for human use in Japan. Heptaplatin, which is approved in the Republic of Korea, has efficient cytotoxicity against cisplatin-resistant cells, with no remarkable systemic toxicity. Lobaplatin is a platinum-based anticancer drug approved in China. It has low systemic cytotoxicity [145].

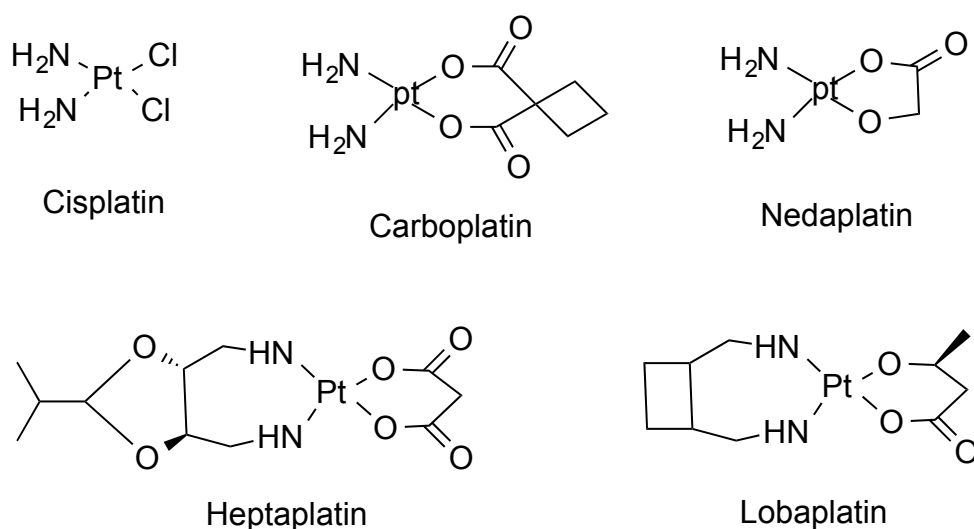


**Figure 0-13. Current platinum-based anticancer drugs approved for human use**

*i. Commercial formulation of Cisplatin*

Cisplatin is available as a sterile aqueous solution for injection in multiple-dose vials in concentration of 1 mg/mL.

## *ii. Nanoformulations of Cisplatin*

As mentioned before, the drawbacks in cisplatin cancer therapy include its systemic side effects. This limitation can be solved by incorporating cisplatin in delivery systems. These systems, are able to accumulate in cancerous tissue through active or passive targeting. Various targeted delivery system have been developed for cisplatin. Polymeric micelles, and liposomal formulations are the most common passive targeting delivery systems. NC-6004 is one of the representative polymeric micelle carriers for cisplatin in phase II clinical trials [147]. NC-6004 is a block copolymer of PEG and poly(glutamic acid) (PGlu) loaded with cisplatin. The *in vitro* release study showed 19.6% and 47.8% cisplatin release after 24 and 96 h, respectively, from this formulation [148]. A phase I clinical trial of NC-6004 carried out in the United Kingdom on patients with solid tumors shows less nephrotoxicity compared to cisplatin administration; nephrotoxicity wasn't induced significantly by administrating of NC-6004 up to 120 mg/m<sup>2</sup>[149,150]. In terms of how much cisplatin accumulated in tumors in animals, C<sub>max</sub> was 2.5-folds higher for NC-6004 compared to free cisplatin [150,151].

Lipoplatin® is a liposomal formulation of cisplatin now in phase III clinical trial. Lipoplatin® is made of dipalmitoyl phosphatidyl glycerol (DPPG), soy phosphatidylcholine, and methoxypoly- ethylene glycol-distearoylphosphatidylethanolamine. A phase I clinical study on 27 patients with pretreated advanced malignant tumors, shows no nephrotoxicity [147,152]. Moreover, Lipoplatin® targets tumor vasculatures and has antiangiogenesis activity in addition to direct anti-cancer activity [153].

## **1.6. Thesis proposal**

### **1.6.1. Rationale**

There is increasing interest in hydrogels in drug delivery and tissue engineering. Hydrogels are three-dimensional polymeric networks that absorb high amount of water, which makes them compatible with living tissues. Moreover, hydrogels are able to hold macromolecules and cells due to cross-linked networks, while the circulation of nutrition and the clearance of by-products can easily be achieved through hydrogels' pores and water filled regions. The combination of water content and polymeric networks renders hydrogels viscoelastic in nature, minimizing irritation to soft tissue. Polymers that form gels in response to temperature introduce an opportunity for more efficient and less invasive delivery of drugs, especially in the form of injectable implants. Compared to conventional implants, thermo-responsive hydrogels can be injected into the site of drug action as solutions. Therefore, there is no need for any surgical operation for inserting the delivery system. Moreover, thermo-responsive solutions can take the shape of the cavity during the sol-gel transition. In a solution state drug molecules or cells can be mixed with polymers in water without the need for adding any organic solvent.

Thermo-responsive *in situ* forming hydrogels show great promise for versatile applications in drug delivery, cell implantation and tissue engineering. However, optimum materials of desired properties are still lacking. Pluronic® F127 displays sol-gel transition around body temperature (37°C) at concentration higher than 20% w/w [88]. However, Pluronic® doesn't display a mechanically strong gel, and is non-biodegradable. Moreover, it has a short resident time at the injection site [85]. ReGel™, on the other hand, is a hydrogel made from biodegradable ABCs. Hence, the degradation of copolymer can be autocatalyzed by the production of lactic, and glycolic acid. Block copolymers consisting of (PEG) and another polyester, i.e., poly( $\epsilon$ -caprolactone) (PCL) are biodegradable block copolymers that

have been studied for their thermoresponsive behaviors. Unlike ReGel™, block copolymers of PEG and PCL degrade more slowly, and don't produce acidic environment [12].

The current PEO-polyester based hydrogels described above; however, lack functional groups in their structure. This may reduce their capacity to incorporate drug molecules with distinct chemical structures. Besides, such structures do not respond to stimuli like pH.

Our research group has previously reported on the development of novel PEO-PCL block copolymers containing pendent functional groups (e.g., benzyl carboxylate and/or carboxyl groups) on PCL [154]. Here, we have synthesized triblock copolymers of PEO and functionalized PCL and investigated the potential of tri- and diblock copolymers within this family in the formation of biodegradable and temperature/pH responsive in situ hydrogel and/or micellar drug delivery systems. The pendent benzylcarboxylate and/or carboxyl groups on the polymers backbone makes them chemically flexible. As a result, it would be easily possible to tailor the properties of polymer for specific needs in drug delivery. For instance through changes in the level of carboxyl to benzyl carboxylate, it would be possible to manipulate the HLB of the polymer for improve micellization or gelation and/or enhance incorporation capacity of drug molecules. Moreover, existence of pendent carboxyl groups can introduce pH sensitivity to block copolymers or enable interaction with hydrogen bond molecules.

### **1.6.2. Hypothesis**

Tri- and diblock copolymers based on PEO and functionalized PCL-containing pendent carboxyl groups, can be prepared and used to develop temperature and pH responsive in situ hydrogels and micellar drug delivery systems for stimulus responsive drug delivery.

### **1.6.3. Objective**

To synthesize tri- and diblock copolymers based on PEG and  $\alpha$ -carbon functionalized poly ( $\epsilon$ -caprolacton) and assess the potential of these ABCs in the formation of thermo and/or pH responsive hydrogels and micelles for depot or tumor targeted drug delivery.

### **1.6.4. Specific aims**

1. To synthesize triblock copolymers based on PEG (as the hydrophilic middle block) and carboxyl and/or benzylcarboxylate substituted PCL (as hydrophobic lateral blocks) at and characterize the temperature and pH sensitive self-assembly of the prepared block copolymers.
2. To assess the characteristics of the prepared block copolymers to form temperature-sensitive in situ hydrogels.
3. To characterize the prepared block copolymers in temperature- and pH-responsive gelation and depot delivery of model macromolecules.
4. To assess the prepared hydrogels for depot delivery of cyclosporine A.
5. To assess the biodegradability and biocompatibility of prepared hydrogels.
6. To assess the potential of multi-functional polymeric micelles formed from GE11-modified PEO (as the shell) and carboxyl substituted PCL (as the core) for tumor targeting of cisplatin.

## References:

- (1) Folkman J, Long DM. The use of silicone rubber as a carrier for prolonged drug therapy. *J Surg Res* 1964;4(3):139-142.
- (2) Hoffman AS. The origins and evolution of “controlled” drug delivery systems. *J Controlled Release* 2008;132(3):153-163.
- (3) Peppas N, Bures P, Leobandung W, Ichikawa H. Hydrogels in pharmaceutical formulations. *European journal of pharmaceutics and biopharmaceutics* 2000;50(1):27-46.
- (4) Van Tomme SR, Storm G, Hennink WE. < i> In situ gelling hydrogels for pharmaceutical and biomedical applications. *Int J Pharm* 2008;355(1):1-18.
- (5) Tan H, Ramirez CM, Miljkovic N, Li H, Rubin JP, Marra KG. Thermosensitive injectable hyaluronic acid hydrogel for adipose tissue engineering. *Biomaterials* 2009;30(36):6844-6853.
- (6) Crompton K, Goud J, Bellamkonda R, Gengenbach T, Finkelstein D, Horne M, et al. Polylysine-functionalised thermoresponsive chitosan hydrogel for neural tissue engineering. *Biomaterials* 2007;28(3):441-449.
- (7) Stile RA, Healy KE. Thermo-responsive peptide-modified hydrogels for tissue regeneration. *Biomacromolecules* 2001;2(1):185-194.
- (8) Gant R, Abraham A, Hou Y, Cummins B, Grunlan M, Coté G. Design of a self-cleaning thermoresponsive nanocomposite hydrogel membrane for implantable biosensors. *Acta biomaterialia* 2010;6(8):2903-2910.
- (9) Fujimoto KL, Ma Z, Nelson DM, Hashizume R, Guan J, Tobita K, et al. Synthesis, characterization and therapeutic efficacy of a biodegradable, thermoresponsive hydrogel designed for application in chronic infarcted myocardium. *Biomaterials* 2009;30(26):4357-4368.
- (10) Moon HJ, Park MH, Joo MK, Jeong B. Temperature-responsive compounds as in situ gelling biomedical materials. *Chem Soc Rev* 2012;41(14):4860-4883.
- (11) Liu R, Fraylich M, Saunders BR. Thermoresponsive copolymers: from fundamental studies to applications. *Colloid Polym Sci* 2009;287(6):627-643.
- (12) He C, Kim SW, Lee DS. < i> In situ gelling stimuli-sensitive block copolymer hydrogels for drug delivery. *J Controlled Release* 2008;127(3):189-207.
- (13) Jeong B, Bae YH, Kim SW. In situ gelation of PEG-PLGA-PEG triblock copolymer aqueous solutions and degradation thereof. *J Biomed Mater Res* 2000;50(2):171-177.
- (14) Jeong B, Kim SW, Bae YH. Thermosensitive sol–gel reversible hydrogels. *Adv Drug Deliv Rev* 2012.
- (15) Torchilin VP. Multifunctional nanocarriers. *Adv Drug Deliv Rev* 2012.
- (16) Nakayama M, Okano T. Multi-targeting cancer chemotherapy using temperature-responsive drug carrier systems. *React Funct Polym* 2011;71(3):235-244.
- (17) Torchilin V. Multifunctional and stimuli-sensitive pharmaceutical nanocarriers. *European Journal of Pharmaceutics and Biopharmaceutics* 2009;71(3):431-444.

- (18) Mahmud A, Xiong X, Aliabadi HM, Lavasanifar A. Polymeric micelles for drug targeting. *J Drug Target* 2007;15(9):553-584.
- (19) Alexandridis P, Lindman B. *Amphiphilic block copolymers: self-assembly and applications*. : Elsevier Science; 2000.
- (20) Förster S, Antonietti M. Amphiphilic block copolymers in structure-controlled nanomaterial hybrids. *Adv Mater* 1998;10(3):195-217.
- (21) Antonietti M, Förster S, Hartmann J, Oestreich S. Novel amphiphilic block copolymers by polymer reactions and their use for solubilization of metal salts and metal colloids. *Macromolecules* 1996;29(11):3800-3806.
- (22) Adams ML, Lavasanifar A, Kwon GS. Amphiphilic block copolymers for drug delivery. *J Pharm Sci* 2003;92(7):1343-1355.
- (23) Young RJ, Lovell PA. *Introduction to polymers*. : Chapman & Hall London; 1991.
- (24) Riess G. Micellization of block copolymers. *Progress in Polymer Science* 2003;28(7):1107-1170.
- (25) Maibaum L, Dinner AR, Chandler D. Micelle formation and the hydrophobic effect. *The Journal of Physical Chemistry B* 2004;108(21):6778-6781.
- (26) Mondal J, Yethiraj A. Driving Force for the Association of Amphiphilic Molecules. *The Journal of Physical Chemistry Letters* 2011;2(19):2391-2395.
- (27) Owen SC, Chan DP, Shoichet MS. Polymeric micelle stability. *Nano Today* 2012;7(1):53-65.
- (28) Loh W. Block copolymer micelles. *Encyclopedia of surface and colloid science* 2002:802-813.
- (29) Alexandridis P, Alan Hatton T. Poly (ethylene oxide)□ poly (propylene oxide)□ poly (ethylene oxide) block copolymer surfactants in aqueous solutions and at interfaces: thermodynamics, structure, dynamics, and modeling. *Colloids Surf Physicochem Eng Aspects* 1995;96(1):1-46.
- (30) Kabanov AV, Chekhonin V, Alakhov VY, Batrakova E, Lebedev A, Melik-Nubarov N, et al. The neuroleptic activity of haloperidol increases after its solubilization in surfactant micelles: micelles as microcontainers for drug targeting. *FEBS Lett* 1989;258(2):343-345.
- (31) Exner AA, Krupka TM, Scherrer K, Teets JM. Enhancement of carboplatin toxicity by Pluronic block copolymers. *J Controlled Release* 2005;106(1):188-197.
- (32) Lin SY, Kawashima Y. Kinetic studies on the stability of indomethacin in alkaline aqueous solution containing poly(oxyethylene)poly(oxypropylene) surface-active block copolymers. *Pharm Acta Helv* 1985;60(12):345-350.
- (33) Lin S, Kawashima Y. Pluronic surfactants affecting diazepam solubility, compatibility, and adsorption from iv admixture solutions. *PDA Journal of Pharmaceutical Science and Technology* 1987;41(3):83-87.
- (34) Kabanov AV, Batrakova EV, Alakhov VY. Pluronic<sup>®</sup> block copolymers for overcoming drug resistance in cancer. *Adv Drug Deliv Rev* 2002;54(5):759-779.
- (35) Batrakova EV, Miller DW, Li S, Alakhov VY, Kabanov AV, Elmquist WF. Pluronic P85 enhances the delivery of digoxin to the brain: in vitro and in vivo studies. *J Pharmacol Exp Ther* 2001;296(2):551-557.

- (36) Batrakova EV, Li S, Vinogradov SV, Alakhov VY, Miller DW, Kabanov AV. Mechanism of pluronic effect on P-glycoprotein efflux system in blood-brain barrier: contributions of energy depletion and membrane fluidization. *J Pharmacol Exp Ther* 2001;299(2):483-493.
- (37) Szakács G, Paterson JK, Ludwig JA, Booth-Genthe C, Gottesman MM. Targeting multidrug resistance in cancer. *Nature Reviews Drug Discovery* 2006;5(3):219-234.
- (38) Regev R, Katzir H, Yeheskely-Hayon D, Eytan GD. Modulation of P-glycoprotein-mediated multidrug resistance by acceleration of passive drug permeation across the plasma membrane. *FEBS Journal* 2007;274(23):6204-6214.
- (39) Batrakova EV, Li S, Alakhov VY, Elmquist WF, Miller DW, Kabanov AV. Sensitization of cells overexpressing multidrug-resistant proteins by pluronic P85. *Pharm Res* 2003;20(10):1581-1590.
- (40) Batrakova EV, Kabanov AV. Pluronic block copolymers: evolution of drug delivery concept from inert nanocarriers to biological response modifiers. *J Controlled Release* 2008;130(2):98-106.
- (41) Gilding D, Reed A. Biodegradable polymers for use in surgery—polyglycolic/poly (actic acid) homo-and copolymers: 1. *Polymer* 1979;20(12):1459-1464.
- (42) Middleton JC, Tipton AJ. Synthetic biodegradable polymers as orthopedic devices. *Biomaterials* 2000;21(23):2335-2346.
- (43) Heuschen J, Jérôme R, Teyssie P. Polycaprolactone-based block copolymers. 1. Synthesis by anionic coordination type catalysts. *Macromolecules* 1981;14(2):242-246.
- (44) Zhou S, Deng X, Yang H. Biodegradable poly ( $\epsilon$ -caprolactone)-poly (ethylene glycol) block copolymers: characterization and their use as drug carriers for a controlled delivery system. *Biomaterials* 2003;24(20):3563-3570.
- (45) Labet M, Thielemans W. Synthesis of polycaprolactone: a review. *Chem Soc Rev* 2009;38(12):3484-3504.
- (46) Yeon Kim S, Gyun Shin I, Moo Lee Y. Methoxy poly (ethylene glycol) and  $\epsilon$ -caprolactone amphiphilic block copolymeric micelle containing indomethacin-II. Micelle formation and drug release behaviours. *J Controlled Release* 1998;51(1):13-22.
- (47) Allen C, Han J, Yu Y, Maysinger D, Eisenberg A. Polycaprolactone- $\beta$ -poly (ethylene oxide) copolymer micelles as a delivery vehicle for dihydrotestosterone. *J Controlled Release* 2000;63(3):275-286.
- (48) Montazeri Aliabadi H, Brocks DR, Lavasanifar A. Polymeric micelles for the solubilization and delivery of cyclosporine A: pharmacokinetics and biodistribution. *Biomaterials* 2005;26(35):7251-7259.
- (49) Diao Y, Li H, Fu Y, Han M, Hu Y, Jiang H, et al. Doxorubicin-loaded PEG-PCL copolymer micelles enhance cytotoxicity and intracellular accumulation of doxorubicin in adriamycin-resistant tumor cells. *International journal of nanomedicine* 2011;6:1955.
- (50) Cai S, Vijayan K, Cheng D, Lima EM, Discher DE. Micelles of different morphologies—advantages of worm-like filomicelles of PEO-PCL in paclitaxel delivery. *Pharm Res* 2007;24(11):2099-2109.
- (51) Gou M, Men K, Shi H, Xiang M, Zhang J, Song J, et al. Curcumin-loaded biodegradable polymeric micelles for colon cancer therapy in vitro and in vivo. *Nanoscale* 2011;3(4):1558-1567.
- (52) Park JS, Woo DG, Sun BK, Chung H, Im SJ, Choi YM, et al. In vitro and in vivo test of PEG/PCL-based hydrogel scaffold for cell delivery application. *J Controlled Release* 2007;124(1):51-59.



- (53) Gong C, Shi S, Dong P, Kan B, Gou M, Wang X, et al. Synthesis and characterization of PEG-PCL-PEG thermosensitive hydrogel. *Int J Pharm* 2009;365(1):89-99.
- (54) Gong C, Shi S, Wu L, Gou M, Yin Q, Guo Q, et al. Biodegradable in situ gel-forming controlled drug delivery system based on thermosensitive PCL-PEG-PCL hydrogel. Part 2: Sol-gel-sol transition and drug delivery behavior. *Acta Biomaterialia* 2009;5(9):3358-3370.
- (55) Gong CY, Dong PW, Shi S, Fu SZ, Yang JL, Guo G, et al. Thermosensitive PEG-PCL-PEG hydrogel controlled drug delivery system: sol-gel-sol transition and in vitro drug release study. *J Pharm Sci* 2009;98(10):3707-3717.
- (56) Mahmud A, Xiong X, Lavasanifar A. Novel Self-Associating Poly (ethylene oxide)-b lock-poly ( $\epsilon$ -caprolactone) Block Copolymers with Functional Side Groups on the Polyester Block for Drug Delivery. *Macromolecules* 2006;39(26):9419-9428.
- (57) Riva R, Schmeits S, Jérôme C, Jérôme R, Lecomte P. Combination of ring-opening polymerization and “click chemistry”: toward functionalization and grafting of poly ( $\epsilon$ -caprolactone). *Macromolecules* 2007;40(4):796-803.
- (58) Jérôme C, Lecomte P. Recent advances in the synthesis of aliphatic polyesters by ring-opening polymerization. *Adv Drug Deliv Rev* 2008;60(9):1056-1076.
- (59) Merisko-Liversidge EM, Liversidge GG. Drug nanoparticles: formulating poorly water-soluble compounds. *Toxicol Pathol* 2008;36(1):43-48.
- (60) Bromberg L. Polymeric micelles in oral chemotherapy. *J Controlled Release* 2008;128(2):99-112.
- (61) Katayose S, Kataoka K. Remarkable increase in nuclease resistance of plasmid DNA through supramolecular assembly with poly (ethylene glycol)—poly (L-lysine) block copolymer. *J Pharm Sci* 1998;87(2):160-163.
- (62) Kakizawa Y, Kataoka K. Block copolymer micelles for delivery of gene and related compounds. *Adv Drug Deliv Rev* 2002;54(2):203-222.
- (63) Fournier E, Dufresne M, Smith DC, Ranger M, Leroux J. A novel one-step drug-loading procedure for water-soluble amphiphilic nanocarriers. *Pharm Res* 2004;21(6):962-968.
- (64) Ma Z, Haddadi A, Molavi O, Lavasanifar A, Lai R, Samuel J. Micelles of poly (ethylene oxide)-b-poly ( $\epsilon$ -caprolactone) as vehicles for the solubilization, stabilization, and controlled delivery of curcumin. *Journal of Biomedical Materials Research Part A* 2008;86(2):300-310.
- (65) Aliabadi HM, Mahmud A, Sharifabadi AD, Lavasanifar A. Micelles of methoxy poly (ethylene oxide)-b-poly ( $\epsilon$ -caprolactone) as vehicles for the solubilization and controlled delivery of cyclosporine A. *J Controlled Release* 2005;104(2):301-311.
- (66) Molavi O, Ma Z, Mahmud A, Alshamsan A, Samuel J, Lai R, et al. Polymeric micelles for the solubilization and delivery of STAT3 inhibitor cucurbitacins in solid tumors. *Int J Pharm* 2008;347(1):118-127.
- (67) Aliabadi HM, Lavasanifar A. Polymeric micelles for drug delivery. 2006.
- (68) Allen C, Maysinger D, Eisenberg A. Nano-engineering block copolymer aggregates for drug delivery. *Colloids and Surfaces B: Biointerfaces* 1999;16(1):3-27.

- (69) Agrawal SK, Sanabria-DeLong N, Coburn JM, Tew GN, Bhatia SR. Novel drug release profiles from micellar solutions of PLA–PEO–PLA triblock copolymers. *J Controlled Release* 2006;112(1):64-71.
- (70) Fang J, Nakamura H, Maeda H. The EPR effect: Unique features of tumor blood vessels for drug delivery, factors involved, and limitations and augmentation of the effect. *Adv Drug Deliv Rev* 2011;63(3):136-151.
- (71) Ranganathan R, Madanmohan S, Kesavan A, Baskar G, Krishnamoorthy YR, Santosham R, et al. Nanomedicine: towards development of patient-friendly drug-delivery systems for oncological applications. *International journal of nanomedicine* 2012;7:1043.
- (72) Maeda H, Bharate G, Daruwalla J. Polymeric drugs for efficient tumor-targeted drug delivery based on EPR-effect. *European Journal of Pharmaceutics and Biopharmaceutics* 2009;71(3):409-419.
- (73) Steichen SD, Caldorera-Moore M, Peppas NA. A review of current nanoparticle and targeting moieties for the delivery of cancer therapeutics. *European Journal of Pharmaceutical Sciences* 2012.
- (74) Vega J, Ke S, Fan Z, Wallace S, Charsangavej C, Li C. Targeting doxorubicin to epidermal growth factor receptors by site-specific conjugation of C225 to poly (L-glutamic acid) through a polyethylene glycol spacer. *Pharm Res* 2003;20(5):826-832.
- (75) Oerlemans C, Bult W, Bos M, Storm G, Nijsen JFW, Hennink WE. Polymeric micelles in anticancer therapy: targeting, imaging and triggered release. *Pharm Res* 2010;27(12):2569-2589.
- (76) Yoo HS, Park TG. Folate receptor targeted biodegradable polymeric doxorubicin micelles. *J Controlled Release* 2004;96(2):273-283.
- (77) Sahoo SK, Ma W, Labhasetwar V. Efficacy of transferrin-conjugated paclitaxel-loaded nanoparticles in a murine model of prostate cancer. *International Journal of Cancer* 2004;112(2):335-340.
- (78) Li Z, Zhao R, Wu X, Sun Y, Yao M, Li J, et al. Identification and characterization of a novel peptide ligand of epidermal growth factor receptor for targeted delivery of therapeutics. *The FASEB journal* 2005;19(14):1978-1985.
- (79) Song S, Liu D, Peng J, Sun Y, Li Z, Gu J, et al. Peptide ligand-mediated liposome distribution and targeting to EGFR expressing tumor in vivo. *Int J Pharm* 2008;363(1):155-161.
- (80) Klutz K, Schaffert D, Willhauck MJ, Grünwald GK, Haase R, Wunderlich N, et al. Epidermal growth factor receptor-targeted 131I-therapy of liver cancer following systemic delivery of the sodium iodide symporter gene. *Molecular Therapy* 2011;19(4):676-685.
- (81) Vasir JK, Reddy MK, Labhasetwar VD. Nanosystems in drug targeting: opportunities and challenges. *Current Nanoscience* 2005;1(1):47-64.
- (82) Bawa P, Pillay V, Choonara YE, du Toit LC. Stimuli-responsive polymers and their applications in drug delivery. *Biomedical materials* 2009;4(2):022001.
- (83) Lee ES, Na K, Bae YH. Polymeric micelle for tumor pH and folate-mediated targeting. *J Controlled Release* 2003;91(1):103-113.
- (84) Vega J, Ke S, Fan Z, Wallace S, Charsangavej C, Li C. Targeting doxorubicin to epidermal growth factor receptors by site-specific conjugation of C225 to poly (L-glutamic acid) through a polyethylene glycol spacer. *Pharm Res* 2003;20(5):826-832.
- (85) Ottenbrite RM, Park K, Okano T. *Biomedical applications of hydrogels handbook*. : Springer; 2010.

- (86) Mano JF. Stimuli-Responsive Polymeric Systems for Biomedical Applications. *Advanced Engineering Materials* 2008;10(6):515-527.
- (87) Hennink W, Van Nostrum C. Novel crosslinking methods to design hydrogels. *Adv Drug Deliv Rev* 2012.
- (88) Ruel-Gariépy E, Leroux J. In situ-forming hydrogels—review of temperature-sensitive systems. *European Journal of Pharmaceutics and Biopharmaceutics* 2004;58(2):409-426.
- (89) Schild H. Poly (< i> N-isopropylacrylamide): experiment, theory and application. *Progress in Polymer Science* 1992;17(2):163-249.
- (90) Taylor LD, Cerankowski LD. Preparation of films exhibiting a balanced temperature dependence to permeation by aqueous solutions—a study of lower consolute behavior. *Journal of Polymer Science: Polymer Chemistry Edition* 1975;13(11):2551-2570.
- (91) Schmolka IR. Artificial skin I. Preparation and properties of pluronic F-127 gels for treatment of burns. *J Biomed Mater Res* 1972;6(6):571-582.
- (92) Katakam M, Ravis WR, Banga AK. Controlled release of human growth hormone in rats following parenteral administration of poloxamer gels. *J Controlled Release* 1997;49(1):21-26.
- (93) Veyries M, Couaraze G, Geiger S, Agnely F, Massias L, Kunzli B, et al. Controlled release of vancomycin from poloxamer 407 gels. *Int J Pharm* 1999;192(2):183-193.
- (94) Ryu J, Chung S, Lee M, Kim C, Shim C. Increased bioavailability of propranolol in rats by retaining thermally gelling liquid suppositories in the rectum. *J Controlled Release* 1999;59(2):163-172.
- (95) Yun Chang J, Oh Y, Soo Kong H, Jung Kim E, Deuk Jang D, Taek Nam K, et al. Prolonged antifungal effects of clotrimazole-containing mucoadhesive thermosensitive gels on vaginitis. *J Controlled Release* 2002;82(1):39-50.
- (96) Wei G, Xu H, Ding PT, Li SM, Zheng JM. Thermosetting gels with modulated gelation temperature for ophthalmic use: the rheological and gamma scintigraphic studies. *J Controlled Release* 2002;83(1):65-74.
- (97) Loh XJ, Li J. Biodegradable thermosensitive copolymer hydrogels for drug delivery. *Expert Opinion* 2007;17:3977-3989.
- (98) Choi S, Kim SW. Controlled release of insulin from injectable biodegradable triblock copolymer depot in ZDF rats. *Pharm Res* 2003;20(12):2008-2010.
- (99) Zentner GM, Rathi R, Shih C, McRea JC, Seo M, Oh H, et al. Biodegradable block copolymers for delivery of proteins and water-insoluble drugs. *J Controlled Release* 2001;72(1):203-215.
- (100) Loh XJ, Li J. Biodegradable thermosensitive copolymer hydrogels for drug delivery. 2007.
- (101) Yin HB, Gong CY, Shi S, Liu XY, Wei YQ, Qian ZY. Toxicity evaluation of biodegradable and thermosensitive PEG-PCL-PEG hydrogel as a potential in situ sustained ophthalmic drug delivery system. *Journal of Biomedical Materials Research Part B: Applied Biomaterials* 2010;92(1):129-137.
- (102) Vermonden T, Censi R, Hennink WE. Hydrogels for Protein Delivery. *Chem Rev* 2012;112:2853-2888.
- (103) Ni PY, Fan M, Qian ZY, Luo JC, Gong CY, Fu SZ, et al. Synthesis and characterization of injectable, thermosensitive, and biocompatible acellular bone matrix/poly (ethylene glycol)-poly ( $\epsilon$ -caprolactone)-poly (ethylene glycol) hydrogel composite. *Journal of Biomedical Materials Research Part A* 2012;100:171-179.

- (104) Jiang ZQ, Deng XM, Hao JY. Novel thermogelling poly ( $\epsilon$ -caprolactone-*co*-lactide)–poly (ethylene glycol)–poly ( $\epsilon$ -caprolactone-*co*-lactide) aqueous solutions. *Chinese Chemical Letters* 2007;18(6):747-749.
- (105) Bae SJ, Joo MK, Jeong Y, Kim SW, Lee W, Sohn YS, et al. Gelation behavior of poly (ethylene glycol) and polycaprolactone triblock and multiblock copolymer aqueous solutions. *Macromolecules* 2006;39(14):4873-4879.
- (106) Bae SJ, Suh JM, Sohn YS, Bae YH, Kim SW, Jeong B. Thermogelling poly (caprolactone-*b*-ethylene glycol-*b*-caprolactone) aqueous solutions. *Macromolecules* 2005;38(12):5260-5265.
- (107) Gong C, Shi S, Wu L, Gou M, Yin Q, Guo Q, et al. Biodegradable in situ gel-forming controlled drug delivery system based on thermosensitive PCL–PEG–PCL hydrogel. Part 2: Sol–gel–sol transition and drug delivery behavior. *Acta Biomaterialia* 2009;5(9):3358-3370.
- (108) Huynh CT, Nguyen MK, Lee DS. Injectable block copolymer hydrogels: Achievements and future challenges for biomedical applications. *Macromolecules* 2011;44(17):6629-6636.
- (109) Moon HJ, Park MH, Joo MK, Jeong B. Temperature-responsive compounds as in situ gelling biomedical materials. *Chem Soc Rev* 2012;41(14):4860-4883.
- (110) Zhang Z, Ni J, Chen L, Yu L, Xu J, Ding J. Biodegradable and thermoreversible PCLA–PEG–PCLA hydrogel as a barrier for prevention of post-operative adhesion. *Biomaterials* 2011;32(21):4725-4736.
- (111) Bawa P, Pillay V, Choonara YE, du Toit LC. Stimuli-responsive polymers and their applications in drug delivery. *Biomedical materials* 2009;4(2):022001.
- (112) Gupta P, Vermani K, Garg S. Hydrogels: from controlled release to pH-responsive drug delivery. *Drug Discov Today* 2002;7(10):569-579.
- (113) Jagur-Grodzinski J. Polymeric gels and hydrogels for biomedical and pharmaceutical applications. *Polym Adv Technol* 2010;21(1):27-47.
- (114) Peppas NA, Klier J. Controlled release by using poly (methacrylic acid-*g*-ethylene glycol) hydrogels. *J Controlled Release* 1991;16(1):203-214.
- (115) Qiu Y, Park K. Environment-sensitive hydrogels for drug delivery. *Adv Drug Deliv Rev* 2012.
- (116) Traitel T, Cohen Y, Kost J. Characterization of glucose-sensitive insulin release systems in simulated in vivo conditions. *Biomaterials* 2000;21(16):1679-1687.
- (117) Nguyen MK, Park DK, Lee DS. Injectable Poly (amidoamine)–poly (ethylene glycol)–poly (amidoamine) Triblock Copolymer Hydrogel with Dual Sensitivities: pH and Temperature. *Biomacromolecules* 2009;10(4):728-731.
- (118) Yin X, Hoffman AS, Stayton PS. Poly (N-isopropylacrylamide-*co*-propylacrylic acid) copolymers that respond sharply to temperature and pH. *Biomacromolecules* 2006;7(5):1381-1385.
- (119) Shim WS, Yoo JS, Bae YH, Lee DS. Novel injectable pH and temperature sensitive block copolymer hydrogel. *Biomacromolecules* 2005;6(6):2930-2934.
- (120) Jiang Z, You Y, Deng X, Hao J. Injectable hydrogels of poly ( $\epsilon$ -caprolactone-*co*-glycolide)–poly (ethylene glycol)–poly ( $\epsilon$ -caprolactone-*co*-glycolide) triblock copolymer aqueous solutions. *Polymer* 2007;48(16):4786-4792.

- (121) Coleman NJ, Craig DQ. Modulated temperature differential scanning calorimetry: a novel approach to pharmaceutical thermal analysis. *Int J Pharm* 1996;135(1):13-29.
- (122) Verdonck E, Schaap K, Thomas LC. A discussion of the principles and applications of modulated temperature DSC (MTDSC). *Int J Pharm* 1999;192(1):3-20.
- (123) Gill P, Moghadam TT, Ranjbar B. Differential scanning calorimetry techniques: applications in biology and nanoscience. *Journal of biomolecular techniques: JBT* 2010;21(4):167.
- (124) Hou Y, Matthews AR, Smitherman AM, Bulick AS, Hahn MS, Hou H, et al. Thermoresponsive nanocomposite hydrogels with cell-releasing behavior. *Biomaterials* 2008;29(22):3175-3184.
- (125) Barnes HA, Hutton JF, Walters K. *An introduction to rheology.* : Elsevier; 1989.
- (126) ROSS-MURPHY SB. RHEOLOGICAL CHARACTERISATION OF GELS1. *J Texture Stud* 1995;26(4):391-400.
- (127) Ross-Murphy SB. Rheology of biopolymer solutions and gels. *The Scientific World Journal* 2003;3:105-121.
- (128) Chung Y, Simmons KL, Gutowska A, Jeong B. Sol-gel transition temperature of PLGA-g-PEG aqueous solutions. *Biomacromolecules* 2002;3(3):511-516.
- (129) Shapiro YE. Structure and dynamics of hydrogels and organogels: An NMR spectroscopy approach. *Progress in Polymer Science* 2011;36(9):1184-1253.
- (130) Schillemans JP, Verheyen E, Barendregt A, Hennink WE, Van Nostrum CF. Anionic and cationic dextran hydrogels for post-loading and release of proteins. *J Controlled Release* 2011;150(3):266-271.
- (131) Lowman AM. *Smart pharmaceuticals* 2008.
- (132) Lin C, Metters AT. Hydrogels in controlled release formulations: network design and mathematical modeling. *Adv Drug Deliv Rev* 2006;58(12):1379-1408.
- (133) Ran Y, Zhao L, Xu Q, Yalkowsky SH. Solubilization of cyclosporin A. *Aaps Pharmscitech* 2001;2(1):23-26.
- (134) Francis MF, Lavoie L, Winnik FM, Leroux J. Solubilization of cyclosporin A in dextran-*g*-polyethyleneglycolalkyl ether polymeric micelles. *European journal of pharmaceutics and biopharmaceutics* 2003;56(3):337-346.
- (135) Kanduru SV, Somayaji V, Lavasanifar A, Brocks DR. An analytical method for cyclosporine using liquid chromatography-mass spectrometry. *Biomedical Chromatography* 2010;24(2):148-153.
- (136) Perry HD, Donnenfeld ED. Topical 0.05% cyclosporin in the treatment of dry eye. *Expert Opin Pharmacother* 2004;5(10):2099-2107.
- (137) Peng C, Chauhan A. Extended cyclosporine delivery by silicone-hydrogel contact lenses. *J Controlled Release* 2011;154(3):267-274.
- (138) Beauchesne PR, Chung NS, Wasan KM. Cyclosporine A: a review of current oral and intravenous delivery systems. *Drug Dev Ind Pharm* 2007;33(3):211-220.

- (139) Li C, Chauhan A. Modeling ophthalmic drug delivery by soaked contact lenses. *Ind Eng Chem Res* 2006;45(10):3718-3734.
- (140) Kapoor Y, Chauhan A. Ophthalmic delivery of Cyclosporine A from Brij-97 microemulsion and surfactant-laden p-HEMA hydrogels. *Int J Pharm* 2008;361(1):222-229.
- (141) Alderden RA, Hall MD, Hambley TW. The discovery and development of cisplatin. *J Chem Educ* 2006;83(5):728.
- (142) Ekborn A. Cisplatin induced ototoxicity: Pharmacokinetics, prediction and prevention. : Institutionen för klinisk neurovetenskap/Department of Clinical Neuroscience; 2003.
- (143) Haxton KJ, Burt HM. Polymeric drug delivery of platinum-based anticancer agents. *J Pharm Sci* 2009;98(7):2299-2316.
- (144) Sarmah A, Roy RK. Understanding the preferential binding interaction of aqua-cisplatin with nucleobase guanine over adenine: a density functional reactivity theory based approach. *RSC Advances* 2013;3(8):2822-2830.
- (145) Wheate NJ, Walker S, Craig GE, Oun R. The status of platinum anticancer drugs in the clinic and in clinical trials. *Dalton Transactions* 2010;39(35):8113-8127.
- (146) Perez R. Cellular and molecular determinants of cisplatin resistance. *Eur J Cancer* 1998;34(10):1535-1542.
- (147) Wang X, Guo Z. Targeting and delivery of platinum-based anticancer drugs. *Chem Soc Rev* 2013;42(1):202-224.
- (148) Matsumura Y. Poly (amino acid) micelle nanocarriers in preclinical and clinical studies. *Adv Drug Deliv Rev* 2008;60(8):899-914.
- (149) Oerlemans C, Bult W, Bos M, Storm G, Nijsen JFW, Hennink WE. Polymeric micelles in anticancer therapy: targeting, imaging and triggered release. *Pharm Res* 2010;27(12):2569-2589.
- (150) Matsumura Y, Kataoka K. Preclinical and clinical studies of anticancer agent-incorporating polymer micelles. *Cancer science* 2009;100(4):572-579.
- (151) Wilson R, Plummer R, Adam J, Eatock M, Boddy A, Griffin M, et al. Phase I and pharmacokinetic study of NC-6004, a new platinum entity of cisplatin-conjugated polymer forming micelles. *J Clin Oncol* 2008;26:2573.
- (152) Stathopoulos GP, Boulikas T, Vougiouka M, Deliconstantinos G, Rigatos S, Darli E, et al. Pharmacokinetics and adverse reactions of a new liposomal cisplatin (Lipoplatin): phase I study. *Oncol Rep* 2005;13(4):589-596.
- (153) Boulikas T. Clinical overview on Lipoplatin™ : a successful liposomal formulation of cisplatin. 2009.
- (154) Mahmud A, Xiong XB, Lavasanifar A. Novel Self-Associating Poly (ethylene oxide)-b lock-poly (ε-caprolactone) Block Copolymers with Functional Side Groups on the Polyester Block for Drug Delivery. *Macromolecules* 2006;39(26):9419-9428.
- (155) Hoffman AS. Stimuli-responsive Polymers: Biomedical Applications and Challenges for Clinical Translation. *Adv Drug Deliv Rev* 2012;65:10-16.

- (156) Li Z, Zhang Z, Liu KL, Ni X, Li J. Biodegradable Hyperbranched Amphiphilic Polyurethane Multiblock Copolymers Consisting of Poly (propylene glycol), Poly (ethylene glycol), and Polycaprolactone as in Situ Thermogels. *Biomacromolecules* 2012;13:3977-3989.
- (157) Rathi RC, Zentner GM, inventors. Anonymous google patent. 1999 .
- (158) Shim MS, Lee HT, Shim WS, Park I, Lee H, Chang T, et al. Poly (D, L-lactic acid-co-glycolic acid)-b-poly (ethylene glycol)-b-poly (D, L-lactic acid-co-glycolic acid) triblock copolymer and thermoreversible phase transition in water. *J Biomed Mater Res* 2002;61(2):188-196.
- (159) Zentner GM, Rathi R, Shih C, McRea JC, Seo M, Oh H, et al. Biodegradable block copolymers for delivery of proteins and water-insoluble drugs. *J Controlled Release* 2001;72(1):203-215.
- (160) Safaei Nikouei N, Lavasanifar A. Characterization of the thermo- and pH-responsive assembly of triblock copolymers based on poly(ethylene glycol) and functionalized poly(epsilon-caprolactone). *Acta Biomater* 2011 Oct;7(10):3708-3718.
- (161) Bae SJ, Suh JM, Sohn YS, Bae YH, Kim SW, Jeong B. Thermogelling poly (caprolactone-b-ethylene glycol-b-caprolactone) aqueous solutions. *Macromolecules* 2005;38(12):5260-5265.
- (162) Loh XJ, Tan YX, Li Z, Teo LS, Goh SH, Li J. Biodegradable thermogelling poly (ester urethane) s consisting of poly (lactic acid)–Thermodynamics of micellization and hydrolytic degradation. *Biomaterials* 2008;29(14):2164-2172.
- (163) Nguyen MK, Lee DS. Injectable biodegradable hydrogels. *Macromolecular bioscience* 2010;10(6):563-579.
- (164) Lee DS, Shim MS, Kim SW, Lee H, Park I, Chang T. Novel thermoreversible gelation of biodegradable PLGA-block-PEO-block-PLGA triblock copolymers in aqueous solution. *Macromolecular rapid communications* 2001;22(8):587-592.
- (165) Wang Q, Li L, Jiang S. Effects of a PPO-PEO-PPO triblock copolymer on micellization and gelation of a PEO-PPO-PEO triblock copolymer in aqueous solution. *Langmuir* 2005 Sep 27;21(20):9068-9075.
- (166) Takeuchi Y, Tsujimoto T, Uyama H. Thermogelation of amphiphilic poly (asparagine) derivatives. *Polym Adv Technol* 2011;22(5):620-626.
- (167) Liu Y, Shao Y, Lü J. Preparation, properties and controlled release behaviors of pH-induced thermosensitive amphiphilic gels. *Biomaterials* 2006;27(21):4016-4024.
- (168) Cheng Y, He C, Ding J, Xiao C, Zhuang X, Chen X. Thermosensitive hydrogels based on polypeptides for localized and sustained delivery of anticancer drugs. *Biomaterials* 2013.
- (169) Huynh CT, Nguyen MK, Lee DS. Injectable block copolymer hydrogels: Achievements and future challenges for biomedical applications. *Macromolecules* 2011;44(17):6629-6636.
- (170) Garbern JC, Hoffman AS, Stayton PS. Injectable pH-and temperature-responsive poly (N-isopropylacrylamide-co-propylacrylic acid) copolymers for delivery of angiogenic growth factors. *Biomacromolecules* 2010;11(7):1833-1839.
- (171) Bae SJ, Suh JM, Sohn YS, Bae YH, Kim SW, Jeong B. Thermogelling poly (caprolactone-b-ethylene glycol-b-caprolactone) aqueous solutions. *Macromolecules* 2005;38(12):5260-5265.

- (172) Safaei Nikouei N, Lavasanifar A. Characterization of the thermo-and pH-responsive assembly of triblock copolymers based on poly (ethylene glycol) and functionalized poly ( $\epsilon$ -caprolactone). *Acta Biomaterialia* 2011;7(10):3708-3718.
- (173) Hamdy S, Haddadi A, Shayeganpour A, Alshamsan A, Aliabadi HM, Lavasanifar A. The immunosuppressive activity of polymeric micellar formulation of cyclosporine A: in vitro and in vivo studies. *The AAPS journal* 2011;13(2):159-168.
- (174) Boudier A, Aubert-Pouëssel A, Louis-Plence P, Gérardin C, Jorgensen C, Devoisselle J, et al. The control of dendritic cell maturation by pH-sensitive polyion complex micelles. *Biomaterials* 2009;30(2):233-241.
- (175) Bezemer J, Radersma R, Grijpma D, Dijkstra P, Feijen J, Van Blitterswijk C. Zero-order release of lysozyme from poly (ethylene glycol)/poly (butylene terephthalate) matrices. *J Controlled Release* 2000;64(1):179-192.
- (176) Xiong X, Ma Z, Lai R, Lavasanifar A. The therapeutic response to multifunctional polymeric nano-conjugates in the targeted cellular and subcellular delivery of doxorubicin. *Biomaterials* 2010;31(4):757-768.
- (177) Xiong X, Mahmud A, Uludağ H, Lavasanifar A. Multifunctional polymeric micelles for enhanced intracellular delivery of doxorubicin to metastatic cancer cells. *Pharm Res* 2008;25(11):2555-2566.
- (178) Oba M, Fukushima S, Kanayama N, Aoyagi K, Nishiyama N, Koyama H, et al. Cyclic RGD peptide-conjugated polyplex micelles as a targetable gene delivery system directed to cells possessing  $\alpha v \beta 3$  and  $\alpha v \beta 5$  integrins. *Bioconjug Chem* 2007;18(5):1415-1423.
- (179) Nishiyama N, Yokoyama M, Aoyagi T, Okano T, Sakurai Y, Kataoka K. Preparation and characterization of self-assembled polymer-metal complex micelle from cis-dichlorodiammineplatinum (II) and poly (ethylene glycol)-poly ( $\alpha$ ,  $\beta$ -aspartic acid) block copolymer in an aqueous medium. *Langmuir* 1999;15(2):377-383.
- (180) Lin C, Metters AT. Hydrogels in controlled release formulations: network design and mathematical modeling. *Adv Drug Deliv Rev* 2006;58(12):1379-1408.
- (181) Wu Y, Yao J, Zhou J, Dahmani FZ. Enhanced and sustained topical ocular delivery of cyclosporine A in thermosensitive hyaluronic acid-based in situ forming microgels. *International journal of nanomedicine* 2013;8:3587.
- (182) Nishiyama N, Okazaki S, Cabral H, Miyamoto M, Kato Y, Sugiyama Y, et al. Novel cisplatin-incorporated polymeric micelles can eradicate solid tumors in mice. *Cancer Res* 2003;63(24):8977-8983.
- (183) Uchino H, Matsumura Y, Negishi T, Koizumi F, Hayashi T, Honda T, et al. Cisplatin-incorporating polymeric micelles (NC-6004) can reduce nephrotoxicity and neurotoxicity of cisplatin in rats. *Br J Cancer* 2005;93(6):678-687.



## Chapter 2

### **Triblock copolymers based on poly(ethylene glycol) and functionalized poly( $\alpha$ -caprolactone): Synthesis and characterization of their thermo/pH responsive assembly**

The content of this chapter has been published in: Safaei Nikouei N, Lavasanifar A. Characterization of the thermo and pH responsive assembly of tri block copolymers based on poly(ethylene glycol) and functionalized poly( $\alpha$ -caprolactone), *Acta Biomaterialia*. 7 (2011) 3708–3718

## 1. Introduction

Amphiphilic block copolymers (ABC)s have been the focus of much interest as versatile excipients for various drug delivery applications. They are known to self-assemble into aggregates of various supramolecular micro/nanostructures in selective solvents [1]. In an aqueous environment, ABCs can self-assemble into polymeric micelles that are composed of hydrophobic segments as the internal core and hydrophilic segments as the surrounding corona [2]. Polymeric micelles have been extensively studied as carriers that can improve the aqueous solubility of hydrophobic therapeutic agents [3-5]. They show better thermodynamic stability than that of conventional surfactant micelles under physiological conditions, owing to a relatively low critical micelle concentration (CMC) [6]. As a result, polymeric micelles may be stable for longer periods upon intravenous administration and be used as carriers for depot drug release. Polymeric micelles formed from self-assembly of ABCs have shown several advantageous properties in drug delivery, such as ease of preparation, efficient drug loading, and potential for controlled drug release [7-10].

At higher concentrations (about 5-10 w/v %), ABCs (or their resulting micelles) can assemble into three dimensional polymeric networks and form a gel [11]. For particular ABC structures, the process of micellar assembly and gel formation can be triggered by changes in environmental factors such as temperature and pH.

Di- and tri- ABCs composed of poly(ethylene glycol) (PEG) and poly( $\epsilon$ -caprolactone) (PCL), have been the subject of several studies for drug delivery applications [7]. Our research group has reported on the development of a new family of block copolymers based on PEG and PCL, where the PCL block has been functionalized through introduction of carboxyl and/or benzyl carboxylate groups on the  $\alpha$ -carbon of  $\epsilon$ -caprolactone. Diblock

copolymers based on this structure were found to form micellar vehicles for the incorporation of therapeutic entities by chemical conjugation [12], physical encapsulation [13], or electrostatic complexation [14, 15]. The thermo- or PH-responsive properties of block polymers based on PEG and functionalized PCL and their potential for the formation of hydrogels have not been investigated, to date. The aim of this study was to synthesize tri block copolymers based on PEG and functionalized PCL, and assess the potential of these ABCs in thermo and/or pH responsive assembly. The gel formation of tri block copolymers containing un-functionalized PCL and PEG is documented in the literature [16, 17] and the gellation of those ABCs in aqueous solution was attributed to micelle packing driven by hydrophobic interactions, as well as partial crystallization of PCL blocks [18].

Our results showed successful synthesis of poly( $\alpha$ -benzyl/carboxyl- $\epsilon$ -caprolactone)-*b*-poly(ethylene glycol)-*b*-poly( $\alpha$ -benzyl/carboxyl- $\epsilon$ -caprolactone) triblock copolymers having different ratios of carboxyl to benzyl carboxylate groups on the hydrophobic block and their self-assembly into micellar structures. The presence of carboxylic group on the PCL chain was shown to introduce pH as well as thermo sensitivity into the assembly of block copolymers. The direction and onset of change in the size of assembled structure was found to be controlled by the ratio of carboxylic to benzyl carboxylated groups on the hydrophobic chain.

## **2. Materials and methods**

### **2.1. Materials**

Hydroxyl-poly(ethylene glycol) (PEG) ( $M_w$ = 1450), diisopropylamine (99%), benzyl chloroformate (tech 95%), sodium (in kerosene), butyllithium (Bu-Li) in hexane (2.5 M

solution), and palladium-coated charcoal were purchased from Sigma, St. Louis, MO.  $\epsilon$ -Caprolactone was purchased from Lancaster Synthesis, UK. Stannous octoate was purchased from MP Biomedical Inc., Germany.

## 2.2. Synthesis of triblock copolymers

Synthesis of triblock copolymers was accomplished in three steps: i) preparation of  $\alpha$ -benzyl carboxylate- $\epsilon$ -caprolactone (BCL) monomer; ii) ring opening polymerization of BCL using dihydroxy PEG as initiator, leading to the formation of poly( $\alpha$ -benzyl carboxylate- $\epsilon$ -caprolactone)-*b*-PEO-*b*-poly( $\alpha$ -benzylcarboxylate- $\epsilon$ -caprolactone) (PBCL-*b*-PEG-*b*-PBCL) triblock copolymers; iii) partial (27, 50, or 75%) or complete debenzoylation of triblock copolymer leading to the preparation of poly[( $\alpha$ -carboxyl- $\epsilon$ -caprolactone)-co-( $\alpha$ -benzylcarboxylate- $\epsilon$ -caprolactone)]-*b*-PEG-*b*-poly[( $\alpha$ -carboxyl- $\epsilon$ -caprolactone)-co-( $\alpha$ -benzylcarboxylate- $\epsilon$ -caprolactone)] (PCBCL-*b*-PEG-*b*-PCBCL) and poly( $\alpha$ -carboxy- $\epsilon$ -caprolactone)-*b*-PEG-*b*-poly( $\alpha$ -carboxy- $\epsilon$ -caprolactone) (PCCL-*b*-PEG-*b*-PCCL), respectively.

Synthesis of benzyl substituted monomer is described in detail in our previous publication [19]. Briefly, BCL was synthesized by anionic activation of  $\epsilon$ -caprolactone (3.1 mL) and further treatment with benzyl chloroformate (4.3 mL). Successful substitution of benzyl carboxylate on the  $\epsilon$ -caprolactone monomer was evidenced by  $^1\text{H}$  NMR spectroscopy. Ring-opening polymerization of BCL (1 g) with hydroxy PEG as initiator (0.5 g) and stannous octoate (16 mg) as catalyst was used to prepare PBCL-*b*-PEG-*b*-PBCL. The obtained PBCL-*b*-PEG-*b*-PBCL triblock copolymer was dissolved in tetrahydrofuran (THF) and then precipitated using anhydrous ethyl ether. The mixture was centrifuged and the supernatant was discarded. Polymer was washed three times by dissolving the precipitate in

THF and repeating the above procedure. The percentage of  $\alpha$ -benzyl carboxylate- $\epsilon$ -caprolactone conversion to PBCL-*b*-PEG-*b*-PBCL was determined comparing the degree of polymerization of PBCL-*b*-PEG-*b*-PBCL measured by  $^1\text{H}$  NMR to the theoretical degree of polymerization. The molar ratio of PEG to catalyst was changed from 2.6:1 to 6.4:1 to optimize the reaction condition further. Partial catalytic debenylation of PBCL-*b*-PEG-*b*-PBCL at different degrees was accomplished using different palladium concentrations ranging from 0 to 10 wt. % on activated charcoal. This led to the production of PCBCL-*b*-PEG-*b*-PCBCL with 27, 50, or 75% of the benzyl groups on PBCL reduced to carboxyl groups. Complete debenylation of 1 g of PCBCL-*b*-PEG-*b*-PCBCL was accomplished with 140 mg of palladium on activated charcoal. Overall, five different block copolymers (characteristics summarized in Table 1) were synthesized and used for further studies.

### 2.3 Characterization of prepared tri block copolymers

$^1\text{H}$  NMR spectroscopy of polymers in  $\text{CDCl}_3$  as solvent was used to study the composition of copolymers. The degree of polymerization for PBCL-*b*-PEG-*b*-PBCL, was identified by comparing peak intensity of  $\text{CH}_2\text{-O-}$  ( $\delta=4.1$  ppm) to the methylene protons of the benzyl carboxylate group ( $\delta=5.15$ ). Percentage of conversion was calculated using the following equation:

$$\text{Conversion (\%)} = \frac{\text{Degree of Polymerization of PBCL-}b\text{-PEO-}b\text{-PBCL from H NMR}}{\text{Theoretical degree of Polymerization of PBCL-}b\text{-PEO-}b\text{-PBCL}} \times 100$$

MALDI-TOF was used to determine the molecular weight and degree of polymerization of synthesized copolymers. 2, 5-dihydroxybenzoic acid (DHB) was used as the matrix, and the polymer samples were dissolved in methanol at a concentration of 5 mg/mL. Sodium chloride (2 mg/mL in methanol) was used as the cationization agent.

Solutions of polymer, matrix, and salt were mixed in a 2:2:1 volume ratio (polymer: matrix: salt) and the mixture was thoroughly vortexed. The sample mixture was then added on a stainless steel target plate and the spots were dried at room temperature prior to insertion into the instrument.

#### **2.4. Characterization of the self-assembly of block copolymers**

Self-assembly of block copolymers was accomplished by direct addition of copolymers to water at a polymer concentration of 1, 2 or 5 mg/mL. For PBCL-b-PEG-b-PBCL block copolymers that did not have any carboxyl groups, the polymer concentration was reduced to 0.5 mg/mL to avoid precipitation. Size of assembled structures at room temperature was measured by dynamic light scattering technique using a MALVERN Nano-ZS90 ZETA-SIZER (Malvern Instruments Ltd., Malvern, U.K). A change in the fluorescence excitation spectra of pyrene in the presence of varied concentrations of block copolymers was used to measure the critical micellar concentration (CMC) of block copolymers in distilled water and phosphate buffer (10  $\mu$ M) with different pHs (4.0, 7.4, and 9.0). Pyrene was dissolved in acetone and added to 5 mL volumetric flasks to provide a final concentration of  $6 \times 10^{-7}$  M. Acetone was then evaporated and replaced with the aqueous polymeric micellar solution in a concentration range of 0.05 to 1000  $\mu$ g/mL. Samples were heated at 65 °C for an hour, cooled to room temperature overnight, and deoxygenated with nitrogen gas prior to fluorescence measurements. The excitation spectra of pyrene for each sample were obtained at room temperature using a Varian Cary Eclipse fluorescence spectrophotometer (Victoria, Australia). The emission wavelength and excitation/emission slit were set at 390 and 5 nm, respectively[19]. The intensity ratio of peaks at 338 nm to those at 333 nm was plotted against the logarithm of copolymer concentration. The CMC was measured from a sharp rise

in intensity ratios ( $I_{338}/I_{333}$ ) at the onset of micellization. The measurement was repeated for three different samples to obtain average CMC.

## **2.5 Assessing the effect of temperature on the self-assembly of triblock copolymers**

The change in the Z average diameter of self-assembled structures as a function of increasing temperature (between 25-55°C) for all block copolymers under study at a polymer concentration of 1 mg/mL was assessed using ZETA-SIZER (Malvern Instruments Ltd., Malvern, U.K). The pH of medium was adjusted to 4.5 by addition of a few drops of HCl 0.05 M. For block copolymers having 27 and 50 % carboxyl substitution, this experiment was repeated at polymer concentrations of 1, 2, and 5 mg/mL. The experiments were repeated for three samples. Changes in micellar size for different block copolymers and/or different polymer concentrations were plotted against temperature and the resulting graphs were used to calculate the temperature for the onset of micellar size change.

## **2.6 Assessing the effect of pH on the self-assembly of triblock copolymers**

The change in the average diameter of self-assembled structures as a function of pH (pHs of 3.0, 4.5, 7.0, and 9.0) at different temperatures (25-55°C) was investigated at a polymer concentration of 1 mg/mL, using ZETA-SIZER (Malvern Instruments Ltd., Malvern, U.K). The pH of the aqueous solution of triblock copolymer was changed to acidic or basic pH by adding 1 N HCL or 1% v/v triethylamine, respectively, as needed. The experiment was repeated for three different samples.

## 2.7. Statistical Analysis

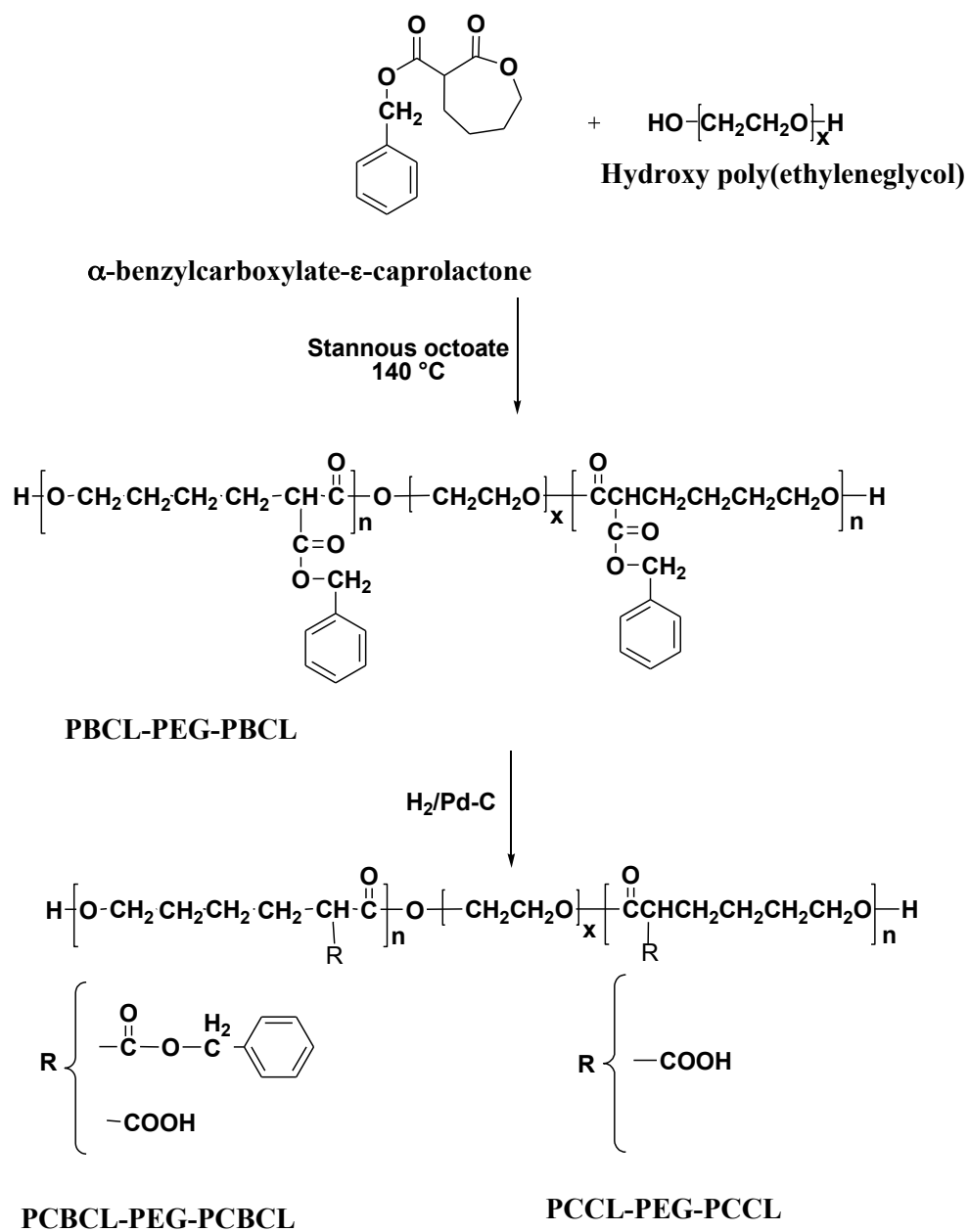
The significance of differences between results was assessed by conducting one-way ANOVA analysis followed by Tukey test, where  $\alpha=0.05$  was set as the level of significance. Curve fitting was conducted by standard curve analysis using Sigmaplot 11.0 software.

## 3. Results

### 3.1. Synthesis and characterization of triblock copolymers

To optimize the polymerization of BCL with dihydroxy PEG, different molar ratios of PEG to catalyst were applied in the ring opening polymerization while the ratio of monomer to PEG was kept constant. Optimum conversion of BCL to PBCL was achieved at a PEG/catalyst molar ratio of 5.8:1. Therefore, this ratio was selected to prepare the triblock copolymers for further studies. This step was followed by the debenylation of PBCL-*b*-PEG-*b*-PBCL block copolymers at different degrees using palladium on activated charcoal at 0 to 14 wt %. The number-average molecular weight of prepared block copolymers was determined from their  $^1\text{H}$  NMR spectra, comparing peak intensity of PEG (-CH<sub>2</sub>CH<sub>2</sub>O-,  $\delta=3.65$  ppm) to that of PCL backbone (-OCH<sub>2</sub>-,  $\delta=4.05$  ppm) using a  $1450\text{ g mol}^{-1}$  molecular weight for PEG (Figure 2-1). The molecular weights, for different block copolymers as determined by  $^1\text{H}$  NMR were in good agreement with the theoretical molecular weights of the prepared block copolymers (Table 2-1).





Scheme 0-1 Synthesis of triblock copolymers

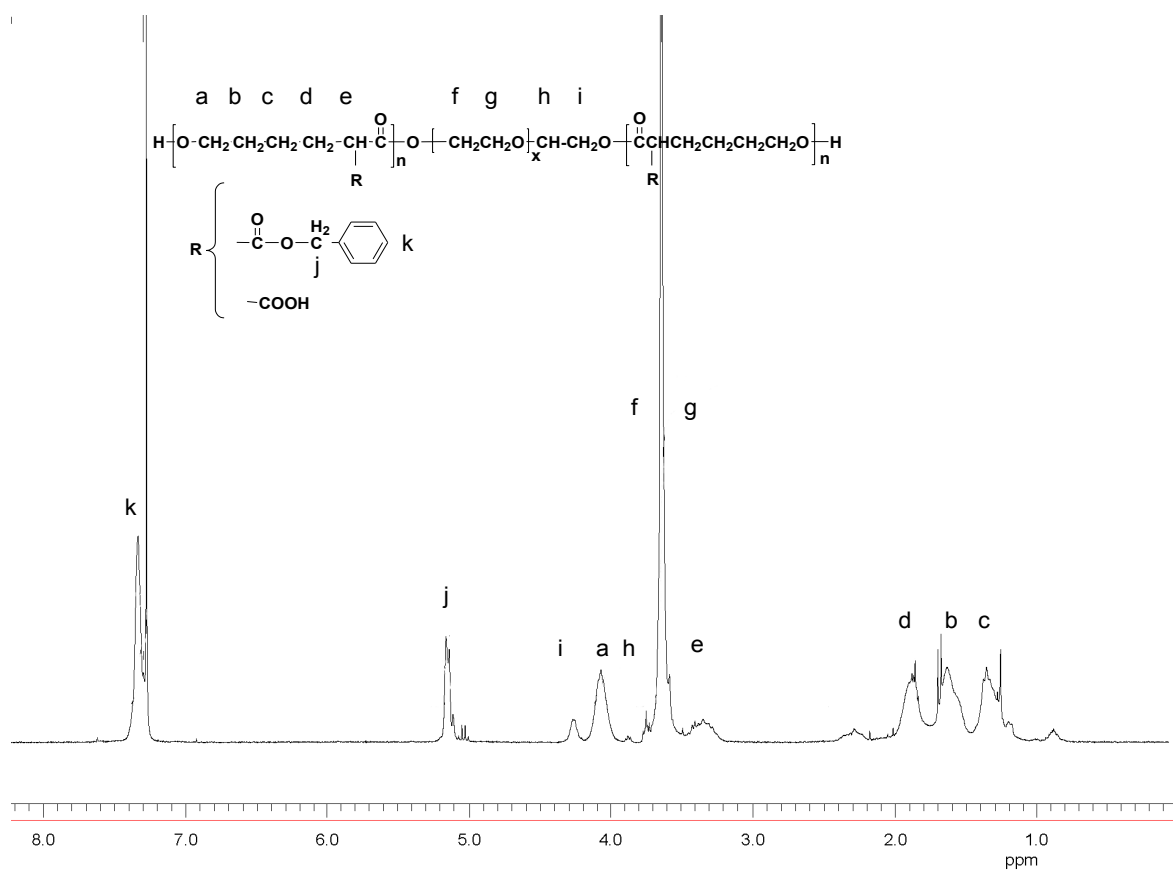


**Figure 0-1**  $^1\text{H}$  NMR spectrum of PCBCL-PEG-PCBCL block copolymers and peak assignments

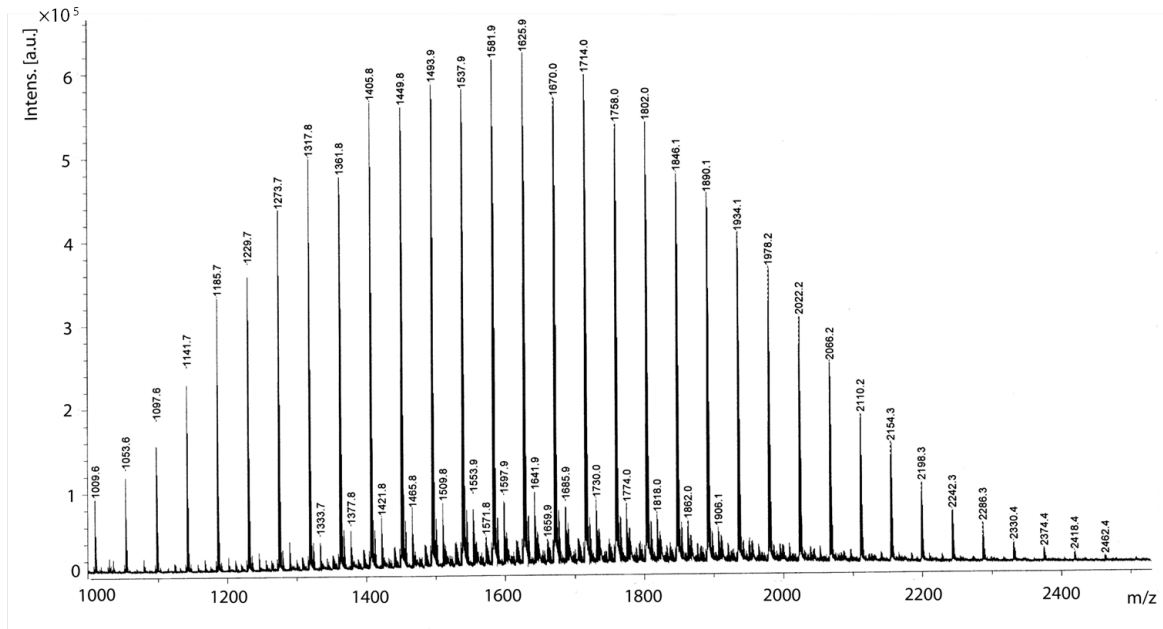
**Table 0-1** Characteristics of the synthesized triblock copolymers

Polymer	Percent of Reduction <sup>a</sup>	Theoretical Mw (g/mol)	Mn <sup>b</sup>	Mn <sup>c</sup>	Degree of polymerization <sup>b</sup>		Degree of polymerization <sup>c</sup>	
					CCL Block	BCL Block	CCL Block	BCL Block
PBCL-PEG-PBCL	0	4428	3683	3435	N/A	9.0	N/A	8
PCBCL-PEG-PCBCL	27	4136	3506	3503	1.9	7.1	2	7
PCBCL-PEG-PCBCL	50	3887	3206	-----	4.3	4.4	4	-----
PCBCL-PEG-PCBCL	75	3618	3303	-----	8.0	2.0	8	-----
PCCL-PEG-PCCL	100	3350	2367	2240	5.8	N/A	5	N/A

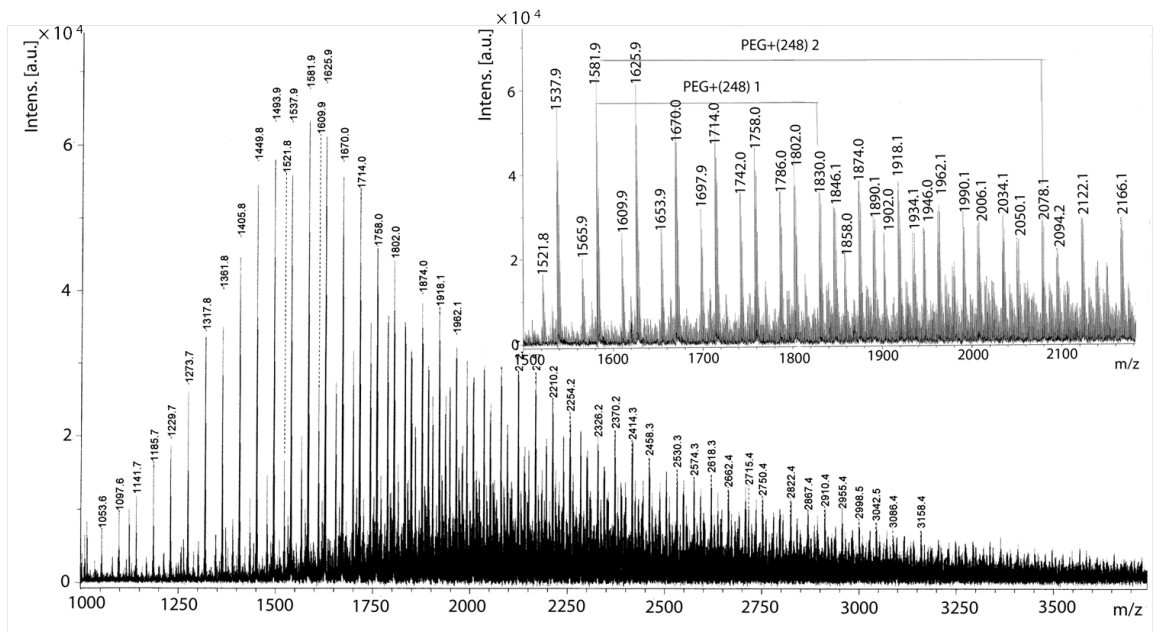
<sup>a</sup> The number shown indicates the percent of debenylation (reduction of benzylcarboxylate to carboxyl groups) in each block copolymer determined by  $^1\text{H}$  NMR spectroscopy. <sup>b</sup> Number average molecular weight measured by  $^1\text{H}$  NMR. <sup>c</sup> Number average molecular weight measured by MALDI-TOF. N/A (not applicable)

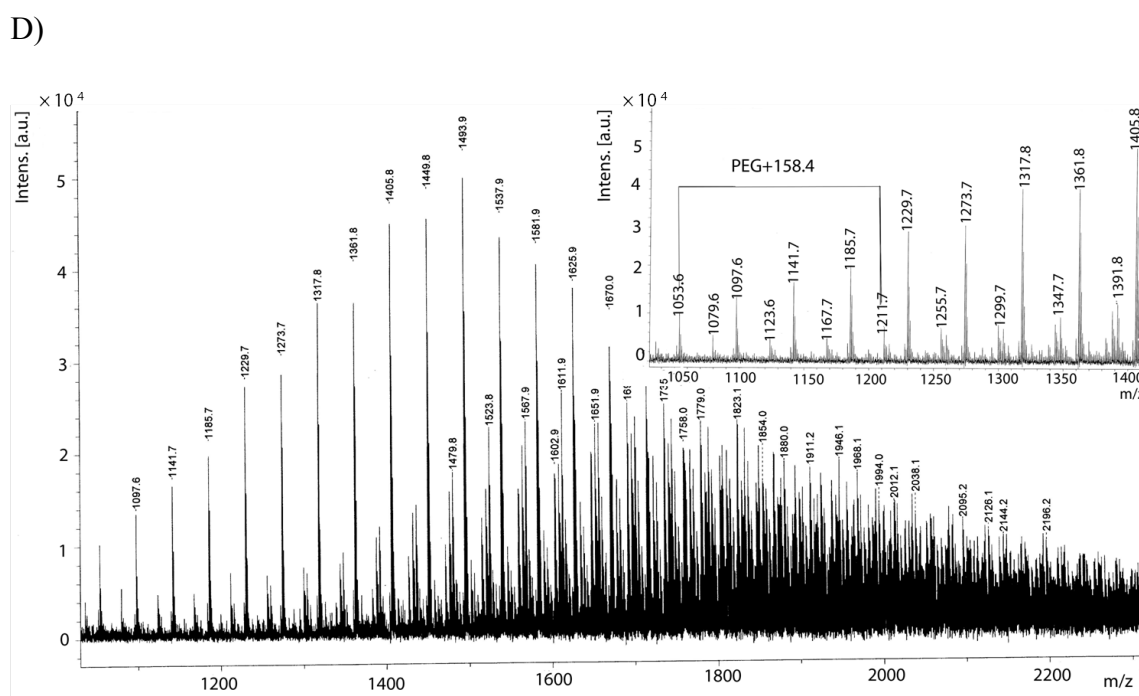
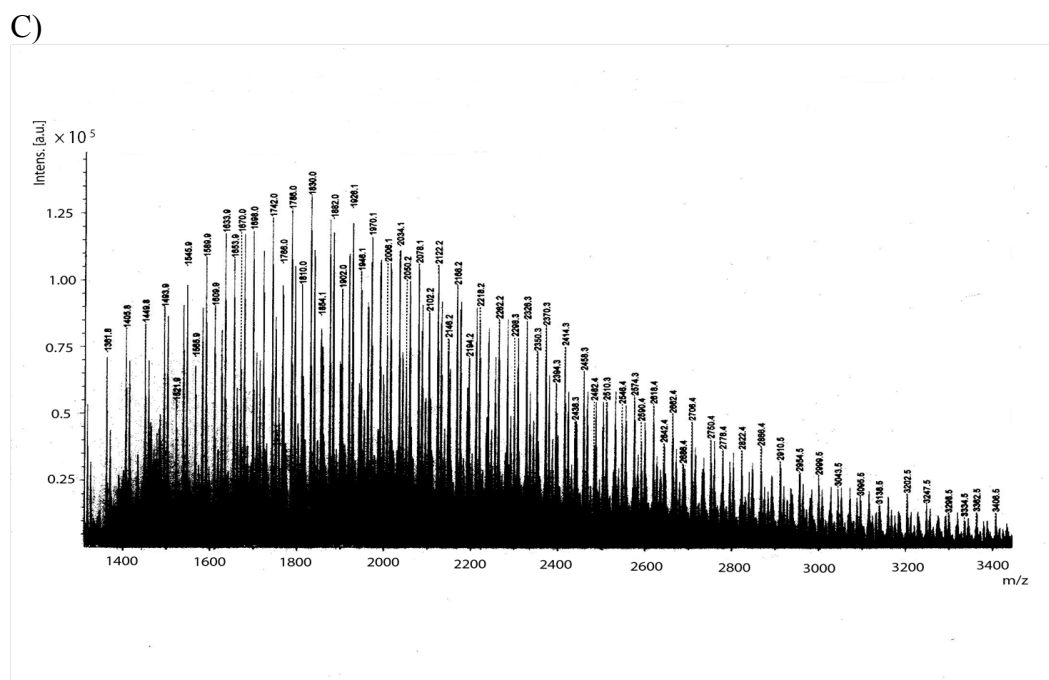
The molecular weight of synthesized copolymers was also determined by MALDI-TOF. 2,5-dihydroxybenzoic acid (DHB) matrix with sodium chloride as a cationization agent was selected for the analysis. The peaks corresponding to each block series observed in the MALDI mass spectra of tri block copolymers were compared with the MALDI mass spectrum of PEG (Figure 2-2A). In the spectra related to triblock copolymers, peaks related to the hydrophobic block containing BCL and CCL units show a peak-to-peak increment of 248 and 158 (Figure 2-2), after subtraction of PEG and sodium cation mass. These numbers correspond to the mass of BCL and CCL, respectively (see windows in Fig 2-2B, and 2-2F, respectively). The spectra of incompletely debenzylated copolymers (Figure 2-2C-E) show polydisperse samples. The peak intensity decreased with increasing  $m/z$  values until the signal was indistinguishable from the baseline at approximately  $m/z$  3200 Da. Due to the rather broad molar mass distribution, there were mass discrimination effects causing a decrease in detection response at higher masses. Lighter molecules are preferentially desorbed and ionized in the MALDI process, suppressing desorption and ionization of higher molar mass molecules [20]. The comparison of the result of molecular weight and degree of polymerization obtained by the  $^1\text{H}$  NMR and MALDI-TOF methods are summarized in Table 2-1. The results were comparable to their respective nominal molecular weights (Table 2-1).

A)



B)





### 3.2. CMC determination

The CMC of block copolymers under study in distilled water, and buffer (pH 4.0, 7.4, and 9.0) was determined by fluorescence spectroscopy, using pyrene as a fluorescence probe, at 25°C (Table 2-2). Prepared block copolymers with no or partial debenzoylation showed low CMC values ranging between 0.34-1.18 µg/mL in water and 0.65-1.72 µg/mL in phosphate buffer (pH 7.4). As expected, a direct relationship between the level of debenzoylation and CMC of block copolymers was observed, where polymers with high level of carboxyl group on the hydrophobic block showed higher CMCs. The CMC of block copolymer with 100 % debenzoylation was 12.51 µg/mL in water. The CMC for 50% debenzoylated block copolymer decreased by changing the pH from basic to acidic (Figure 2-5B), perhaps as a result of deionization of carboxyl group on hydrophobic block leading to higher tendency for self-assembly of block copolymers indicated by a decrease in CMC. On the other hand, copolymer without any carboxyl group showed no significant change in CMC value at different pHs. The CMC of copolymers with 27 % carboxyl groups showed a decreasing trend when pH was changed from basic to acidic, although it was statistically not significant (P=0.08, paired students' t test).

**Table 0-2. Characterization of the self- assembly of different triblock copolymers under study**

Percentage of Debzoylation	CMC ± SD (µg/mL) <sup>a</sup> In water	CMC ± SD (µg/mL) <sup>b</sup> pH 7.4	Size ± SD (nm) pH 4.5	Temperature for onset of micellar size change <sup>d(°C)</sup>	pH of onset of micellar size change <sup>e</sup>
0	0.34±0.04	0.65±0.03	284.3±8.4 <sup>c</sup>	N/A	N/A
27	0.65±0.07	0.90±0.1	42.2±2.5 <sup>d</sup>	29	4.5
50	0.86±0.05	1.41±0.13	52.4±1.2 <sup>d</sup>	32	4.5
75	1.18±0.09	1.72±0.044	65.4±1.3 <sup>d</sup>	36	4.5
100	12.5±0.17	----	139±4.3 <sup>d</sup>	32	----

<sup>a</sup> determined at room temperature (25°C), in water; <sup>b</sup> determined at room temperature, at phosphate buffer (10µM, pH 7.4); <sup>c</sup> determined at a polymer concentration of 0.5 mg/mL and pH=4.5; <sup>d</sup> determined at a polymer concentration of 1 mg/mL and pH=4.5; <sup>e</sup> determined at room temperature and a polymer concentration of 1 mg/mL; NA (Not applicable); SD (Standard deviation of repeat or size distribution, n=3)

### 3.3. Thermo-responsive size change of polymeric micelles

The average aggregate size (*Z* average) for the synthesized copolymers containing both carboxyl and benzyl carboxylate groups on their hydrophobic block (measured at room temperature and pH 4.5) varied between 42.2 to 65.4 nm (Table 2-2). Polymers with 100 % carboxyl groups (no benzyl groups) on the PCL block formed particles of 139 nm under the same conditions (measured at room temperature and pH 4.5). Triblock copolymers of PBCL-*b*-PEG-*b*-PBCL, that had no carboxyl but 100 % benzyl carboxylate groups on the PCL backbone, formed large particles (284.3 nm) under the same self-assembly condition. The micellar size change as a function of temperature for this polymer was assessed at a lower concentration (0.5 mg/mL), due to solubility problems.

With an increase in temperature, sigmoidal changes ( $r^2 > 0.98$ ) in the micellar size were noticed for all block copolymers under the study conditions (pH=4.5) (Figure 2-3 B-E). The only exception was the polymer with no carboxylic group, i.e., PBCL-*b*-PEG-*b*-PBCL, for which the correlation to sigmoidal curve was lower ( $r^2=0.65$ ) (Figure 2-3A). The average diameter of self-assembled structures for 50, 75 and 100 % debenzylated copolymers at pH 4.5 showed a sigmoidal decrease as temperature increased (Figure 2-3 C-E). In contrast, under identical conditions, the 27 % debenzylated copolymer showed a sigmoidal increase in micelle size as the temperature was increased (Figure 2-3B). The onset of micellar size change for 27, 50, 75 and 100 % debenzylated polymer was calculated at 29, 32, 36 and 32 °C, respectively.

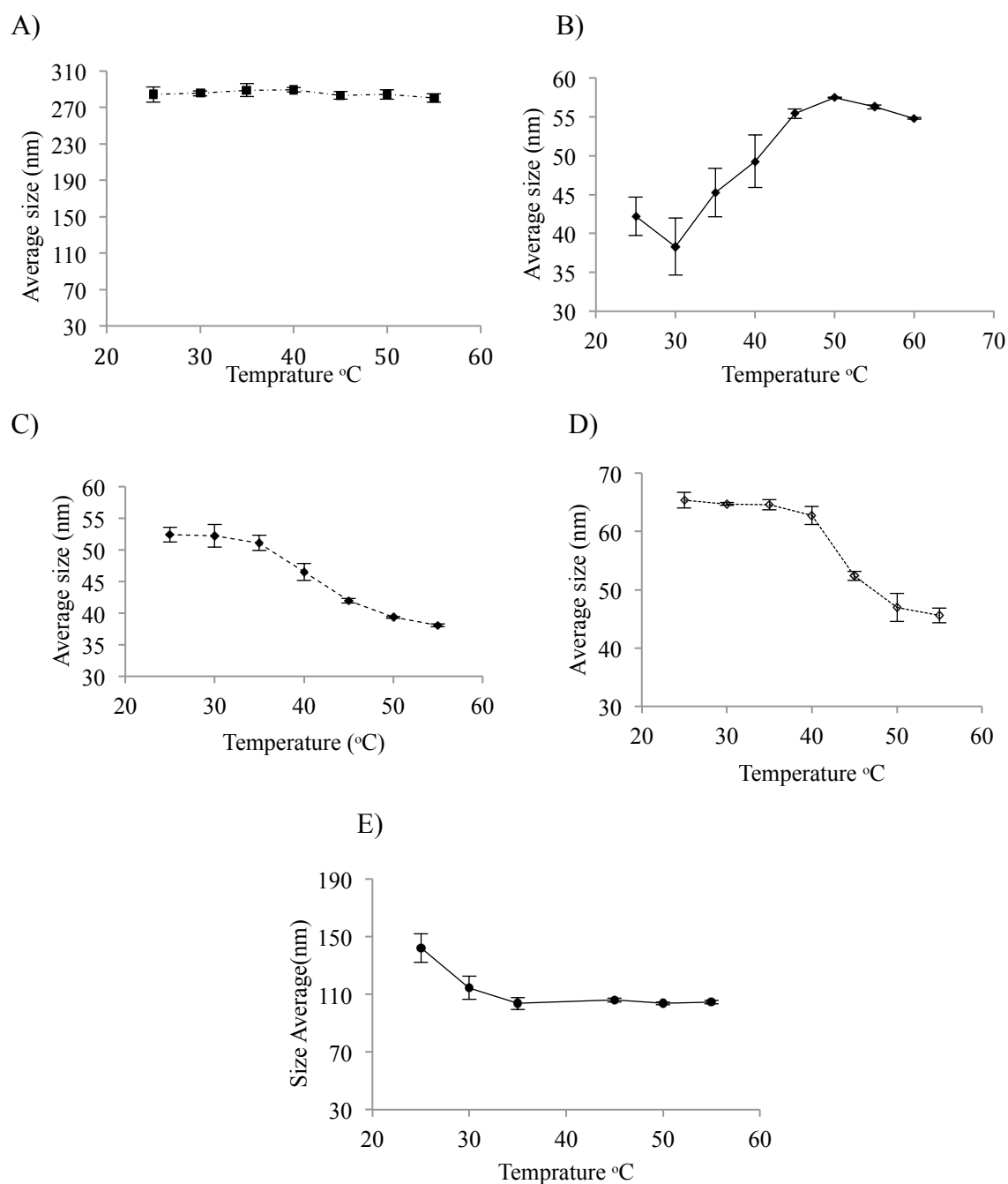


**Figure 0-3. Micellar size change of A) 0, B) 27, C) 50, D) 75, and E) 100% debenzylated block copolymers as a function of temperature assessed for a polymer aqueous solution at 1 mg/mL concentration at pH=4.5 (n=3)**

The effect of polymer concentration on thermo-responsive self-assembly of block copolymers with 27 and 50 % debenzylation in aqueous media (pH=4.5) was investigated using DLS, as well. Figures 2-4 A and B show the thermoresponsive micellar size change of



27 and 50 % debenzylated block copolymers as a function of polymer concentration, respectively. The direction of change in the size of self-assembled structures for both polymers was not affected by polymer concentration. It can also be seen that by increasing the concentration, the thermoresponsive increase in size for self-assembly of 27 % debenzylated polymer became more noticeable. At 1 mg/mL polymer concentration, an increase of 14 nm is observed between self-assembled structures formed at 25 °C compared to those at 55 °C ( $P < 0.01$ , paired students' t test). For polymer concentrations of 2 and 5 mg/mL this difference in size is raised to 29 and 59 nm, respectively. The temperature for the onset of size change in case of the 27 % debenzylated polymer was also reduced from 29 to 26°C as the polymer concentration was raised from 1 to 5 mg/mL. This trend was not observed for triblock copolymers with 50 % debenzylation (Figure 2-4B). The latter copolymer solution became turbid when the temperature was increased, at a polymer concentration of 5 mg/mL.

### **3.4. pH-sensitive assembly of block copolymers**

The pH-sensitivity of the self-assembly process was examined by measuring particle size change as a function of pH using DLS. Figure 2-5 demonstrates that at room temperature polymeric micelles of copolymers with different carboxylic content show significant reduction in size as pH is lowered to 4.5 from 3.0, while micelles made of copolymer with no carboxyl group showed negligible size change as a function of pH. Above pH 4.5, the micellar size at room temperature was stable and remained constant for carboxyl- containing block copolymers, independent from the level of carboxyl group substitution.

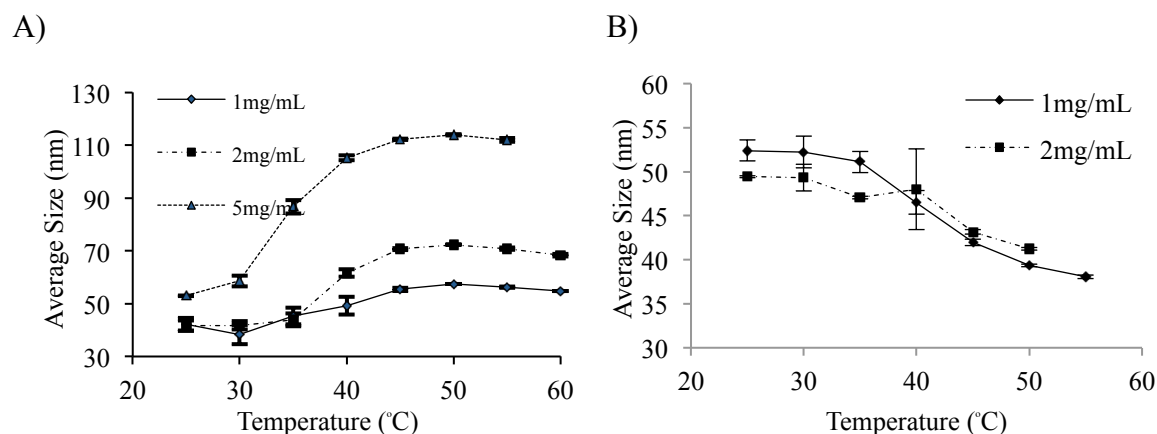


**Figure 0-4. Micellar size change as a function of temperature for different concentrations of A) 27 % and B) 50 % debenzylated PCBCL-*b*-PEG-*b*-PCBCL aqueous solutions at pH 4.5 (n=3)**

Thermo-responsive behavior of polymeric micelles at different pHs (pH 4.5, 7.0 and 9.0) was assessed for each copolymer by increasing the temperature (Figure 2-6). Micellar size change for 27, 50, and 75 % debenzylated block copolymers followed the same trend at pH 7.0 and 9.0 as what was previously observed for pH 4.5, where an increase in size was observed for 27 % debenzylated polymer and a decrease in size was observed for 50 and 75 % debenzylated polymers as a function of rising temperature. The 27% debenzylated block copolymer showed an increase in micellar size from 55.7 to 86.9 nm at pH 7.0 as the temperature was raised. The same block copolymers showed an increase in micellar size from 41.2 to 61.5 nm at pH 9.0. The increase in micellar size for pH values of 4.5 and 9.0 was about 14 and 20 nm, respectively. This difference in size was about 30 nm at pH 7.0. Temperature-dependent reduction in size for 50 and 75% debenzylated block copolymers was more extensive at pH of 4.5 than at pH 7.0 or pH 9.0.

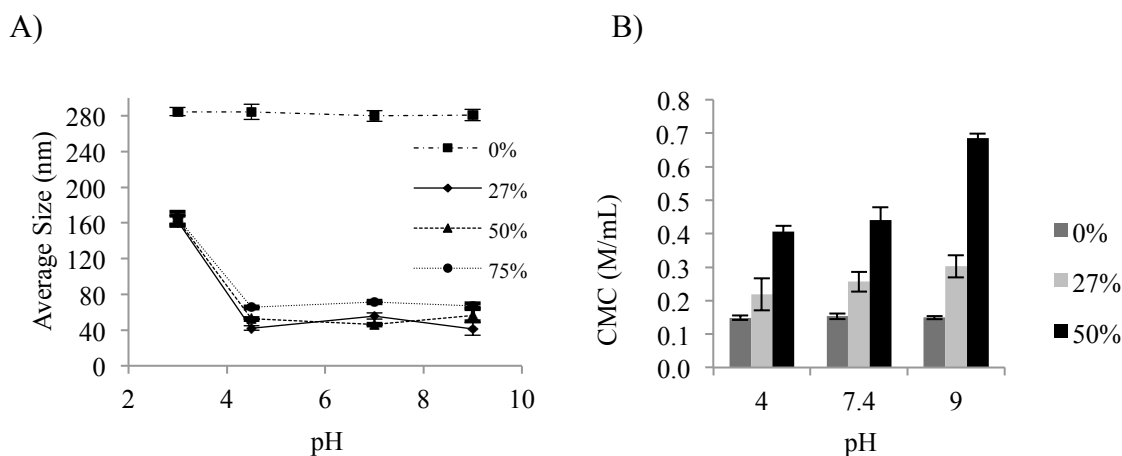


**Figure 0-5. Micellar size change for block copolymers having different degrees of debenzylation. B) Changes in CMC values of block copolymers, as a function of pH at room temperature (n=3)**

#### 4. Discussion

The main objective of this study was to investigate the potential of triblock copolymers based on PEG and functionalized PCL for the formation of thermo and/or pH responsive micelles and gels. To this end, a series of novel triblock copolymers composed of PEG in the middle and PCL as lateral blocks, containing benzyl carboxylate, carboxyl or a mixture of the two on the  $\alpha$ -carbon of  $\epsilon$ -caprolactone units, were successfully synthesized. The synthesis of polymers was carried out first, through ring opening polymerization of BCL, using dihydroxy PEG as an initiator and stannous octoate as a catalyst. To achieve the optimum yield, the molar ratio of PEG:catalyst was varied during the polymerization reaction, and the optimum conversion occurred at a PEG:catalyst molar ratio of 5.8:1. While lower catalyst concentrations led to incomplete conversion of monomer, at higher catalyst concentrations an organogel was formed. Theoretically, in the absence of any competing initiator, a dihydroxy

PEG to catalyst molar ratio of 1:1 should yield 100 % conversion of monomer within 50 min at 130 °C [21, 22]. A higher molar ratio of initiator to catalyst (i.e., lower catalyst concentrations) was needed in this study for 100 % conversion of BCL monomer to PBCL within 24 h for the preparation of PBCL-PEG-PBCL. This may be attributed to the longer reaction time used here, which is an appropriate condition for undesirable side reactions during the polymerization reaction (e.g., chain back biting or inter-chain trans-esterification reactions), leading to the formation of organogel-forming polymers at higher catalyst concentrations. The presence of two carboxyl groups in the case of  $\alpha$ -benzyl carboxylate- $\epsilon$ -caprolactone, providing additional electrophilic groups for the attack of the initiator, might have also contributed to this observation. On the other hand, an excess amount of initiator in the reaction (PEG:catalyst >5.8:1) may lead to incomplete copolymerization and/or formation of shorter copolymers than what expected because of the generation of less active initiator chain ends. [22] Further studies assessing the kinetics of polymerization at different PEG:catalyst ratios are needed to find the optimum reaction time and catalyst concentration that can minimize the chance of side reactions while maximizing the percentage of monomer to polymer conversion, leading to the preparation of more monodisperse polymers.

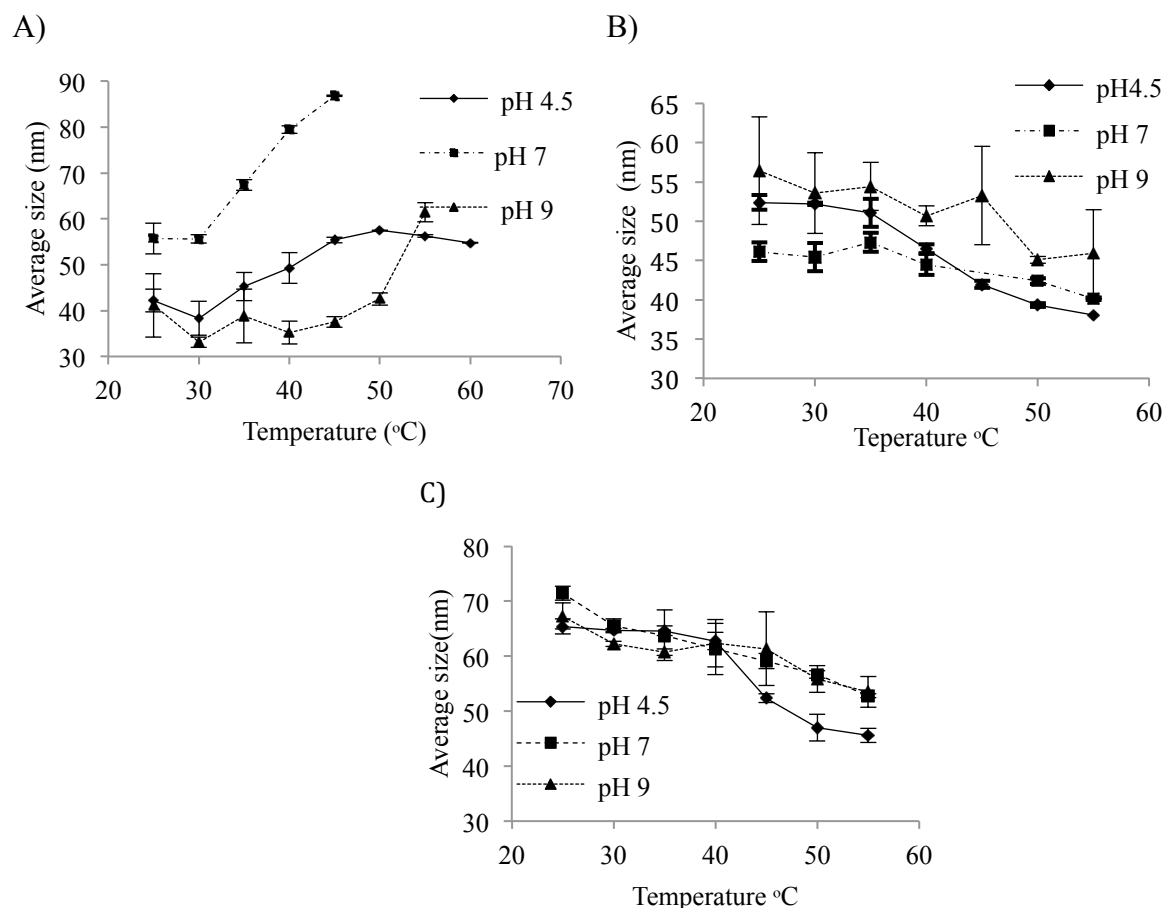


**Figure 0-6** The effect of pH on thermoresponsive changes in the size of micelles for A) 27%, B) 50 % and C) 75% debenzylated PCBCL-*b*-PEG-*b*-PCBCL block copolymers. Polymer concentration was 1 mg/mL (n=3).

In the second step, the PBCL-*b*-PEG-*b*-PBCL block copolymer was completely or partially debenzylated. The percentage of debenzylation was controlled by adjusting the amount of catalyst in the debenzylation reaction. The molecular weight and degree of polymerization of synthesized block copolymers calculated using  $^1\text{H}$  NMR spectra (Figure 2-1) were consistent with the results obtained by MALDI-TOF (Figure 2-2) and similar to what is predicted theoretically (Table 2-1). This shows the reliability of these two methods for

estimating molecular weight as well as degree of polymerization. The results of MALDI-TOF also revealed a relatively high polydispersity of the prepared polymers.

The micelle formation of block copolymers in an aqueous media was assessed by CMC measurement. The values are low for all of the block copolymers, indicating that micelles formed from triblock copolymers are thermodynamically stable. The hydrophilic/lipophilic balance (HLB) of triblock copolymers can be controlled by changing the percentage of debenzoylation of the polymers, and the PEG:PCBCL molar ratios. At a constant PEG:PBCL molar ratio, a higher degree of debenzoylation lead to an increase in the HLB of polymers. In the current study, an increase in the HLB of our triblock copolymers, introduced by an increase in the level of carboxyl groups on the hydrophobic block, led to an increase in the CMC of block copolymers, reflecting a reduction in their thermodynamic stability as a function of the degree of polymer debenzoylation (Table 2-2). Moreover, change in the percentage of carboxyl group on the polymer backbone resulted in a pH dependent change in CMC of block copolymers. Block copolymers containing carboxyl groups on their structure showed an increase in CMC as a result of an increase in pH of the media. In contrast, the copolymer without carboxyl group in its structure did not show any change in its CMC (Figure 2-5B). The higher CMC values at basic pHs reflect the ionization of COOH groups leading to an increase in HLB of copolymers. A positive correlation between CMC value and degree of COOH substitution on the polymeric backbone at all pHs under study, also confirms this explanation.

For ABCs containing carboxyl groups on their hydrophobic block, a direct relationship between the size of self-assembled structures and the number of carboxylic groups of the

block copolymers was observed (Table 2-2). This can be attributed to the presence of water clustering around carboxylic groups in the assembled structures and/or aggregation of micelles introduced by hydrogen bonds between COOH groups on different polymer chains. The PBCL-*b*-PEG-*b*-PBCL copolymer, on the other hand, formed the largest particle size. This could imply inter-micellar hydrophobic interactions between PBCL chains, resulting in the formation of planar association [23].

In further studies, the potential use of these block copolymers in thermo and pH responsive self-assembly was assessed. Block copolymers containing  $\geq 50$  % carboxyl groups on their hydrophobic block (50, 75 and 100 % debenzylated polymers) showed a decrease in the size of their assembled structures as a result of an increase in temperature (Figure 2-3 C-E). Block copolymers with complete debenzylation (100%), containing the highest amount of carboxylic groups on the caprolactone chain, showed the sharpest decrease in the micelle size as temperature was increased (Figure 2-3E). This observation may be attributed to the release of water clusters from the micellar structure and/or breakdown of hydrogen bonds between COOH groups on different polymer chains, leading to the dissociation of polymer aggregates at higher temperatures (Figure 2-7A). Both possibilities are introduced by a high COOH content on the PCBCL block. Further studies are needed to clarify the mechanism behind this observation.

Micellar size for polymers without carboxyl groups, i.e., PBCL-*b*-PEG-*b*-PBCL, showed a decreasing trend in size as temperature was raised. However, the decrease in size was not as pronounced as the previous structures (Figure 2-3A). On the other hand, the copolymer with 27% carboxyl groups on its hydrophobic block showed the opposite behavior, an increase in micellar size as a function of a rise in temperature (Figure 2-3B). The

temperature for the onset of micellar size increase for 27 % debenzylated polymer was about 29° C at low polymer concentrations (1 mg/mL). When the polymer concentration was raised to 5 mg/mL, the onset of micellar size increase was reduced to 26 ° C (Figure 2-4 A). For block copolymers containing 27 % carboxyl groups on their PCBCL block, the release of water molecules from the core at increased temperatures may lead to inter-micellar hydrophobic interactions and the formation of larger aggregates [24] (Figure 2-7 B). This explanation is in line with our observations regarding the effect of polymer concentration on temperature-induced micellar size change. At higher polymer concentrations the chance of micellar interaction and aggregation will be enhanced, leading to the formation of larger aggregates and reduced transition temperatures. Temperature induced association of micelles may lead to the formation of thermo-reversible gels that are liquid at lower temperatures, but form gels at higher temperatures. A similar phenomenon has been reported for PEG-*b*-poly(lactide glycolide)-*b*-PEG (PEG-*b*-PLGA-*b*-PEG), where an increase in polymer concentration leads to an enhanced chance of micellar association [25-27]. For pharmaceutical application as injectable implants, it is advisable that the onset of micellar association and gel formation be a few degrees below physiological temperature, which is what we have observed for the 27 % debenzylated polymer in this study [28].



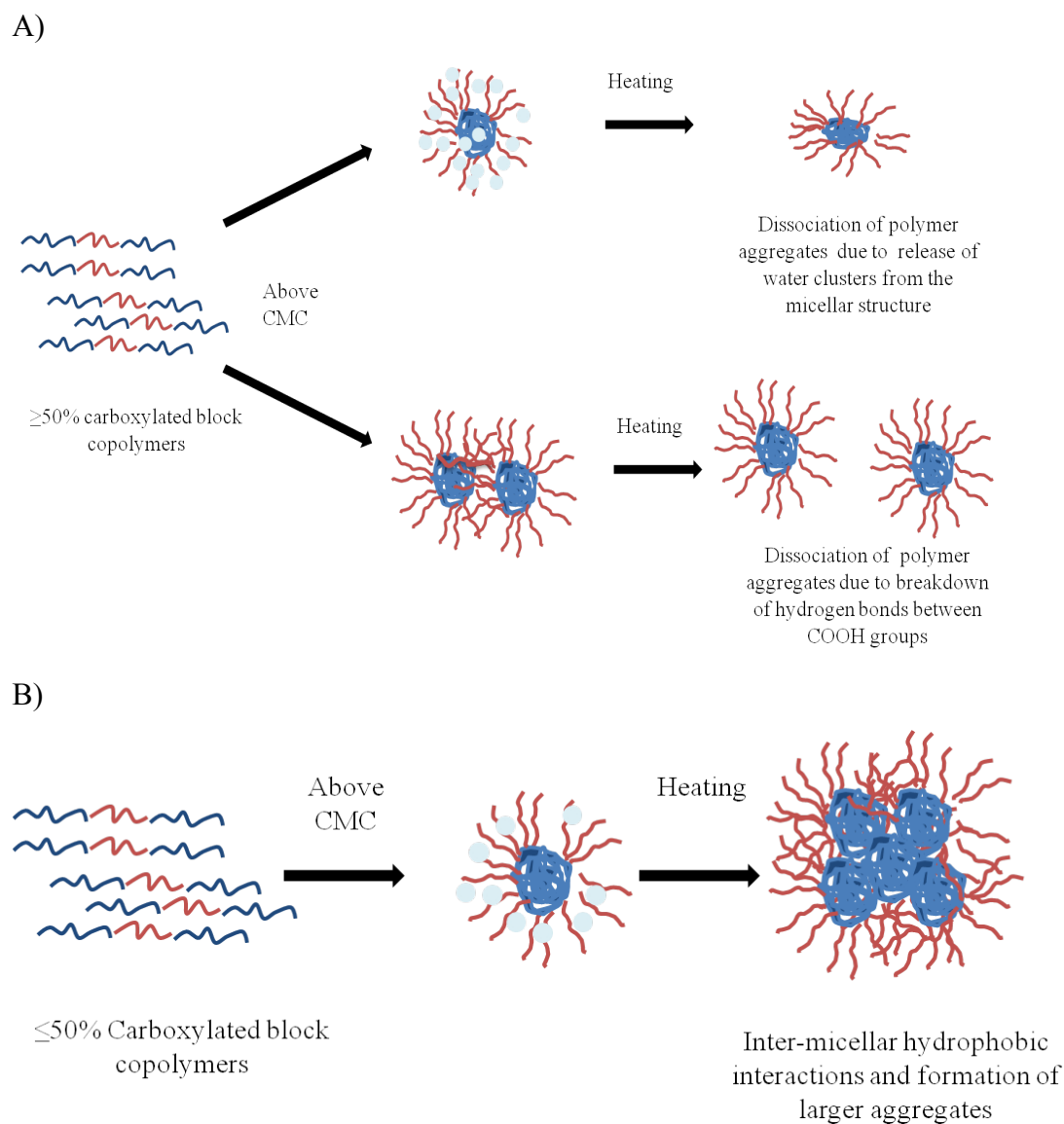


**Figure 0-7 Proposed mechanisms for thermo-responsive aggregate size change for different block copolymer structures under study**

Conversion of  $\alpha$ -benzyl carboxylate to a carboxyl group on the caprolactone chain introduced pH responsiveness into the block copolymers (Figure 2-5). By decreasing the pH of polymeric solutions to below 4.5, which is near the  $PK_a$  of carboxyl groups, the

equilibrium shifts towards their un-ionization. This will induce higher hydrophobicity to the PCBCL block and a tendency for inter-micellar hydrophobic interactions of these blocks, leading to micellar size increase. In this study, this trend was similar for all block copolymers that contained carboxyl groups on their structure. For polymeric micelles with no carboxyl group (i.e., PBCL-*b*-PEG-*b*-PBCL), on the other hand, no significant change in the size of aggregates was observed at different pHs, indicating the necessity for carboxylic groups on the polymer chain for pH- sensitivity.

The pH sensitivity of the self-assembly process as a function of temperature increase was then assessed. At pH 3.0, when the temperature was increased, the micellar solutions became turbid. This could have been caused by un-ionization of carboxylic groups; increased hydrophobicity of the PCBCL block in structures under study, followed by hydrophobic interaction between micelles at higher temperatures, leading to the formation of large aggregates, and/or precipitation of the polymer chains or aggregates out of the aqueous solution.

Polymeric micelles made from 27, 50 and 75 % debenzylated copolymers showed a similar trend in thermo-responsive behavior at pH 7.0 and 9.0 to what was observed at pH 4.5, an increase in the size of polymer aggregates for 27 % debenzylated polymer and a decrease in aggregate size for 50 and 75 % debenzylated polymers as a function of temperature increase (Figure 2-6 A-C). For 50 and 75 % debenzylated polymers the decrease in aggregate size was more significant at pH 4.5 than at pH 7.0 or 9.0. This observation can be a reflection of the ionization of COOH groups and the improved hydration of PCBCL block at pH 7.0 and 9.0 over pH 4.5. However, the extent of increase in aggregate size as a function of temperature for 27% debenzylated polymer was higher at pH 7.0 than pHs 4.5 or

9.0 (Figure 2-6 A). Excessive ionization of COOH groups at pH 9.0, leading to polymer chain repulsion, may counteract the hydrophobic interaction and aggregation of micelles at this pH. Further studies are required to clarify the reason behind this observation.

## **5. Conclusions**

Triblock copolymers based on PEG and functionalized PCL were successfully synthesized. The self-assembly of prepared block copolymers was shown to be affected by the ratio of carboxyl:benzyl carboxylate groups on the hydrophobic block. This ratio also controlled the response of the self-assembled structures to temperature and pH of the environment. In the current study, the block copolymers with 27% debenzylation showed thermo-reversible micellar association. This indicates a potential for 27 % PCBCL-PEG-PCBCL polymers to form thermo-reversible gels with transition temperatures about a few degrees below physiological temperature.

## **Acknowledgements:**

This study was supported by funding from the Natural Science and Engineering Research Council of Canada (NSERC).

## Reference:

- [1] Huang X, Du F, Cheng J, Dong Y, Liang D, Ji S, et al. Acid-sensitive polymeric micelles based on thermoresponsive block copolymers with pendent cyclic orthoester groups. *Macromolecules* 2009;42:783-90.
- [2] Jeong JH, Byun Y, Park TG. Synthesis and characterization of poly(L-lysine)-g-poly(D,L-lactic-co-glycolic acid) biodegradable micelles. *Journal of Biomaterials Science, Polymer Edition* 2003;14:1-11.
- [3] Liggins RT, Burt HM. Polyether-polyester diblock copolymers for the preparation of paclitaxel loaded polymeric micelle formulations. *Advanced Drug Delivery Reviews* 2002;54:191-202.
- [4] Gaucher G, Dufresne MH, Sant VP, Kang N, Maysinger D, Leroux JC. Block copolymer micelles: Preparation, characterization and application in drug delivery. *Journal of Controlled Release* 2005;109:169-88.
- [5] Jones M-C, Gao H, Leroux J-C. Reverse polymeric micelles for pharmaceutical applications. *Journal of Controlled Release* 2008;132:208-15.
- [6] Inoue T, Chen G, Nakamae K, Hoffman AS. An AB block copolymer of oligo(methyl methacrylate) and poly(acrylic acid) for micellar delivery of hydrophobic drugs. *Journal of Controlled Release* 1998;51:221-9.
- [7] Kataoka K, Harada A, Nagasaki Y. Block copolymer micelles for drug delivery: design, characterization and biological significance. *Advanced Drug Delivery Reviews* 2001;47:113-31.
- [8] Lavasanifar A, Samuel J, Kwon GS. Poly(ethylene oxide)-block-poly(-amino acid) micelles for drug delivery. *Advanced Drug Delivery Reviews* 2002;54:169-90.
- [9] Nishiyama N, Bae Y, Miyata K, Fukushima S, Kataoka K. Smart polymeric micelles for gene and drug delivery. *Drug Discovery Today: Technologies* 2005;2:21-6.
- [10] Nishiyama N, Kataoka K. Current state, achievements, and future prospects of polymeric micelles as nanocarriers for drug and gene delivery. *Pharmacology & Therapeutics* 2006;112:630-48.
- [11] Ma Y, Tang Y, Billingham NC, Armes SP, Lewis AL. Synthesis of biocompatible, stimuli-responsive, physical gels based on ABA tri block copolymers. *Biomacromolecules* 2003;4:864-8.
- [12] Shahin M, Lavasanifar A. Novel self-associating poly(ethylene oxide)-b-poly( $\epsilon$ -caprolactone) based drug conjugates and nano-containers for paclitaxel delivery. *International Journal of Pharmaceutics*;389:213-22.
- [13] Binkhathlan Z, Hamdy DA, Brocks DR, Lavasanifar A. Development of a polymeric micellar formulation for valspodar and assessment of its pharmacokinetics in rat. *European Journal of Pharmaceutics and Biopharmaceutics*;75:90-5.
- [14] Xiong XB, Uludag H, Lavasanifar A. Biodegradable amphiphilic poly(ethylene oxide)-block-polyesters with grafted polyamines as supramolecular nanocarriers for efficient siRNA delivery. *Biomaterials* 2009;30:242-53.
- [15] Xiong XB, Uludag H, Lavasanifar A. Virus-mimetic polymeric micelles for targeted siRNA delivery. *Biomaterials*;31:5886-93.
- [16] Gong CY, Shi S, Dong PW, Yang B, Qi XR, Guo G, et al. Biodegradable in situ gel-forming controlled drug delivery system based on thermosensitive PCL-PEG-PCL hydrogel: Part 1—synthesis, characterization, and acute toxicity evaluation. Wiley Subscription Services, Inc., A Wiley Company; 2009. p. 4684-94.
- [17] Ma G, Miao B, Song C. Thermosensitive PCL-PEG-PCL hydrogels: Synthesis, characterization, and delivery of proteins. *Journal of Applied Polymer Science*; 2010. 116:1985-93.

- [18] Liu CB, Gong CY, Huang MJ, Wang JW, Pan YF, Zhang YD, et al. Thermoreversible gel-sol behavior of biodegradable PCL-PEG-PCL tri block copolymer in aqueous solutions. *J Biomed Mater Res B Appl Biomater* 2008;84:165-75.
- [19] Mahmud A, Xiong XB, Lavasanifar A. Novel self-associating poly(ethylene oxide)-block-poly(epsilon-caprolactone) block copolymers with functional side groups on the polyester block for drug delivery. *Macromolecules* 2006;39:9419-28.
- [20] Adamus G, Hakkarainen M, Hoglund A, Kowalczyk M, Albertsson AC. MALDI-TOF MS reveals the molecular level structures of different hydrophilic-hydrophobic polyether-esters. *Biomacromolecules* 2009;10:1540-6.
- [21] Albertsson A-C, Varma IK. Recent Developments in Ring Opening Polymerization of Lactones for Biomedical Applications. *Biomacromolecules* 2003;4:1466-86.
- [22] Storey RF, Sherman JW. Kinetics and Mechanism of the Stannous Octoate-Catalyzed Bulk Polymerization of  $\epsilon$ -Caprolactone. *Macromolecules* 2002;35:1504-12.
- [23] Nikolic MS, Olsson C, Salcher A, Kornowski A, Rank A, Schubert R, et al. Micelle and Vesicle Formation of Amphiphilic Nanoparticles. *Angewandte Chemie International Edition* 2009;48:2752-4.
- [24] Wei H, Zhang XZ, Zhou Y, Cheng SX, Zhuo RX. Self-assembled thermoresponsive micelles of poly(N-isopropylacrylamide-*b*-methyl methacrylate). *Biomaterials* 2006;27:2028-34.
- [25] Jeong B, Choi YK, Bae YH, Zentner G, Kim SW. New biodegradable polymers for injectable drug delivery systems. *Journal of Controlled Release* 1999;62:109-14.
- [26] Jeong B, Kim SW, Bae YH. Thermosensitive sol-gel reversible hydrogels. *Advanced Drug Delivery Reviews* 2002;54:37-51.
- [27] Jeong B, Bae YH, Kim SW. Thermoreversible Gelation of PEG-PLGA-PEG Tri block Copolymer Aqueous Solutions. *Macromolecules* 1999;32:7064-9.
- [28] Nguyen MK, Lee DS. Injectable Biodegradable Hydrogels. *Macromolecular Bioscience*;10:563-79.

## Chapter 3

### **Thermo-reversible Hydrogels based on Triblock Copolymers of PEG and functionalized Poly( $\epsilon$ -caprolactone)**

The content of this chapter has been submitted in: Safaei Nikouei N, Vakili M, Akbari A, Wu J, Lavasanifar A. Biodegradable Thermo-reversible Hydrogels based on Triblock Copolymers of PEG and Functionalized Poly( $\epsilon$ -caprolactone). *Biomaterials*

## 1. Introduction

Thermal gelling polymers which undergo sol-to-gel transition in aqueous media at temperatures a few degrees below the physiological temperature, i.e.,  $< 37\text{ }^{\circ}\text{C}$ , are the focus of much attention for their potential application as vehicles for regional drug delivery, or as scaffolds for cell implantation and/or tissue engineering purposes [1]. Thermo-gelling materials made as injectable aqueous fluids before administration, but immediately turn into standing in situ gels within the desired tissue, organ, or body cavity. This unique characteristics, exempts the need for surgical procedures for the implantation of the gel. In addition, the in situ forming hydrogel with thermo-reversible properties will be able to take the shape of the body cavity in which they are inserted upon administration in a liquid sol form at room temperature, then turn into a gel following a raise in their temperature to body temperature. Various therapeutic molecules such as small molecule drugs or therapeutic macromolecules such as peptides and proteins can be incorporated into the gel by simply mixing the drug with the gel-forming material in sol state at room temperature [2,3]. The in situ forming hydrogels can also be used as a scaffold for the implantation of cells providing a protective barrier. .

A common problem associated with the use of existing thermo-gelling materials as in situ hydrogels for biomedical applications, is their inadequate safety and/or degradation profile of the gel-forming polymer. In 1990s one of the first examples of relatively safe and degradable thermo-gelling materials based on polyesters was introduced [5]. The gel forming material (known as ReGel<sup>®</sup>) was composed of poly(lactide-co-glycolide)-*block*-poly(ethylene glycol)-*block*-poly(lactide-co-glycolide) (PLGA-PEG-PLGA) triblock copolymers, which are water soluble copolymers at room temperature and form gel at concentrations of 5–30 wt%

and elevated temperatures ( $\sim$  °C) (6,7). ReGel<sup>®</sup> was found to enhance the solubility of poorly soluble drugs (e.g., PTX and CyA) by 400 to > 2000-folds. The gel was used for depot drug delivery with release times ranging from 1 to 6 weeks. For instance, an excellent control over the release of PTX for approximately 50 days was achieved using ReGel<sup>®</sup> [8]. Release studies on proteins (e.g., pGH, G-CSF, insulin, rHbsAg) revealed continuous release without any signs of burst release for up to 10–14 days .

Block copolymers consisting of (PEG) and another polyester, i.e., poly( $\epsilon$ -caprolactone) (PCL) (10,11), have also been widely studied for drug delivery or tissue engineering applications (10,12,13). The sol-gel transition of these block copolymers have been studied by several groups recently, including Bae *et al.* who suggested that the sol-gel transition of PCL-PEG-PCL block copolymers to be prompted by micellar aggregation [14,15]. At a temperature much lower than the sol–gel transition temperature, small micelles flow freely in the aqueous solution. The micelle size increased slightly as the temperature is increased, but the micelles remained in the sol state. With further increase in temperature to around the sol–gel transition temperature, the micelle size increased rapidly, leading to sol–gel transition [16].

Our research group has reported on the development of a new family of block copolymers based on PEG and PCL, where the PCL block has been functionalized through the introduction of carboxyl and/or benzyl carboxylate groups on the  $\alpha$ -carbon of  $\epsilon$ -caprolactone [17]. In the previous chapter, we reported on successful synthesis of triblock copolymers based on PEG and benzyl carboxylate/carboxyl substituted PCL and investigated the thermo- or pH-responsive assembly of prepared block copolymers to polymeric micelles and their aggregates [18]. In the current study, the synthetic condition for



the preparation of triblock copolymers based on PEG as the hydrophilic block and poly( $\alpha$ -benzyl carboxylate-co- $\alpha$ -carboxyl- $\epsilon$ -caprolactone) (PCBCL) as the hydrophobic block was further optimized. This optimization led to the production of PCBCL-PEG-PCBCL triblock copolymers with controlled levels of  $\alpha$ -carboxyl substitution on the PCBCL block. The sol-gel transition of prepared polymers at a 7-15 w/w% concentration range in an aqueous environment in response to changes in the temperature was then characterized by inverse flow method, dynamic mechanical analysis (DMA) and differential scanning calorimetry (DSC).  $^1\text{H}$  NMR spectroscopy was used to investigate the temperature responsive mechanism of gel formation. The effect of the degree of  $\alpha$ -carboxyl group substitution on the hydrophobic block as well as copolymer concentration on the transition temperature and rheological behavior of hydrogels was also investigated.

## **2. Materials and methods**

### **2.1. Materials**

Dihydroxy-poly(ethylene glycol) (PEG) ( $M_w = 1450$  Da) and Palladium, 10% on activated charcoal (Pd/C) were purchased from Sigma, St. Louis, MO.  $\alpha$ -benzyl carboxylate- $\epsilon$ -caprolactone (BCL) was synthesized by Alberta Research Chemicals Inc (ARCI), Edmonton, Canada. All other chemicals and reagents were analytical grade.

### **2.2. Synthesis of triblock copolymers**

Polymerization of BCL (0.6 g) by dihydroxylated PEG as initiator (0.19 g) was conducted in the absence of any catalyst at  $140^\circ\text{C}$  for 3 h, and then continued at  $160^\circ\text{C}$  for 15 h. This led to the production of poly( $\alpha$ -benzyl carboxylate- $\epsilon$ -caprolactone)-PEG-poly( $\alpha$ -benzyl carboxylate- $\epsilon$ -caprolactone) (PBCL-PEG-PBCL) triblock copolymer. Prepared block

copolymer was dissolved in dichloromethane and then precipitated in hexane. The mixture was centrifuged and the supernatant was discarded. Polymer was washed three times by dissolving the precipitate in dichloromethane and repeating the above procedure. In the second step, partial catalytic reduction of PBCL-PEG-PBCL at different levels was accomplished using varying amount of palladium 10% on activated charcoal ranging from 5 to 20 wt. % and different reaction times ranging from 30 to 90 minute. This led to the production of PCBCL-PEG-PCBCL with 30, 54, or 97% of debenylation. Four different block copolymers (characteristics summarized in Table 3-1) were synthesized and used for further studies.

### 2.3 Characterization of prepared triblock copolymers

#### a) $^1\text{H NMR}$

$^1\text{H NMR}$  spectroscopy in  $\text{CDCl}_3$  was used to study the composition of copolymers. The degree of polymerization for the PBCL blocks in PBCL-PEG-PBCL was identified by comparing peak intensity of PEG ( $-\text{CH}_2\text{CH}_2\text{O}-$ ,  $\delta=3.65$  ppm) to that of PBCL ( $-\text{O}-\text{CH}_2-$ ,  $\delta=4.1$  ppm). Percentage of conversion was calculated using the following equation:

$$\text{Conversion (\%)} = \frac{\text{Degree of Polymerization of PBCL from } ^1\text{H NMR}}{\text{Theoretical degree of Polymerization of PBCL}} \times 100$$

The degree of benzyl carboxylate substitution on the polymer backbone was estimated by comparing the peak integration of PCBCL backbone ( $-\text{CH}_2\text{O}-$ ,  $\delta= 4.1$  ppm) to the peak integration of the methylene protons of the benzyl carboxylate group ( $-\text{CH}_2-\text{O}-\text{C}=\text{O}$ ,  $\delta=5.15$ ). The percentage of reduction (i.e., debenylation) in PCBCL-PEG-PCBCL was then calculated according to the following formula:

Reduction (%) =

$$\frac{(\text{Degree of polymerization of PCBCL}) - (\text{Degree of benzyl carboxylate substitution on PCBCL})}{\text{Degree of polymerization of PCBCL}} \times 100$$

## 2.4 Characterization of PCBCL-PEG-PCBCL Thermo-Responsive Sol-Gel Transition

### *a) Visual observation of sol-gel transition by tube inversion method*

The sol to gel transition of the synthesized copolymer solutions was first determined by the tube inversion method [19,20]. Aqueous solution of PCBCL-PEG-PCBCL block copolymers were prepared using distilled water, at concentrations of 7, 10, and 15% w/w. The 15x45 mm vials containing 1 mL polymer aqueous solution were immersed in a waterbath where the temperature was set at 25°C. The temperature of the waterbath was allowed to increase by 1°C every 5 min up to 60°C. Phase transition (flow/no flow) was assessed by inverting the incubated tube vertically to allow a visual assessment of the aqueous polymer sample. The copolymer solution was considered gel when the solution did not flow for 1 minute upon inversion of vial. The incubation temperature, at which this phenomenon was observed, was recorded as the transition temperature.

### *b) Modulated Differential Scanning Calorimetry (MDSC)*

Thermal analysis was performed with Q series<sup>TM</sup> 2000 modulated differential scanning calorimeter. Aqueous solutions of 30, 54, and 97% reduced triblock copolymer in deionized water at concentrations of 7, 10, and 15% wt. were prepared, and kept in refrigerator overnight. Each sample (10 mg) was hermetically sealed in an aluminum pan. The samples were first heated to 70°C, and kept for 5 minute at this temperature to eliminate their thermal history. Heating thermograms were recorded using modulated mode with amplitude of 0.2°C

in 60s and ramping of 0.5°C per minute. Scans were conducted from 8 to 10°C. This was followed by holding the sample at 10°C for 15 minutes, and then increasing the temperature to 70°C with the same rate under nitrogen gas. The pan filled with distilled water was used as reference.

### *c) Rheological analysis*

The storage moduli and loss moduli curves for polymer solutions were determined using a Physica MCR xx0 rheometer equipped with a peltier heating/cooling plate. Polymer solutions in distilled water (7, 10, and 15% w/w) were placed between two parallel plates. Temperature sweeps (20-60°C) were conducted at a fixed strain of 1% using an angular frequency of 10 rad/s. Sweeps were conducted at 1°C min<sup>-1</sup>. The change in the storage modulus and loss modulus as a function of temperature was plotted. The transition temperature of solutions was estimated by dividing loss modulus to storage modulus values. The temperature after which the ratio of loss modulus to storage modulus was < 1 was considered sol-gel transition temperature. In a separate experiment, three heating and cooling periods (between 25°C and 38°C) were conducted for the 30% reduced triblock copolymer at 10% w/w concentration in distilled water to evaluate the repeatability of sol-gel transition of polymer solutions.

## **2.5 <sup>1</sup>H NMR study**

The <sup>1</sup>H NMR spectra of PCBCL-PEG-PCBCL (30 and 54% reduced) in D<sub>2</sub>O (10 mg/mL) were obtained as a function of temperature raising from 7 to 60 °C. Temperature was raised at a rate of 2°C every 6 minutes. The ratio of the integration of peaks related to PEG protons ( $\delta=3.65$  ppm), methylene protons of the PCBCL backbone (-CH<sub>2</sub>-CH<sub>2</sub>-CH<sub>2</sub>-,  $\delta= 1.2$ ,

1.4, and 1.9 ppm), phenyl protons ( $\delta = 7.4$  ppm), or methylene protons of benzyl carboxylate substituent ( $\delta = 5.15$  ppm) to the integration of peaks related to a standard, i.e., dimethyl sulfone protons ( $\delta = 3.2$  ppm), added at a known concentration to the  $^1\text{H}$  NMR samples, were compared as a function of temperature.

## 2.6 Statistical analysis

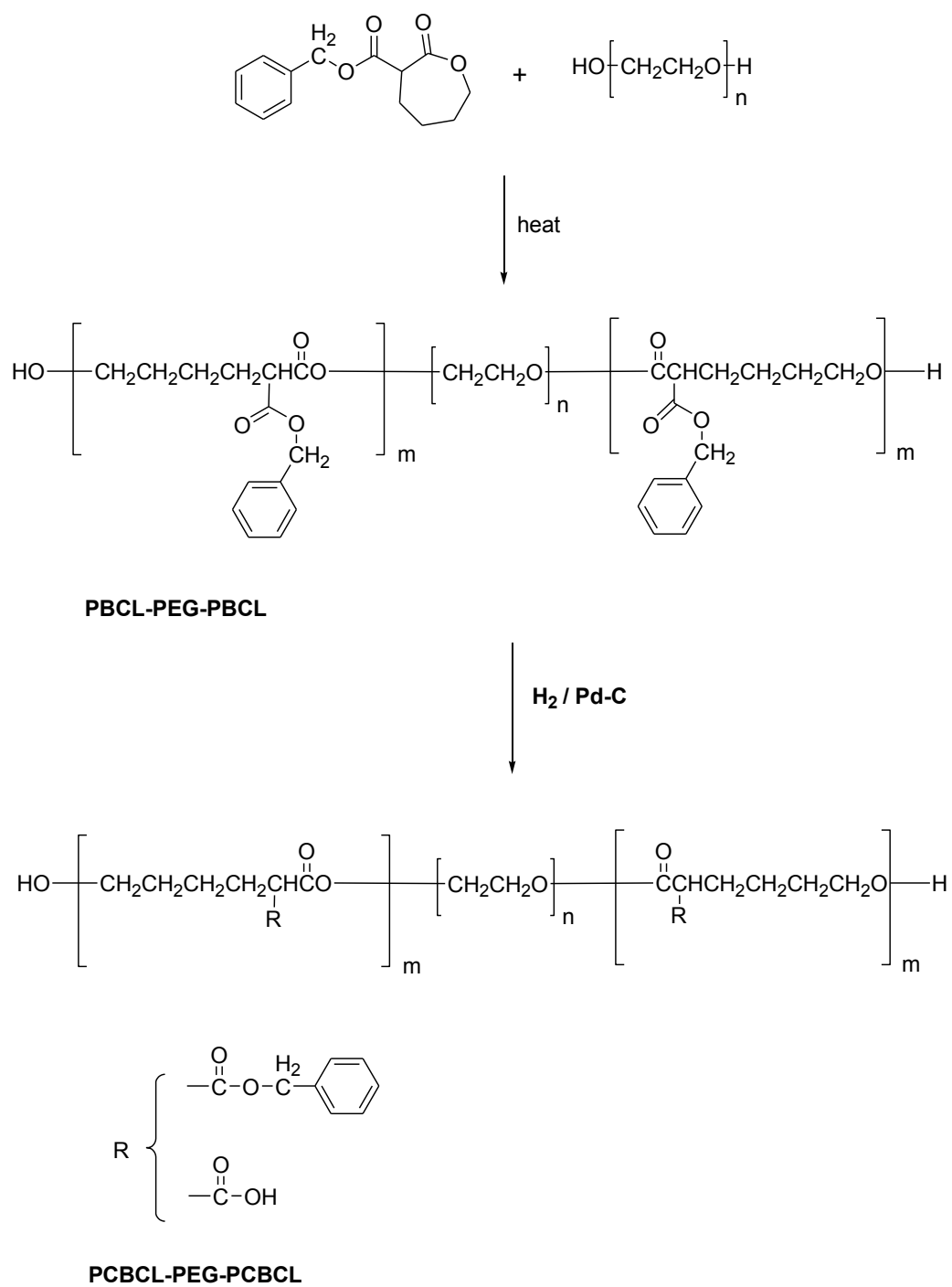
The significance of differences between results was assessed using unpaired Student's *t* test. The level of significance was set at  $\alpha = 0.05$ .

## 3. Results and Discussion

### 3.1. Synthesis and characterization of triblock copolymers

Synthesis of PCBCL-PEG-PCBCL copolymer was carried out following a two-step procedure (Scheme 3-1) reported before [18] with some modifications: First, triblock copolymers composed of PEG in the middle and PBCL on the sides were synthesized through ring opening polymerization of BCL in the absence of any catalyst. Number-average molecular weight of prepared block copolymers was determined from their  $^1\text{H}$  NMR spectra, comparing peak intensity of PEG ( $-\text{CH}_2\text{CH}_2\text{O}-$ ,  $\delta = 3.65$  ppm) to that of PBCL ( $-\text{OCH}_2-$ ,  $\delta = 4.1$  ppm) assuming a  $1450 \text{ g mol}^{-1}$  molecular weight for PEG (Figure 3-1A). This step was followed by the catalytic reduction [17] of PBCL-PEG-PBCL block copolymers, in the presence of continuous hydrogen gas stream. In the current work, the second step of the synthetic procedure, i.e., reduction of benzyl carboxylate substituents to free carboxyl groups, was optimized to achieve block copolymers with controllable composition. This was achieved through changes in the duration of the reduction reaction and/or level of palladium to control the level of benzyl carboxylate to carboxyl conversion. Towards this, palladium on activated

charcoal at concentrations of 5 to 20% by weight of the polymer mass and different reaction times (30 to 90 minute) was used to achieve block copolymers with various degrees of reduction. The  $^1\text{H}$  NMR spectra of PBCL-PEG-PBCL (Figure 3-1A) as well as  $^1\text{H}$  NMR and  $^{13}\text{C}$  NMR of PCBCL-PEG-PCBCL (Figure 3-1B and C, respectively) were used to confirm the synthesis and structural composition of each polymer product. A peak related to the COOH group was observed in the spectra of PCBCL-PEG-PCBCL in  $^{13}\text{C}$  NMR at  $\delta = 168$  ppm. Moreover, Compared to the  $^1\text{H}$  NMR spectrum for PBCL-PEG-PBCL, the ratio of the area under the peak for both phenyl and methylene of the benzyl protons to that of PEG was reduced after reduction of PBCL to PCBCL confirming the success of reduction reaction. Level of reduction was defined as described in the method section for each polymer prepared under different reduction time or catalyst concentration.



**Scheme 0-1 synthetic scheme for the preparation of PBCL-PEG-PBCL, and PCBCL-PEG-PCBCL triblock copolymers**





C)

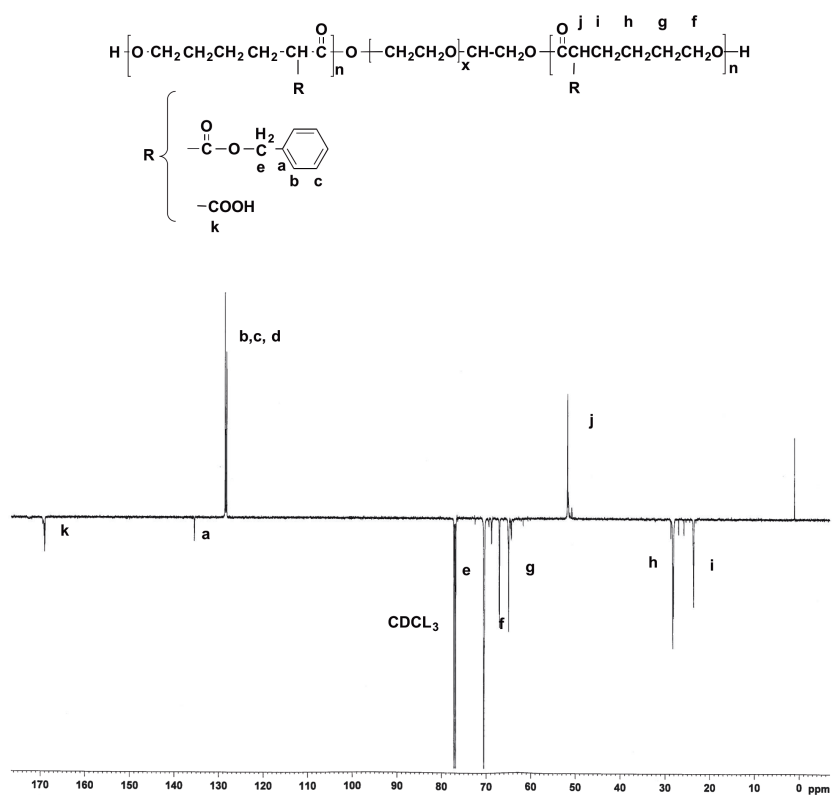


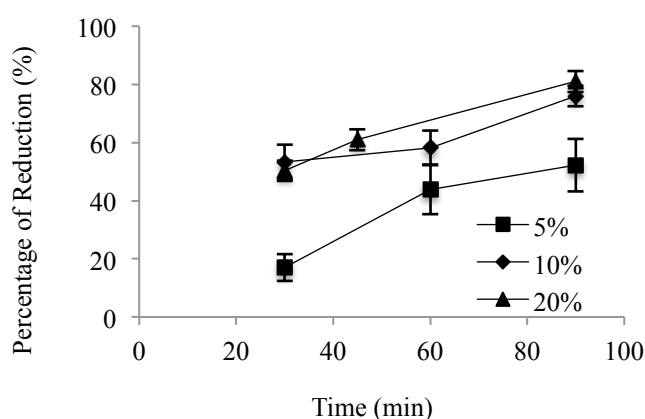
Figure 0-1 A typical  $^1\text{H}$  NMR spectrum of A) PBCL-PEG-PBCL; and B) PCBCL-PEG-PCBCL block copolymers (54% reduced) in  $\text{CDCl}_3$  and peak assignments. C)  $^{13}\text{C}$  NMR of PCBCL-PEG-PCBCL (54% reduced) in  $\text{CDCl}_3$  and peak assignments

Table 0-1 Characteristic of synthesized triblock copolymers

Polymer	Percent of Reduction <sup>a</sup>	$M_n^b$	The number of pendent groups per PCL polymer chain <sup>b</sup>	
			Carboxyl	Benzyl carboxylate
PBCL-PEG-PBCL	0	4179	0	11
PCBCL-PEG-PCBCL	30	3882	3.3	7.7
PCBCL-PEG-PCBCL	54	3648	5.9	5.1
PCBCL-PEG-PCBCL	97	3216	10.7	0.3

<sup>a</sup> The number shown indicates the percentage of reduction of benzyl carboxylate to carboxyl group in each block copolymer determined by  $^1\text{H}$  NMR spectroscopy. <sup>b</sup> Based on data from  $^1\text{H}$  NMR.

Figure 3-2 shows the effect of reaction time on the percentage of reduction for different amounts of catalyst. Increasing the amount of catalyst from 5 to 10 % significantly increased the level of PBCL reduction, but an increase in the level of catalyst above 10 % (up to 20 %) did not have any significant effect on the PBCL reduction level. For instance, using 5 % catalyst, after 90 minutes reaction, the level of reduction was 52% compared to 76 and 81% reduction using 10, and 20% catalyst, respectively. Additionally, using 5 % catalyst, the degree of reduction increased significantly when reaction time was increased from 30 to 60 min. However, increasing reaction time above 60 min did not affect the degree of reduction in the presence of 5% catalyst. In the presence of 10 and 20 % activated charcoal, on the other hand, reduction level did not plateau and increased with an increase in the reaction time. In general, increasing activated charcoal to 10 or 20 % was shown to promote the reduction more effectively than increasing the reaction time at 5% activated charcoal. We then used a catalyst concentration of 10 % and changed the reaction time to achieve PCBCL-PEG-PCBCL block copolymers at different levels of reduction (as summarized in Table 3-1) for use in further studies.



**Figure 0-2 The effect of the duration of reaction on the percentage of PBCL reduction in triblock copolymers, using different amounts of catalyst (w/w % of used polymer) (n=3)**

### **3.2 Characterization of the thermo-responsive phase transition of aqueous block copolymer solutions**

Block copolymers were solubilized in double distilled water and characterized for their sol-gel transition using three different methods.

#### *a) Inverse Flow Method*

Among different polymers under study (Table 3-1), only the 30 and 54 % reduced PCBCL-PEG-PCBCL showed a sol-gel transition as a function of temperature and polymer concentration. Figure 3.3 shows a typical temperature dependent transition curve obtained using inverse flow method for aqueous solutions of PCBCL-PEG-PCBCL triblock copolymers with 30 and 54 % reduction at 7, 10 and 15 % concentration. The 54% reduced polymer formed a transparent gel at 31°C at a concentration of 7% w/w. This is the temperature used to identify the lower transition point in Figure 3-3. With further increase in temperature, the transparent gel became turbid, and upon further heating at 41 °C, a turbid solution was observed. This is the temperature used to plot the upper transition curve in Figure 3-3 For the 30% reduced polymer at the concentration of 7%, the lower and upper transition temperatures were measured at 35 and 45°C, respectively.

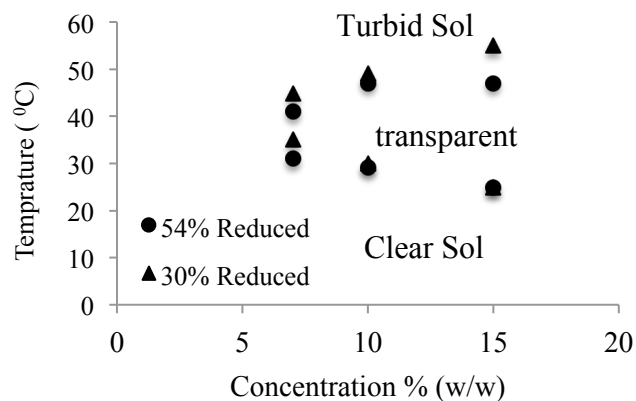


**Figure 0-3 Sol-gel phase transition diagrams of PCBCL-PEG-PCBCL 30, and 54% reduced block copolymer solution at 7, 10, and 15 % w/w concentration in distilled water**

For both polymers, the lower transition temperature decreased as the concentration of polymer increased. For example, for 54% reduced copolymer, the lower transition temperature decreased from 31 to 25°C when the concentration of the polymer was increased from 7 to 15 wt%. For the 30 % reduced PCBCL-PEG-PCBCL, the lower transition temperature decreased from 35°C to 25°C when the concentration of polymer was increased from 7 to 15 wt%. The upper transition temperature; however, was increased by increasing the concentration of block copolymers. For example, when the concentration increased from 7 to 15 wt %, the upper transition temperature rose from 45 to 55°C and from 41°C to 47°C for 30% and 54% reduced copolymers, respectively.

The observed lower transition temperature may reflect the increase in the aggregation of micelles leading to gel formation (21) , whereas the observed upper transition temperature may reflect the physical dehydration of the block copolymer micelles leading eventually to phase separation. A reduction in the lower transition temperature as a result of an increase in polymer concentration can be attributed to an increase in the aggregation and packing interaction between micelles at higher polymer concentrations [22,23]. At higher temperatures, the hydrophilic segments of the copolymer may undergo dehydration [22],

leading to phase separation. Increasing the concentration of copolymers can push the temperature needed for effective dehydration of system to higher degrees. Nevertheless, the results illustrate an opportunity for adjusting the transition temperatures of the developed copolymers by applying different polymer concentrations in an aqueous media.

Unlike 30 and 54 % reduced polymers, the 97% reduced block copolymer did not show any sol-gel transition when applied up to concentration of 15 w/w % in aqueous media. This implies a role for hydrophobic interaction between benzyl carboxylate side chains in driving the micellar packing leading to gelation of 30 and 54% reduced copolymer solutions. The hydrophobicity of the side group can promote the dehydration and the aggregation of the amphiphilic polymer in the aqueous solution [24]. The more hydrophilic nature of 97% reduced copolymer can reduce tendency for gelation and keep the polymer in soluble form in water. On the other hand, PBCL-PEG-PBCL (with 0 percent reduction) was found to be water insoluble.

#### *b) Modulated DSC*

Figure 3-4 illustrates the thermographs of aqueous solutions of 30 and 54% reduced block copolymers at a concentration of 10% w/w using modulated DSC. The 30% reduced block copolymer showed two endothermic peaks. The first peak which appeared at 35.05 °C can indicate the lower sol-gel transition temperature of aqueous solution of this block copolymer, while the second peak at 45.71 °C coincides with the second transition. The MDSC analysis of 54% reduced block copolymer hydrogel also showed two transition endothermic peaks at 33.57 °C and 45.21 °C. These temperatures are also close to sol-gel and gel-sol transition temperatures of 54 % reduced polymer measured by inverse flow method,

respectively. The transition enthalpy for 30% reduced copolymer was 0.07 J/g (35.05 °C) and 0.44 J/g (45.71 °C), while these values were 0.31 J/g (33.57 °C) and 1.58 J/g (45.21 °C) for the 54% reduced block copolymer.

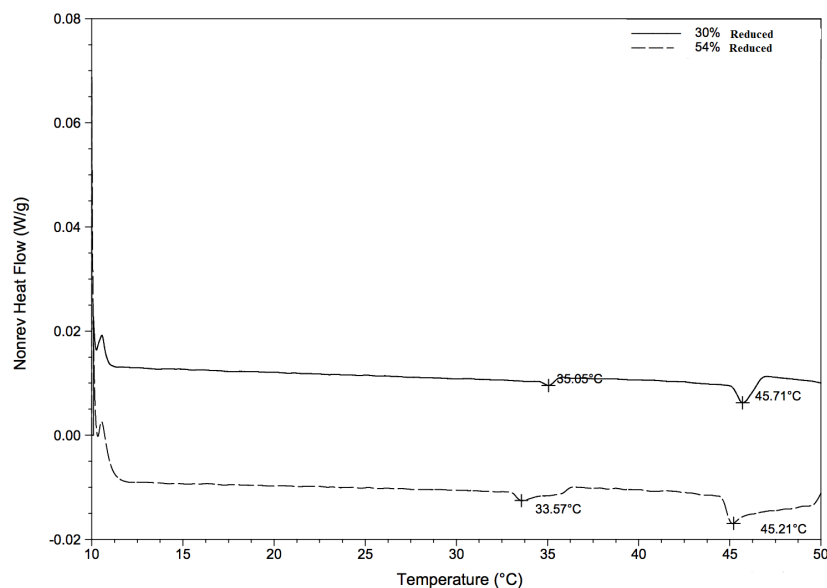


**Figure 0-4 Modulated DSC thermograms of 30, and 54% reduced block copolymer solution in distilled water at 10% w/w concentration of copolymers**

The endothermic nature of the peaks and their comparative enthalpy values imply a role for the breaking of hydrogen bonds between water/ polymer or polymer/polymer (through pendent carboxyl groups) within the micelle core in the thermo-responsive transition processes. The first transition (around 33 and 35 °C) may reflect breaking of hydrogen bonds between water and the hydrophilic parts of PCBCL (i.e., COOH groups) and/or intramicellar hydrogen bonds between COOH groups [25]. This may be followed by the association of micelles through intermicellar bridging of the hydrophobic parts of the tri block copolymers. This explanation is also in line with the lower enthalpy of transition observed for the 30% reduced copolymer that has lower number of COOH groups in its structure compared to the

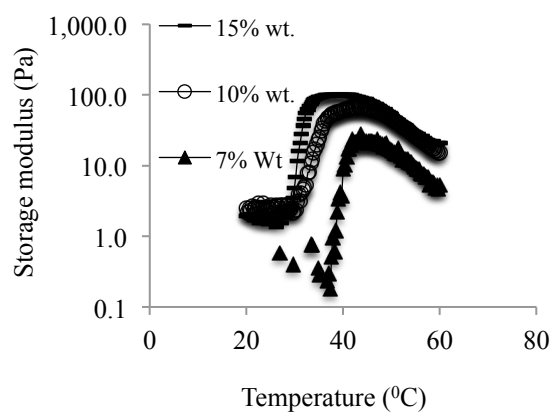
54 % reduced copolymer which has higher number of free COOH groups in its structure (0.07 versus 0.31 J/g for 30 and 54 % reduced block copolymers). The second transition, on the other hand, may reflect the dehydration of PEG and/or a change in micellar conformation leading to phase separation [23].

*c) Dynamic Mechanical Analysis (DMA)*

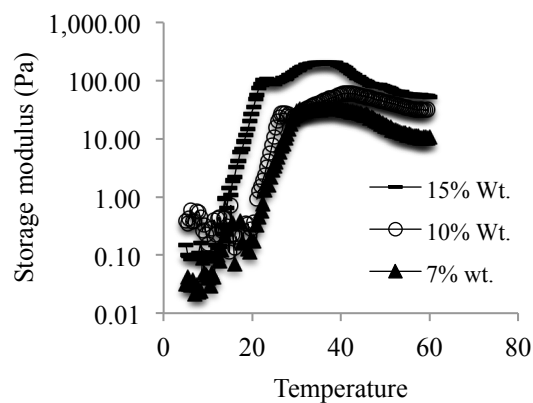
The changes in the storage modulus,  $G'$ , and loss modulus,  $G''$ , of aqueous solutions of 30 and 54% reduced copolymer as a function of a change in temperature was also used to evaluate gel formation (Figure 3.5 and 3.6). Storage modulus,  $G'$ , is related to the stiffness or resistance of material to deformation [26] , while loss modulus is related to the viscos properties of materials and their resistance to flow.

Figure 3-5A and B shows changes in the storage modulus,  $G'$ , of 30 and 54% reduced tri block copolymers as a function of temperature for different polymer concentrations. For both 30 and 54 % reduced block copolymers, we observed a sharp increase in  $G'$  at a certain temperature (Figure 3-5A and B). Moreover, the temperature at which a sharp rise in  $G'$  was observed decreased as the concentration of triblock copolymer was increased. For 30 % reduced block copolymer,  $G'$  reached its maximum value at 49, 46 and 44 °C at polymer concentrations of 7, 10 and 15 w/w %, respectively, and started to decline above these temperatures. For 54 % reduced polymer,  $G'$  reached its maximum value at 30, 41 and 37 °C at polymer concentrations of 7, 10 and 15 %, respectively. The  $G'$  for the 54% reduced block copolymer remained in plateau up to 60°C, indicating formation of more stable hydrogels from this block copolymer. The maximum value of  $G'$  is a reflection of the elastic properties of polymer in the gel form [27].

A)



B)

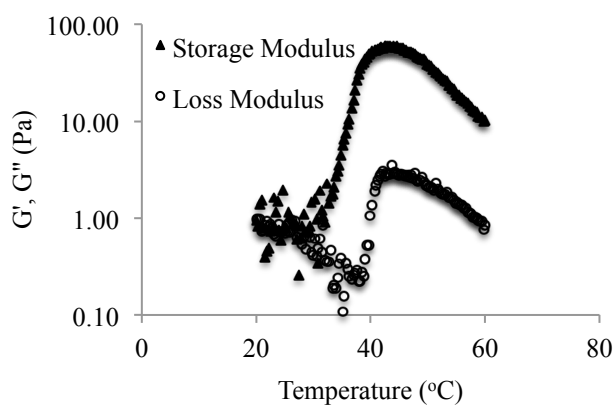


**Figure 0-5** Changes in the storage modulus,  $G'$ , as a function of temperature for A) 30 %, and B) 54% reduced PCBCL-PEG-PCBCL block copolymer solutions in water at 7, 10, and 15% w/w as a function of raising temperature at  $1^{\circ}\text{C min}^{-1}$ ; The graph shows the average of 3 measurement ( $n=3$ ).

Changes in the storage modulus,  $G'$ , to loss modulus,  $G''$ , as a function of temperature are compared for 30 and 54 % reduced block copolymers at a concentration of 10 % w/w in Figure 3-5 A and B. The loss modulus of aqueous solution of both 30 and 54 % reduced triblock copolymers was found to be mostly similar to the storage modulus at low temperatures, indicating a typical liquid state. Both storage and loss modulus increased at a certain temperature, but the level of increase in loss modulus was lower compared to increase in storage modulus. This indicated gel formation [27]. The temperature at which the ratio of loss modulus to storage modulus passed one and stayed below one was considered as sol-gel transition temperature. This temperature was found to be 30 and 33  $^{\circ}\text{C}$  for 30 and 54 % reduced triblock copolymers at 10 % concentration, respectively. In line with our earlier results, transition temperature was found to be dependent on the chemical structure and concentration of copolymers under study (Table 3-2).



A)



B)

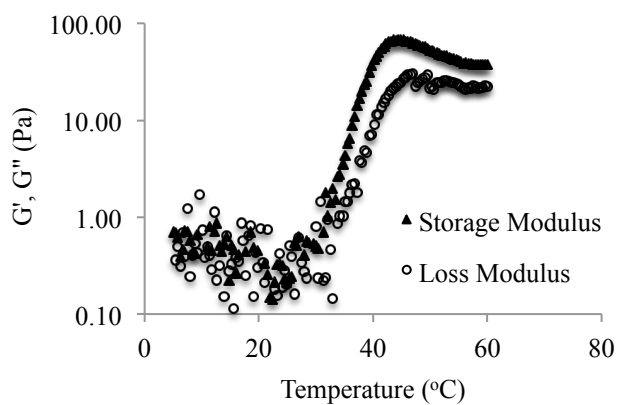


**Figure 0-6 Increases in storage modulus ( $G'$ ) and loss modulus ( $G''$ ) of A) 30%, and B) 54% reduced polymer (10% w/w) as a function of rising temperature at  $1^{\circ}\text{C min}^{-1}$ . The graph represents the average of 3 measurement ( $n=3$ ).**

**Table 0-2 Transition temperature of 30 and 54 % reduced PCBCL-PEG-PCBCL copolymer at different concentrations in water measured by Dynamic Mechanical Analysis (n=3)**

Polymer	Concentration of polymer (w/v %)	Sol-gel Transition Temperature (°C) ± SD
30 % reduced	7	38 ± 0.60
	10	30 ± 0.45
	15	27 ± 0.75
54 % reduced	7	33 ± 0.43
	10	33 ± 0.55
	15	28 ± 0.43

The sol-gel transition temperature of both copolymer aqueous solutions under study measured by different methods is compared for the 10% w/w concentration in Table 3-3. The results indicate a good agreement between different methods of measurement and point to a transition temperature around 30-35 ° C for 30 % and around 29-34 °C for the 54% reduced block copolymer solutions. Between the two polymers, the 54% reduced polymer formed a more stable gel at temperatures above its transition temperature, but the sol to gel transition for this polymer was not as rapid as the 30 % reduced polymer.

**Table 0-3 Comparison of the sol-gel transition temperature for PCBCL-PEG-PCBCL aqueous samples prepared at 10 % w/w concentration measured by different methods**

Polymer	Inverse Flow Method (°C)	DSC (°C)	Dynamic Mechanical Analysis (°C)
30 % reduced	30	35	30
54 % reduced	29	34	33

Figure 3-7 shows the reproducibility of temperature responsive viscosity changes in 30% reduced PCBCL-PEG-PCBCL in distilled water for repeated heating/cooling cycles between 25 °C and 38 °C. Symmetric peaks were observed for each cycle, indicating fully reversible properties. Therefore, PCBCL-PEG-PCBCL hydrogel seem promising for repeated applications as they show reproducible sol-gel and gel-sol transition between room and body temperature.

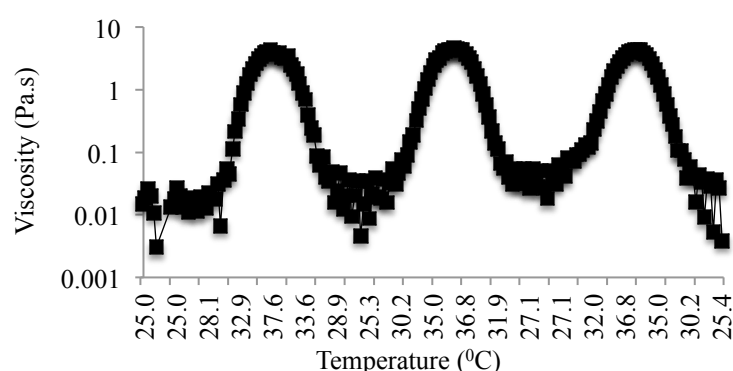


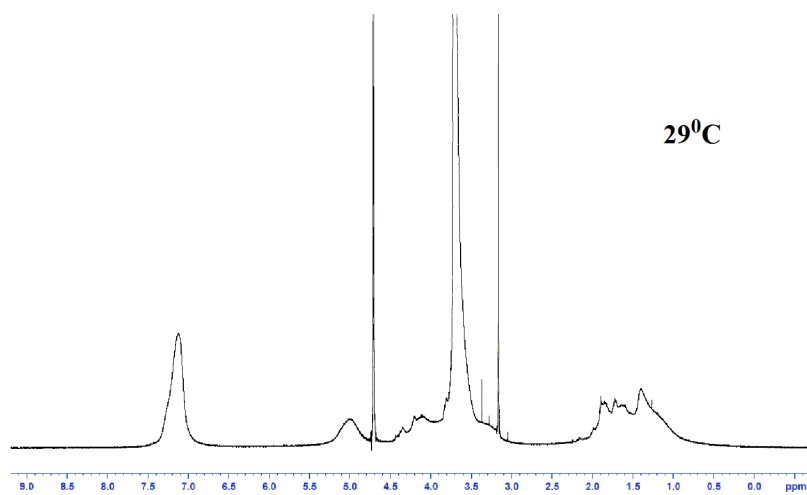
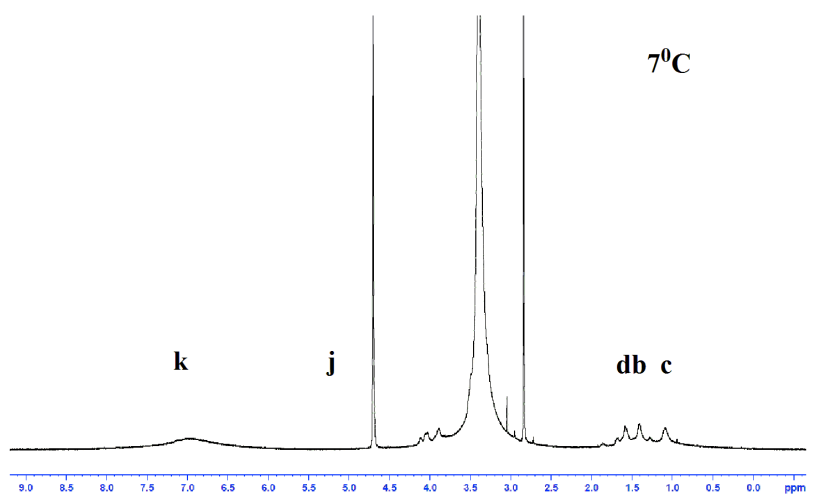
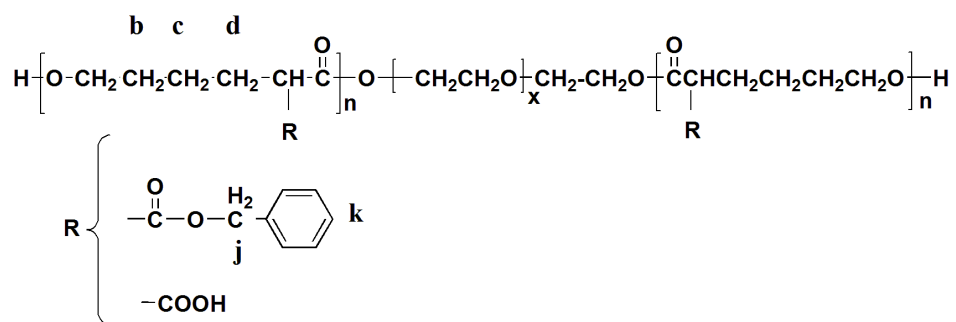
**Figure 0-7** Plot of viscosity as a function of time and temperature (3 heating/cooling cycles between 25, and 38 °C) for the 30% reduced PCBCL-PEG-PCBCL copolymer in distilled water at a concentration of 10% w/w (n=3).

### 3.3 $^1\text{H}$ NMR Study in $\text{D}_2\text{O}$

Figure 3-8A shows the  $^1\text{H}$  NMR spectra of 54% reduced copolymer solution in  $\text{D}_2\text{O}$  (10 mg/mL polymer) at 7, and 29°C, respectively. Dimethyl sulfone was used as standard in the  $^1\text{H}$  NMR spectra. The  $^1\text{H}$  NMR spectrum at above transition temperature exhibited, a marked increase in the integration of the methylene protons of benzyl group ( $-\text{CH}_2-\text{O}-\text{C}=\text{O}$ ,  $\delta=5.15$ ); phenyl protons of benzyl group ( $-\text{C}_6\text{H}_5$ ,  $\delta=7.2$  ppm) and methylene protons on PCBCL backbone ( $-\text{CH}_2-\text{CH}_2-\text{CH}_2-\text{CH}_2-\text{O}$ ,  $\delta= 1.2, 1.4,$  and  $1.9$  ppm). Figure 3.8B shows the temperature dependence of the ratio of area under the peak for protons on the phenyl ring, methylene of benzylcarboxylate group, or  $\text{CH}_2$  on PCBCL to that of dimethyl sulfone ( $-\text{CH}_3$ ,

$\delta = 3.2$  ppm) for both copolymers under study (30 and 54% PCBCL-PEG-PCBCL) in  $D_2O$ . Temperature dependency in peak integration was only observed for the protons related to the PCBCL (hydrophobic) block. The ratio for the integration of peak related to PEG protons to the peak related to dimethyl sulfone protons did not show significant change as a function of increasing temperature, however. This may reflect better mobility of the core-forming block at elevated temperatures that can facilitate formation of hydrophobic bridges between micelles leading to micellar aggregation and gel formation.

A)



B)

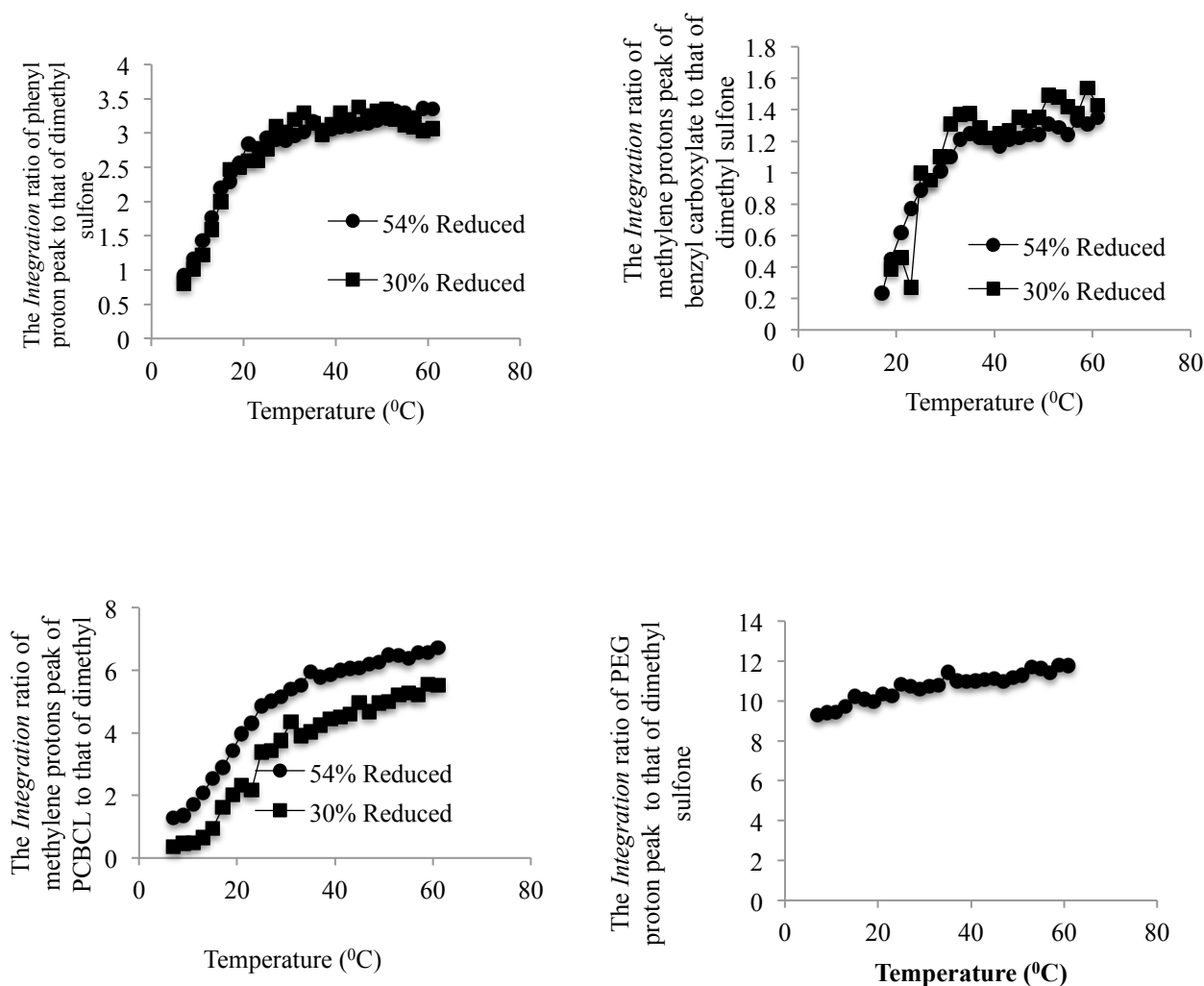


**Figure 0-8 A)  $^1\text{H}$  NMR spectra of 54% reduced PCBCL-PEG-PCBCL solution (10 mg/mL) in  $\text{D}_2\text{O}$  at 23°C and 29°C B) The change in  $^1\text{H}$  NMR ratio integration of phenyl protons, methylene protons of the benzyl carboxylate group on PCBCL, methylene protons of the PCBCL backbone, and PEG protons to the integration of dimethyl sulfone protons as a function of temperature**

Based on the results of this study, a mechanism for the sol-gel transition for triblock copolymer solutions is proposed in Figure 3-9. Formation of a micellar network is proposed to be responsible for gel formation. The micellar network formation as a function of increasing temperature is proposed to be induced by mobilization of the PCBCL segment of the block copolymer out of the micellar structure, accompanied by its dehydration and inter micellar bridging. At higher temperatures (above second transition temperature), dehydration

of PEG segment may lead to the formation of turbid gels followed by phase separation (Figure 3-9). This mechanism can also explain the endothermic nature of two peaks observed in MDSC thermograms as the dehydration of hydrophobic chains and PEG segments are both heat-absorbing processes. In addition to responsiveness to temperature, the developed materials are expected to show pH sensitivity owing to the presence of pending COOH groups.

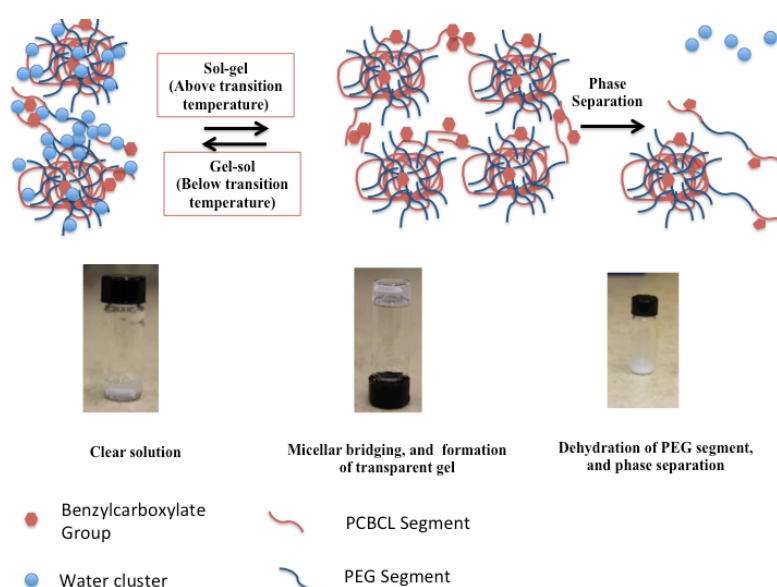


**Figure 0-9 Schematic diagram for the sol-gel and gel-sol transition mechanisms of prepared triblock copolymers in aqueous solution as a function of increasing temperature.**

#### 4. Conclusions

Triblock copolymers formed from PEG as the middle block and different levels of benzylcarboxylate to carboxyl substituted PCL (i.e., PCBCL) as the lateral blocks were studied for their potential in the formation of thermo-responsive gels. Among different block copolymers under study, those with partial carboxyl substitution showed a concentration dependent sol-gel transition at temperatures a few degrees below body temperature (~ 30-35 °C) as defined by inverse flow method, DSC and dynamic mechanical analysis. Overall, a

good agreement between different methods of measurement in defining the transition temperature of block copolymers was observed. The transition temperature of polymer solutions and viscoelastic properties of hydrogels was found to be dependent on the level of benzylcarboxylate to carboxyl substitution on the PCBCL backbone as well as the triblock copolymer concentration. Developed materials have great potential for application as biodegradable injectable implants for depot drug/protein delivery, thermo-responsive hydrogels for mucosal drug administration or scaffolds for cell implantation and tissue engineering.

### **Acknowledgement:**

The authors would like to thank Dr. Ali Akbari and Dr. Jianping Wu for providing rheometer equipment for this study.



## References:

- (1) Hoffman AS. Stimuli-responsive Polymers: Biomedical Applications and Challenges for Clinical Translation. *Adv Drug Deliv Rev* 2012;65:10-16.
- (2) Li Z, Zhang Z, Liu KL, Ni X, Li J. Biodegradable Hyperbranched Amphiphilic Polyurethane Multiblock Copolymers Consisting of Poly (propylene glycol), Poly (ethylene glycol), and Polycaprolactone as in Situ Thermogels. *Biomacromolecules* 2012;13:3977-3989.
- (3) Ruel-Gariépy E, Leroux J. In situ-forming hydrogels—review of temperature-sensitive systems. *European Journal of Pharmaceutics and Biopharmaceutics* 2004;58(2):409-426.
- (4) Vermonden T, Censi R, Hennink WE. Hydrogels for Protein Delivery. *Chem Rev* 2012;112:2853-2888.
- (5) Rathi RC, Zentner GM, inventors. Anonymous google patent. 1999 .
- (6) Shim MS, Lee HT, Shim WS, Park I, Lee H, Chang T, et al. Poly (D, L-lactic acid-co-glycolic acid)-b-poly (ethylene glycol)-b-poly (D, L-lactic acid-co-glycolic acid) triblock copolymer and thermoreversible phase transition in water. *J Biomed Mater Res* 2002;61(2):188-196.
- (7) Loh XJ, Li J. Biodegradable thermosensitive copolymer hydrogels for drug delivery. *Expert Opinion* 2007;17:3977-3989.
- (8) Zentner GM, Rathi R, Shih C, McRea JC, Seo M, Oh H, et al. Biodegradable block copolymers for delivery of proteins and water-insoluble drugs. *J Controlled Release* 2001;72(1):203-215.
- (9) Zentner GM, Rathi R, Shih C, McRea JC, Seo M, Oh H, et al. Biodegradable block copolymers for delivery of proteins and water-insoluble drugs. *J Controlled Release* 2001;72(1):203-215.
- (10) Yin HB, Gong CY, Shi S, Liu XY, Wei YQ, Qian ZY. Toxicity evaluation of biodegradable and thermosensitive PEG-PCL-PEG hydrogel as a potential in situ sustained ophthalmic drug delivery system. *Journal of Biomedical Materials Research Part B: Applied Biomaterials* 2010;92(1):129-137.
- (11) Gong C, Shi S, Dong P, Kan B, Gou M, Wang X, et al. Synthesis and characterization of PEG-PCL-PEG thermosensitive hydrogel. *Int J Pharm* 2009;365(1):89-99.
- (12) Ni PY, Fan M, Qian ZY, Luo JC, Gong CY, Fu SZ, et al. Synthesis and characterization of injectable, thermosensitive, and biocompatible acellular bone matrix/poly (ethylene glycol)-poly ( $\epsilon$ -caprolactone)-poly (ethylene glycol) hydrogel composite. *Journal of Biomedical Materials Research Part A* 2012;100:171-179.
- (13) Jiang ZQ, Deng XM, Hao JY. Novel thermogelling poly ( $\epsilon$ -caprolactone-co-lactide)-poly (ethylene glycol)-poly ( $\epsilon$ -caprolactone-co-lactide) aqueous solutions. *Chinese Chemical Letters* 2007;18(6):747-749.
- (14) Bae SJ, Joo MK, Jeong Y, Kim SW, Lee W, Sohn YS, et al. Gelation behavior of poly (ethylene glycol) and polycaprolactone triblock and multiblock copolymer aqueous solutions. *Macromolecules* 2006;39(14):4873-4879.
- (15) Bae SJ, Suh JM, Sohn YS, Bae YH, Kim SW, Jeong B. Thermogelling poly (caprolactone-b-ethylene glycol-b-caprolactone) aqueous solutions. *Macromolecules* 2005;38(12):5260-5265.
- (16) Gong C, Shi S, Wu L, Gou M, Yin Q, Guo Q, et al. Biodegradable in situ gel-forming controlled drug delivery system based on thermosensitive PCL-PEG-PCL hydrogel. Part 2: Sol-gel-sol transition and drug delivery behavior. *Acta Biomaterialia* 2009;5(9):3358-3370.

- (17) Mahmud A, Xiong XB, Lavasanifar A. Novel Self-Associating Poly (ethylene oxide)-b lock-poly ( $\epsilon$ -caprolactone) Block Copolymers with Functional Side Groups on the Polyester Block for Drug Delivery. *Macromolecules* 2006;39(26):9419-9428.
- (18) Safaei Nikouei N, Lavasanifar A. Characterization of the thermo- and pH-responsive assembly of triblock copolymers based on poly(ethylene glycol) and functionalized poly(epsilon-caprolactone). *Acta Biomater* 2011 Oct;7(10):3708-3718.
- (19) Bae SJ, Suh JM, Sohn YS, Bae YH, Kim SW, Jeong B. Thermogelling poly (caprolactone-b-ethylene glycol-b-caprolactone) aqueous solutions. *Macromolecules* 2005;38(12):5260-5265.
- (20) Loh XJ, Tan YX, Li Z, Teo LS, Goh SH, Li J. Biodegradable thermogelling poly (ester urethane) s consisting of poly (lactic acid)-Thermodynamics of micellization and hydrolytic degradation. *Biomaterials* 2008;29(14):2164-2172.
- (21) Nguyen MK, Lee DS. Injectable biodegradable hydrogels. *Macromolecular bioscience* 2010;10(6):563-579.
- (22) Lee DS, Shim MS, Kim SW, Lee H, Park I, Chang T. Novel thermoreversible gelation of biodegradable PLGA-block-PEO-block-PLGA triblock copolymers in aqueous solution. *Macromolecular rapid communications* 2001;22(8):587-592.
- (23) Wang Q, Li L, Jiang S. Effects of a PPO-PEO-PPO triblock copolymer on micellization and gelation of a PEO-PPO-PEO triblock copolymer in aqueous solution. *Langmuir* 2005 Sep 27;21(20):9068-9075.
- (24) Takeuchi Y, Tsujimoto T, Uyama H. Thermogelation of amphiphilic poly (asparagine) derivatives. *Polym Adv Technol* 2011;22(5):620-626.
- (25) Liu Y, Shao Y, Lü J. Preparation, properties and controlled release behaviors of pH-induced thermosensitive amphiphilic gels. *Biomaterials* 2006;27(21):4016-4024.
- (26) Hou Y, Matthews AR, Smitherman AM, Bulick AS, Hahn MS, Hou H, et al. Thermoresponsive nanocomposite hydrogels with cell-releasing behavior. *Biomaterials* 2008;29(22):3175-3184.
- (27) Cheng Y, He C, Ding J, Xiao C, Zhuang X, Chen X. Thermosensitive hydrogels based on polypeptides for localized and sustained delivery of anticancer drugs. *Biomaterials* 2013.

## Chapter 4

### **Characterization of pH dependent thermo-gelation and TMR-D delivery by triblock copolymers based on PEG and functionalized PCL**

The content of this chapter is part of the following manuscript which is in preparation: Safaei Nikouei N, Shahin M, Lavasanifar A. Characterization of pH dependent thermo-gelation and TMR-D delivery by tri block copolymers based on PEG and functionalized PCL

## 1. Introduction

Thermo-reversible gel forming materials that are in sol phase in aqueous media and become gel as a result of an increase in temperature are of particular interest in biomedical field. This is due to their versatile potential applications including use in tissue engineering [1-3], as scaffolds for cell implantation, application in the formation of biosensors membranes [4], as bulking agents in the treatment of chronic infarcted myocardium [5], use in the prevention of post-surgical adhesion [6], and as noninvasive delivery systems for proteins, peptides and small molecule drugs.

One of the most important advantages of such materials in drug delivery and tissue engineering is that the drug molecules or living cells can simply be mixed with the polymer solution, then embedded within the gel network once it is formed in response to stimuli like temperature. In this case, the hydrogel network is formed without using any organic solvent or cross-linker making the hydrogel even more compatible with the drug and biological system [7,8]. Changes in the composition of polymer, can be used to induce a change in the amount of water entrapped within the polymeric network, or manipulate the degradation rate of the gel, and/or drug incorporation and release properties [9].

Amphiphilic block copolymers of specific structure are shown to be able to form micelles and then go through temperature responsive micellar association leading to the formation of thermo-reversible hydrogels. Among those are block copolymers consisting of (PEG) and poly( $\epsilon$ -caprolactone) (PCL) [10-12] which have been widely studied for drug delivery or tissue engineering applications [10,13,14]. Our research group has reported on the development of a new family of block copolymers based on PEG and PCL, where the PCL block has been functionalized through introduction of carboxyl and/or benzyl carboxylate groups to the  $\alpha$ -carbon of  $\epsilon$ -caprolactone units. In the previous chapters, we have

reported on the successful synthesis of triblock copolymers based on PEG (as the middle block) and  $\alpha$ -carboxyl/ $\alpha$ -benzyl carboxylate substituted PCL (as the lateral blocks), micellization of the prepared tri block copolymers and temperature/pH responsive association of prepared polymeric micelles [15]. In further studies, temperature responsive sol-gel transition of prepared block copolymers was characterized and the effect of pendent  $\alpha$ -carboxyl to  $\alpha$ -benzyl carboxylate ratio on the transition temperature and viscoelasticity of the gel was assessed [27]. This structure is expected to be responsive to pH in addition to temperature, because of the existence of free carboxyl groups on the polymeric backbone.

Introduction of pH sensitive moieties to temperature responsive polymer may, in fact, be used to narrow down the sol-gel transition temperature range of the thermo-gelling material; in other words, make the transition sharper [16]. Oligosulfamethazine–poly(lactide-co-caprolactone)–PEG–poly(lactide-co-caprolactone)–oligosulfa-methazine (OSM–PCLA–PEG–PCLA–OSM) is one example of pH/thermo-responsive polymers prepared through derivatization of PCLA-PEG-PCLA with a pH sensitive structure [17]. The OSM–PCLA–PEG–PCLA–OSM structure, formed a thermo-reversible gel at pH 7.4 at 37°C, but the gel was not formed at pH > 8 or < 6.5. Poly(N-isopropylacrylamide-co-acrylic acid), and poly(N-isopropylacrylamide-co-propylacrylic acid) copolymers are another examples of pH/temperature responsive copolymers where sections with pH and temperature responsiveness are incorporated in one copolymer structure [18]. Poly(N-isopropylacrylamide-co-acrylic acid) has been used to provide regional delivery of vascular endothelial growth factor (VEGF) in acidic environment like tumors, wounds, or ischemic regions. The copolymer didn't form gel at physiological pH (7.4), however lowering pH to 5.5 or below led to gel formation at 37°C. The release of VEGF was sustained by the gel for up to three weeks. In this case, a change in the pH of biological environment where the gel is

incorporated to 7.4 through healing of the wound, or improvement of ischemic condition was hypothesized to lead to gradual dissolution of the copolymer [19]. . In the current chapter, we report on the effect of using Tris buffer (instead of water) as the media on the temperature responsive sol-gel transition of the PCBCL-PEG-PCBCL triblock copolymers. The effect of a change in the pH of the media on the sol-gel transition temperature as well as the release of a model macromolecular fluorescence probe, i.e., tetramethylrhodamin-dextran (TMR-D), at two different molecular weights of 10 and 40 kDa from the prepared thermo-gelling material was also investigated.

## **2. Materials and methods**

### **2.1. Materials**

Dihydroxy-poly(ethylene glycol) (PEG) (Mw= 1450 Da) and Palladium, 10% on activated charcoal (Pd/C) were purchased from Sigma, St. Louis, MO.  $\alpha$ -benzyl carboxylate- $\epsilon$ -caprolactone (BCL) was synthesized by Alberta Research Chemicals Inc (ARCI), Edmonton, Canada. Tetramethylrhodamine Dextran (TMR-D) was purchased from Sigma-aldrich. All other chemicals and reagents were analytical grade.

### **2.2 Synthesis and characterization of triblock copolymer**

Triblock copolymer was synthesized as previously reported. Briefly, PBCL-PEG-PBCL was synthesized by ring opening polymerization of BCL using dihydroxy PEG as initiator in the absence of any catalyst. The polymerization was completed in 15 h at 160°C, after 3 hs of preheating at 140 °C. The resultant polymer went through partial debenzoylation under hydrogen gas using activated charcoal (5 %w/w) as catalyst. The degree of reduction was controlled by adjusting the time of reaction on 20 minutes. This led to the production of

poly( $\alpha$ -carboxyl-co- $\alpha$ -benzylcaboxylate- $\epsilon$ -caprolactone)-b-PEG-b-poly( $\alpha$ -carboxyl-co- $\alpha$ -benzylcaboxylate- $\epsilon$ -caprolactone) (PCBCL-b-PEG-b-PCBCL) triblock copolymer with 30 % reduction on the lateral blocks. In each step, the copolymer was washed by dichloromethane, and then precipitated in hexane. The washing process of each polymer was repeated three times. The composition of block copolymer (degree of polymerization and level of COOH substitution) was defined by  $^1\text{HNMR}$  as described before [27].

## **2.3 Characterization of the sol-gel transition of PCBCL-PEG-PCBCL solutions**

### **2.3.1. Inverse flow method**

The sol to gel transition of the synthesized polymer solutions was first determined by the tube inversion method [20]. Aqueous solutions of PCBCL-PEG-PCBCL block copolymer at concentrations of 7, 10, and 15% w/w were prepared using Tris buffer (pH 6.0). The 15x45 mm vials containing 1 mL polymer solutions in Tris buffer were immersed in a waterbath where the temperature was set at 25 $^{\circ}\text{C}$ . The temperature of the waterbath was allowed to increase by 1  $^{\circ}\text{C}$  every 5 min up to 60  $^{\circ}\text{C}$ . Phase transition (flow/no flow) was assessed by inverting the incubated tube vertically to allow a visual assessment of the aqueous polymer sample. The copolymer solution was considered gel when the solution did not flow for 1 minute upon inversion of vial. The incubation temperature, at which this phenomenon was observed, was recorded as the transition temperature. The pH of media was changed through addition of a few drops of 0.5 N HCl or NaOH solutions to reach pH 3.0 and 9.0, respectively. The effect of pH on the sol-gel transition of the triblock copolymer solution was assessed using the inverse flow methods as described above procedure as a function of temperature.

### **2.3.2. Dynamic Mechanical Analysis (DMA)**

The storage modulus,  $G'$ , and loss modulus,  $G''$ , for the copolymer solution in Tris buffer was determined using a Physica MCR xx0 rheometer equipped with a peltier heating/cooling plate and compared to that in water. Polymer solutions in Tris buffer (7, 10, and 15% w/w) were placed between two parallel plates. Temperature sweeps (20-60°C) were conducted at a fixed strain of 1% using an angular frequency of 10 rad/s. Sweeps were conducted at 1°C min<sup>-1</sup>. The change in the storage modulus and loss modulus as a function of temperature was plotted. The transition temperature of solution was estimated by dividing loss modulus to storage modulus values. The temperature after which the ratio of loss modulus to storage modulus was < 1 was considered sol-gel transition temperature.

### **2.3.3 Modulated Differential Scanning Calorimetry (MDSC)**

Thermal analysis was performed with Q series<sup>TM</sup> 2000 modulated differential scanning calorimeter. Sample of triblock copolymer at a concentration of 10% w/w in distilled water was prepared, and kept in refrigerator overnight. The samples were first heated to 70°C, and kept for 5 minute at this temperature to eliminate their thermal history. Heating scans were recorded using modulated mode with amplitude of 0.2°C in 30s and ramping of 0.5°C per minute. Scanning was conducted from 8 to 10°C, followed by holding the sample at 10°C for 15 minute, and then increased to 70°C. The pan filled with distilled water was used as reference.

## **2.4. Characterization of tetramethylrhodamin-dextran (TMR-D) loaded hydrogels**

Tetramethylrhodamine-Dextran (TMR-D) at two different molecular weights of 10000 and 40000 Da was loaded in the hydrogel as a model for large molecular weight drugs . The



incorporation of TMR-D into polymeric network was accomplished by mixing of dried polymer and TMR-D in water until the clear solution was achieved. TRM-D loaded hydrogel was then characterized for its rheological behavior using dynamic mechanical analysis as well as sol-gel transition temperature using Physica MCR xx0 rheometer equipped with a peltier heating/cooling plate as described before for unloaded hydrogels [27].

## **2.5. In vitro release of TMR-D from hydrogels**

The release profile of TMR-Ds of different molecular weights from the hydrogel was studied by adding pre-warmed (37 °C) Tris buffer (10 mL) on the hydrogel (0.2 mL) in a glass vial. While shaking in the waterbath at 37° C, 1 mL samples were withdrawn from media at specific intervals (0.08, 0.25, 0.5, 1, 2, 4, 8, 24, 48, 72, 96, and 120 h) and replaced with equal volume of fresh media. The amount of TMR-D released into media was determined by Synergy <sup>TM</sup>fluorescence spectroscopy with absorption and emission at 555 and 580 nm. The cumulative release percentage of TMR-D was calculated and plotted versus time. The release study was repeated at 25 and 50°C. In a separate experiment, few drops of 0.5 N HCl or NaOH solution was added to Tris buffer to change the pH of the media to 5.0 and 9.0, respectively, while keeping the salt concentration constant. The effect of pH of the medium on the release of TMR-D from hydrogel was then evaluated as described above.

### **2.3.6 Statistical analysis**

The significance of differences between results was assessed using unpaired Student's t test. The level of significance was set at  $\alpha=0.05$ .

### 3. Results and discussions

#### 3.1 The effect of aqueous media (Tris buffer versus water) on the thermoresponsive sol-gel transition of PCBCL-PEG-PCBCL

Figure 4-1 shows temperature dependent transition of PCBCL-PEG-PCBCL triblock copolymer (30% reduction) solution in Tris buffer. The polymer solution at a concentration of 7% w/w, formed a transparent gel at 29°C. This is the temperature used to identify the lower sol-gel transition point in the diagram. With further increase in temperature, the transparent gel became turbid, and upon further heating at 45 °C, a turbid solution was observed. This temperature was used as the upper transition point in the diagram. As illustrated in Figure 4-1, and similar to what has been observed for water [27], the lower transition temperature of blockcopolymer solution decreased by increasing the concentration of polymer in Tris buffer,. At a concentration of 15% w/w of polymer, lower transition temperature reached 8°C (compared to 29°C for the 7% w/w concentration). A reduction in the lower transition temperature as a result of an increase in polymer concentration can be attributed to an increase in the aggregation and packing interaction between micelles at higher polymer concentrations [21,22].

In general, the PCBCL-PEG-PCBCL solution showed lower transition temperature in Tris buffer compared to water at corresponding concentrations of polymer (7,10, and 15% w/w.) [27,28]. For instance at a 10 % polymer concentration, the sol-gel transition temperature was 27 °C in Tris buffer versus 30 °C in water, as determined by the inverse flow method. At the same polymer concentration, the upper transition was observed at 47 °C in Tris buffer versus 49 °C in water. The lower sol-gel transition temperatures observed in buffer compared to water can be attributed to the presence of electrolytes in buffer solution leading to salting-out effect [21]. In this case, Tris buffer will become a less favorable

solvent for the polymer than the pure water, thus copolymer will form gel at lower temperatures.

Changes in the storage modulus,  $G'$  as a function of temperature for the triblock copolymer solution in Tris buffer at different polymer concentrations is shown in Figure 4-2 A. The change in storage modulus,  $G'$ , as a function of temperature is compared to that for loss modulus,  $G''$ , in Figure 4-2B. In line with our findings using the inverse flow method, the lower transition temperature was shown to decrease by increasing the concentration of polymer in Tris buffer. A similar trend was observed in water as the media in our previous studies [27]. The loss modulus of triblock copolymer solution in Tris buffer was found to be mostly similar to the storage modulus at low temperatures, indicating a typical liquid state. Both storage and loss modulus increased at a certain temperature, but the level of increase in loss modulus was lower compared to increase in the storage modulus. This indicated gel formation [23]. The temperature at which the ratio of loss modulus to storage modulus passed one and stayed below one was considered as sol-gel transition temperature. This temperature was found to be 28°C for the triblock copolymer under study at 10 % concentration, which is in good agreement with the transition temperature defined by inverse flow method (Table 4-1).

A comparison between the temperatures responsive behavior of the triblock copolymer under study at a concentration of 10 % w/w in deionized water versus Tris buffer in terms of changes in storage modulus is shown in Figure 4-3. The sharp change in the mechanical properties of hydrogels in Tris buffer happened at lower temperatures compared to the same samples in distilled water. This observation is in line with lower sol-gel transition temperature of prepared block copolymers in Tris buffer observed by the inverse flow method.

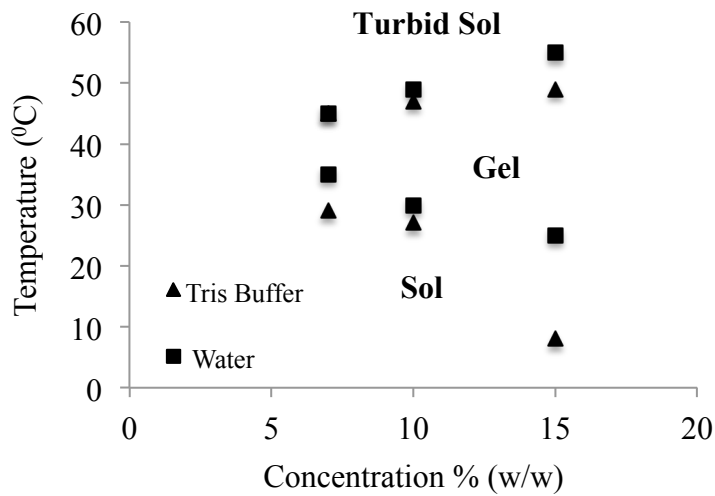


**Figure 0-1** Temperature dependent sol-gel transition of PCBCL-PEG-PCBCL 30% reduced polymer at different concentrations in Tris buffer versus water as defined by Inverse flow method. . Data in water is reproduced from Chapter 3, Figure 3.

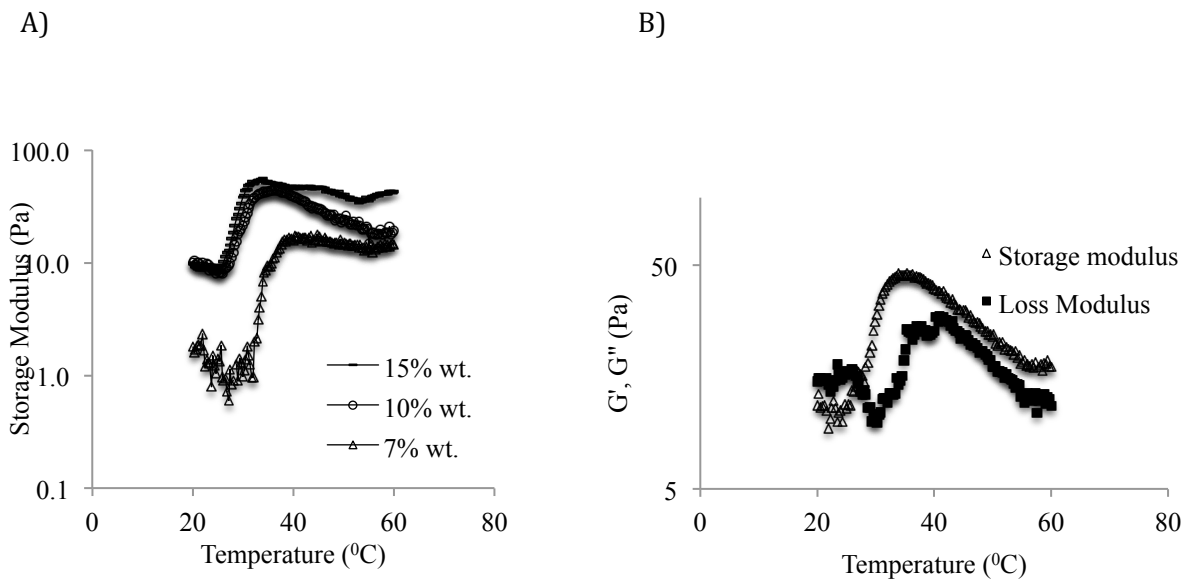


**Figure 0-2** A) Increases in storage modulus ( $G'$ ) of PCBCL-PEG-PCBCL of different concentrations as a function of temperature. B) Increase in storage modulus ( $G'$ ) and loss modulus ( $G''$ ) of PCBCL-PEG-PCBCL polymer at 10 % concentration as a function of rising temperature at  $1^\circ\text{C min}^{-1}$  ( $n=3$ ).

**Table 0-1 Comparison between the sol-gel transition temperatures of PCBCL-PEG-PCBCL copolymer solutions in Tris buffer at different concentrations as defined by inverse flow method versus DMA.**

Concentration of polymer (w/v %)	Sol-gel Transition Temperature ( $^{\circ}\text{C}$ ) <sup>a</sup>	
	Inverse flow method	DMA
7	29	32
10	27	26
15	8	16

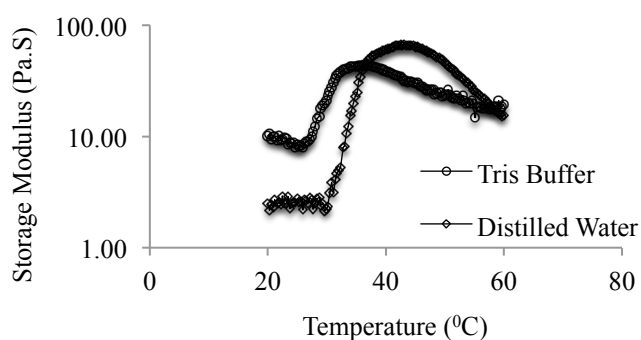


**Figure 0-3 Changes in the storage modulus of PCBCL-PEG-PCBCL block copolymer solution in water versus Tris buffer (10 % w/w) as defined by DMA (n=3).**

### **3.2 The effect of pH on the thermo-responsive sol-gel transition of PCBCL-PEG-PCBCL**

Figure 4-4 shows the temperature responsive gelation of triblock copolymer solution under study at concentration of 10% w/w at different pHs, i.e., pH of 3.0, 5.0, 6.0, 7.4, and 9.0. It can be seen from the graph that the polymer solution only forms gel at pHs  $\geq 5.0$ . Gel is not formed at pH 3.0. The transition temperature of the polymer solution to gel; however, was not affected by the pHs  $\geq 5.0$ . This is an interesting observation that can be attributed to differences in the ionization state of the substituted COOH on the PCBCL block. At pH 3.0, the COOH groups become mostly unionized. This can increase the tendency for micelle

formation and hiding of PCBCL segment within the micellar core. At higher pHs; however, the COOH group become ionized mostly. This may induce the mobilization of PCBCL segment out of the micellar core making it more prone to formation of micellar aggregates and networks through inter-micellar bridging of the hydrophobic units of PCBCL [24]. A material with pH responsive properties observed here, i.e., one that can form a stable gels at physiological pH but turn into solutions at slightly acidic pH, can find several applications in the field of drug delivery.

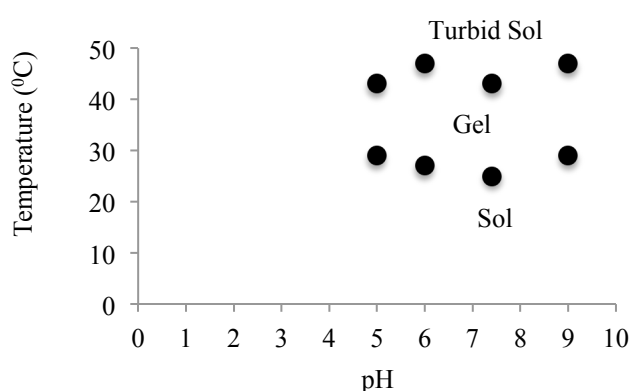


**Figure 0-4 pH and temperature dependent sol-gel transition of PCBCL-PEG-PCBCL solution in Tris buffer (10 % w/w) as defined by inverse flow method**

### **3.3. The effect of TMR-D loading on the thermo-responsive sol-gel transition of PCBCL-PEG-PCBCL**

We have loaded TMR-D of two different molecular weights in the PCBCL-PEG-PCBCL polymer solution in water as a mimic of a large molecular weight drug and assessed the effect of TMR-D loading on sol-gel transition of the polymer solution at 10 % w/w concentration. In general, loading of TMR-D did not appear to interfere with the gelation of the triblock copolymer solution in water but its presence affected the transition temperature of the block copolymer solution as defined by inverse flow method (Table 4-2); DMA and DSC (Figure 4-5 and 4-6). Moreover, storage modulus of hydrogel loaded with TMR-D was shown

to be higher compared with unloaded hydrogel indicating that addition of TMR-D can increase the mechanical strength of the hydrogel (Figure 4-5).

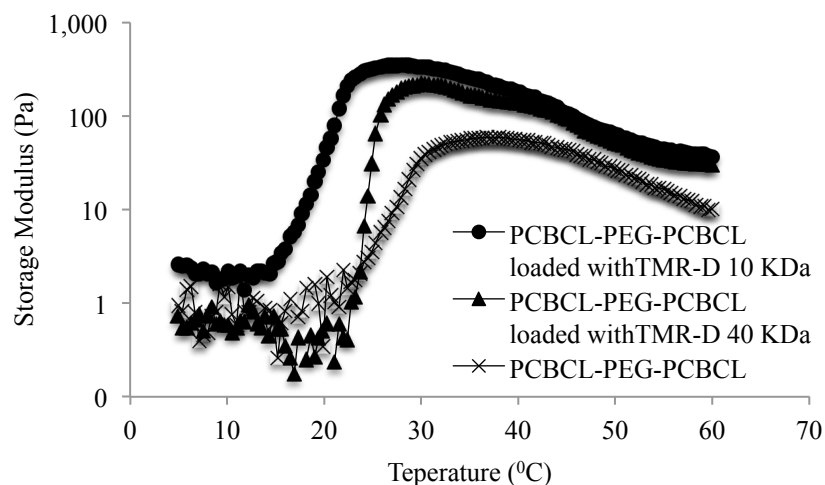


**Figure 0-5 Changes in storage modulus as a function of temperature for PCBCL-PEG-PCBCL block copolymer solution in water (10% w/w) alone or loaded with TMR-D 10 or 40k Da (n=3)**

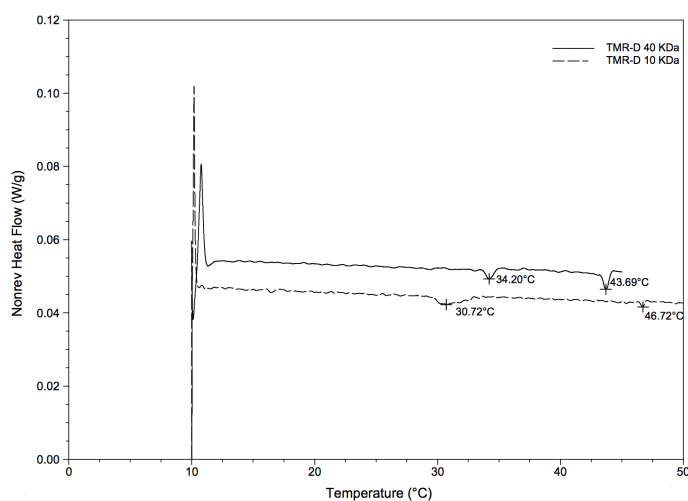


**Figure 0-6 DSC thermogram of TMR-D loaded PCBCL-PEG-PCBCL solution in Tris buffer**

**Table 0-2 Comparison between the sol-gel transition temperatures of PCBCL-PEG-PCBCL (10% w/w) loaded with TMR-D 10, or 40kDa using different methods of measurement**

PCBCL-PEG-PCBCL Sample	TMR-D Loading (w/w%)	Sol-gel Transition Temperature (°C)		
		Inverse flow method	DMA	DSC
loaded with TMR-D 10kDa	0.01	27	21	30
loaded with TMR-D 40kDa	0.01	29	24	34
unloaded	0	30	30	35

Table 4-2 summarizes the transition temperature of the triblock copolymer solution in water loaded with TMR-D 10 kDa, or 40 kDa as defined through inverse flow methods, DMA and DSC analysis. For comparison data related to unloaded triblock copolymer solution is also presented in the same Table. It can be seen that the addition of TMR-D 10 kDa led to a lower sol-gel transition temperature compared to TMRD 40 kDa irrespective of the method of measurement for the transition temperature. This can be attributed to the better solubility of TMR-D 10kDa in water that may promote the salting out of the polymeric solution leading to gel network formation. Another possibility is the stabilizing role of TMR-D on the formation of inter-micellar bridges, which is hypothesized to be responsible for the formation of the gel network.

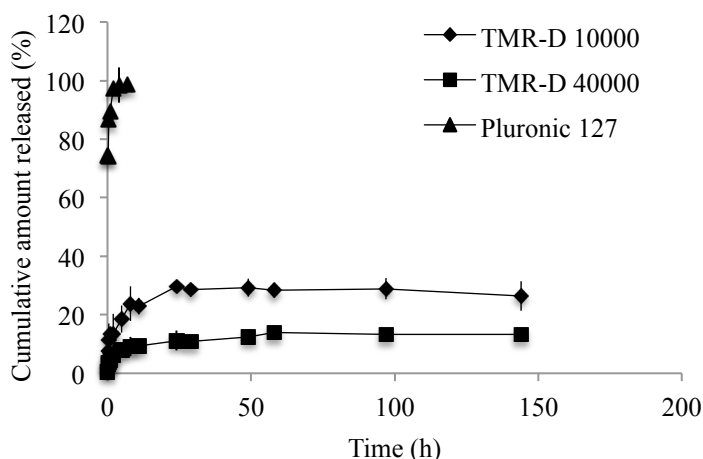
### **3.4 Temperature and pH responsive release of TMR-D from the prepared gels**

The release profile of TMR-D 10 kDa is compared with that for TMR-D 40 kDa from PCBCL-PEG-PCBCL gels in Tris buffer (pH=7.4) in Figure 4-7. For comparison the release



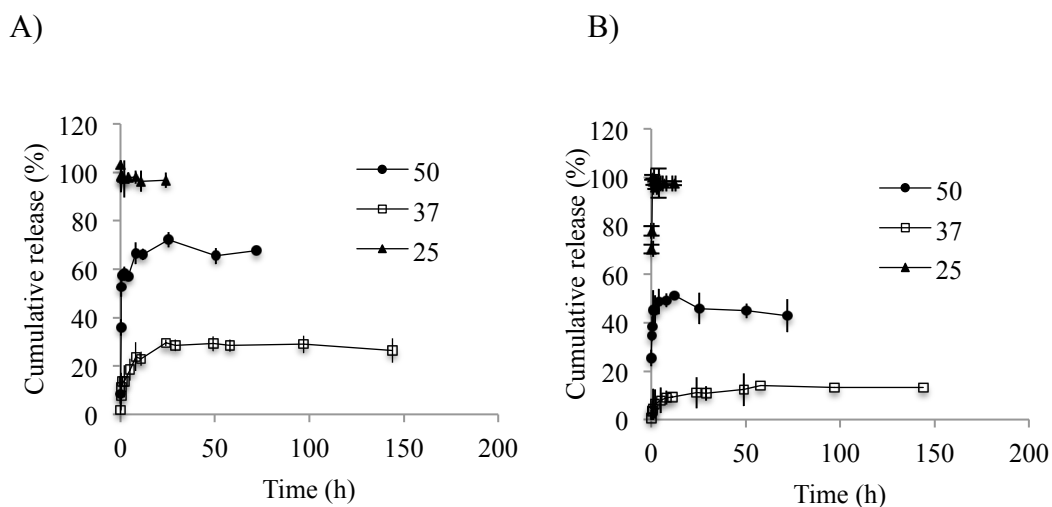
profile of TMR-D from Pluronic® F127 is reported. In general, the diffusion of large molecular weight drugs through diffusion is expected to be very limited and slow from the gel network. In line with this expectation, the release of TMR-D (both molecular weights) was very slow from the prepared gel at 37 °C. For both molecular weights, a burst release was seen within the first few hours of sampling. This was followed by a much slower release rate. In contrast, under the same conditions, TMR-D was released rapidly from Pluronic® F127 gel, perhaps because of the low mechanical strength of this gel. The results of this control sample; however, shows existence of sink condition under conditions in which the study was performed.

The initial burst release phase observed for TMR-D from PCBCL-PEG-PCCL gel, is most likely due to the diffusion of the adsorbed TMRD, TMRD encapsulated in the vicinity of the gel surface or TMRD release from pores close to the surface of the gel that are larger than the size of the encapsulated TMRD. The release of TMR-D appeared to plateau after 24 and 48 hs for 10 and 40 kDa TMR-D, respectively. The cumulative release of TMR-D 10kDa was 23.7% compared to 13.2% for 40kDa at 144 h reflecting a slower diffusion of the larger macromolecule from the pores within the gel network. For drugs with the molecular size comparable to or larger than the gel pore size, further release will most likely be achieved by erosion/degradation of the polymer network, which does not appear to be happening in this case during the time line of the study (150 min) [26]. In fact the results of our degradation study (Data reported in Chapter 5) shows this is the case.



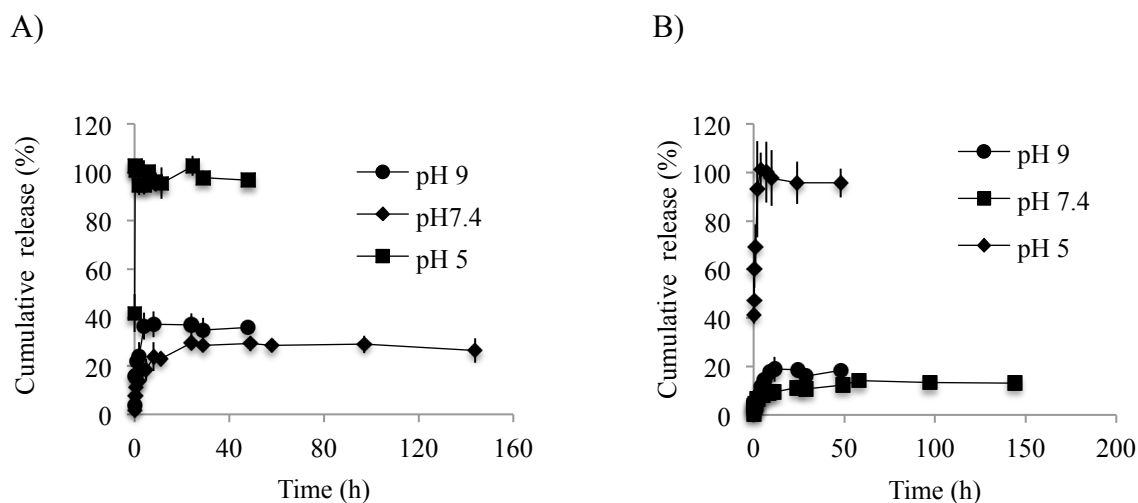
**Figure 0-7 Release profile of TMR-D 10 and 40 kDa, or pluronic 127 from PCBCL-PEG-PCBCL gels in Tris Buffer (pH 7.4) at 37 °C (n=3).**

Figure 4-8A and B show the effect of temperature on the release profile of TMR-D 10 and 40kDa, respectively. At room temperature 100 % of the loaded TMR-D was released in the media within 0.5 h irrespective of the TMR-D molecular weight. TMR-D release was dramatically increased at 50° C for both TMR-D molecular weights (release of 46% for TMR-D 40 kDa and 72% for TMR-D 10 kDa within 24 h) compared to release at 37 °C (release of 11% for TMR-D 40 kDa and 27% for TMR-D 10 kDa at the same time point). The increase in the release rate from 37 to 50°C can be explained by differences in the rigidity and stiffness of the hydrogels at these two different temperatures. At 50°C the PCBCL-PEG-PCBCL hydrogel show lower mechanical strength compared to 37°C (Figure 4-5). The cumulative release of TMR-D 40 kDa was still lower than that of TMR-D 10 kDa even at 50 °C.



**Figure 0-8 Temperature dependent release profile of TMR-D A) 10kDa and B) 40kDa from prepared hydrogels in Tris buffer (pH=7.4) (n=3).**

The release experiments were also conducted at pH 5.0, 7.4, and 9.0 for block copolymers loaded with TMR-D 10 and 40 kDa. The results are presented in Figure 4-9A and B. For TMR-D 10 kDa, the release rate from the hydrogel significantly was increased at pH 9.0 compared to the release rate at pH 7.4 ( $P < 0.05$ , student's t test). For TMR-D 40 kDa similar release in both pH was seen ( $P > 0.05$ , student's t test). The cumulative release % of TMR-D10 and 40 kDa after 24 h was 37 and 18 % at pH 9.0 compared to 28, and 11% release of TMR-D at pH 7.4 within the same timeframe, respectively. Similar to pH 7.4, release of TMR-D 40 kDa was lower than the release of TMR-D 10 kDa at pH 9.0. At pH 5.0, both TMR-Ds were released very rapidly from the hydrogel within 0.25 and 4 hours for TMR-D 10 kDa and 40 kDa respectively. The fast release of TMR-D at pH 5.0 may reflect a tendency for dissociation of the gel network at pH 5.0.



**Figure 0-9 pH dependent release profile of TMR-D A) 10 and B) 40 kDa from the prepared hydrogel at 37°C (n=3).**

#### 4. Conclusion

The use of Tris buffer instead of water lowered the sol-gel transition temperature of PCBCL-PEG-PCBCL block copolymer and also made the gel more stable. PCBCL-PEG-PCBCL block copolymer showed thermo-reversible sol-gel transition at or above pH 5.0, but did not form gel at pH 3.0. The transition temperature of the block copolymer was independent of the pH of the media at pHs above 5.0, however. The PCBCL-PEG-PCBCL gel was able to restrict the release of model large molecular weight molecules, i.e., TMR-D, at physiological temperature (37 °C) and pH (7.4). The cumulative release of TMR-D was inversely proportional to the molecular weight of the TMR-D. . When pH was kept at physiological pH, a faster TMR-D release was observed at room temperature and 50 °C. At 37 °C, rapid release of TMR-D was observed at slightly acidic pH of 5.0. TMR-D release was also higher at pH 9.0 than 7.4 at physiological temperature. The results show the potential of developed polymer for application as biodegradable temperature and pH responsive biomaterials for drug/protein delivery.

**Acknowledgement:**

The authors would like to thank Dr. Ali Akbari and Dr. Jianping Wu for providing rheometer equipment for this study.

## References:

- (1) Tan H, Ramirez CM, Miljkovic N, Li H, Rubin JP, Marra KG. Thermosensitive injectable hyaluronic acid hydrogel for adipose tissue engineering. *Biomaterials* 2009;30(36):6844-6853.
- (2) Crompton K, Goud J, Bellamkonda R, Gengenbach T, Finkelstein D, Horne M, et al. Polylysine-functionalised thermoresponsive chitosan hydrogel for neural tissue engineering. *Biomaterials* 2007;28(3):441-449.
- (3) Stile RA, Healy KE. Thermo-responsive peptide-modified hydrogels for tissue regeneration. *Biomacromolecules* 2001;2(1):185-194.
- (4) Gant R, Abraham A, Hou Y, Cummins B, Grunlan M, Coté G. Design of a self-cleaning thermoresponsive nanocomposite hydrogel membrane for implantable biosensors. *Acta biomaterialia* 2010;6(8):2903-2910.
- (5) Fujimoto KL, Ma Z, Nelson DM, Hashizume R, Guan J, Tobita K, et al. Synthesis, characterization and therapeutic efficacy of a biodegradable, thermoresponsive hydrogel designed for application in chronic infarcted myocardium. *Biomaterials* 2009;30(26):4357-4368.
- (6) Moon HJ, Park MH, Joo MK, Jeong B. Temperature-responsive compounds as in situ gelling biomedical materials. *Chem Soc Rev* 2012;41(14):4860-4883.
- (7) Peppas N, Bures P, Leobandung W, Ichikawa H. Hydrogels in pharmaceutical formulations. *European journal of pharmaceutics and biopharmaceutics* 2000;50(1):27-46.
- (8) Van Tomme SR, Storm G, Hennink WE. < i> In situ gelling hydrogels for pharmaceutical and biomedical applications. *Int J Pharm* 2008;355(1):1-18.
- (9) Lowman AM. *Smart pharmaceuticals* 2008.
- (10) Yin HB, Gong CY, Shi S, Liu XY, Wei YQ, Qian ZY. Toxicity evaluation of biodegradable and thermosensitive PEG-PCL-PEG hydrogel as a potential in situ sustained ophthalmic drug delivery system. *Journal of Biomedical Materials Research Part B: Applied Biomaterials* 2010;92(1):129-137.
- (11) Gong C, Shi S, Dong P, Kan B, Gou M, Wang X, et al. Synthesis and characterization of PEG-PCL-PEG thermosensitive hydrogel. *Int J Pharm* 2009;365(1):89-99.
- (12) Vermonden T, Censi R, Hennink WE. Hydrogels for Protein Delivery. *Chem Rev* 2012;112:2853-2888.
- (13) Ni PY, Fan M, Qian ZY, Luo JC, Gong CY, Fu SZ, et al. Synthesis and characterization of injectable, thermosensitive, and biocompatible acellular bone matrix/poly (ethylene glycol)-poly ( $\epsilon$ -caprolactone)-poly (ethylene glycol) hydrogel composite. *Journal of Biomedical Materials Research Part A* 2012;100:171-179.
- (14) Jiang ZQ, Deng XM, Hao JY. Novel thermogelling poly ( $\epsilon$ -caprolactone-< i> co-lactide)-poly (ethylene glycol)-poly ( $\epsilon$ -caprolactone-< i> co-lactide) aqueous solutions. *Chinese Chemical Letters* 2007;18(6):747-749.
- (15) Safaei Nikouei N, Lavasanifar A. Characterization of the thermo- and pH-responsive assembly of triblock copolymers based on poly(ethylene glycol) and functionalized poly(epsilon-caprolactone). *Acta Biomater* 2011 Oct;7(10):3708-3718.
- (16) Huynh CT, Nguyen MK, Lee DS. Injectable block copolymer hydrogels: Achievements and future challenges for biomedical applications. *Macromolecules* 2011;44(17):6629-6636.

- (17) Shim WS, Yoo JS, Bae YH, Lee DS. Novel injectable pH and temperature sensitive block copolymer hydrogel. *Biomacromolecules* 2005;6(6):2930-2934.
- (18) Yin X, Hoffman AS, Stayton PS. Poly (N-isopropylacrylamide-co-propylacrylic acid) copolymers that respond sharply to temperature and pH. *Biomacromolecules* 2006;7(5):1381-1385.
- (19) Garbern JC, Hoffman AS, Stayton PS. Injectable pH-and temperature-responsive poly (N-isopropylacrylamide-co-propylacrylic acid) copolymers for delivery of angiogenic growth factors. *Biomacromolecules* 2010;11(7):1833-1839.
- (20) Bae SJ, Suh JM, Sohn YS, Bae YH, Kim SW, Jeong B. Thermogelling poly (caprolactone-b-ethylene glycol-b-caprolactone) aqueous solutions. *Macromolecules* 2005;38(12):5260-5265.
- (21) Wang Q, Li L, Jiang S. Effects of a PPO-PEO-PPO triblock copolymer on micellization and gelation of a PEO-PPO-PEO triblock copolymer in aqueous solution. *Langmuir* 2005 Sep 27;21(20):9068-9075.
- (22) Lee DS, Shim MS, Kim SW, Lee H, Park I, Chang T. Novel thermoreversible gelation of biodegradable PLGA-block-PEO-block-PLGA triblock copolymers in aqueous solution. *Macromolecular rapid communications* 2001;22(8):587-592.
- (23) Cheng Y, He C, Ding J, Xiao C, Zhuang X, Chen X. Thermosensitive hydrogels based on polypeptides for localized and sustained delivery of anticancer drugs. *Biomaterials* 2013.
- (24) Bae SJ, Suh JM, Sohn YS, Bae YH, Kim SW, Jeong B. Thermogelling poly (caprolactone-b-ethylene glycol-b-caprolactone) aqueous solutions. *Macromolecules* 2005;38(12):5260-5265.
- (25) Safaei Nikouei N, Lavasanifar A. Characterization of the thermo-and pH-responsive assembly of triblock copolymers based on poly (ethylene glycol) and functionalized poly ( $\epsilon$ -caprolactone). *Acta Biomaterialia* 2011;7(10):3708-3718.
- (26) Schillemans JP, Verheyen E, Barendregt A, Hennink WE, Van Nostrum CF. Anionic and cationic dextran hydrogels for post-loading and release of proteins. *J Controlled Release* 2011;150(3):266-271.
- (27) Safaei Nikouei N, Vakili M, Akbari A, Wu J, Lavasanifar A. Biodegradable Thermo-reversible Hydrogels based on Triblock Copolymers of PEG and Functionalized Poly( $\epsilon$ -caprolactone). *Biomaterials*, submitted (2013)
- (28) Safaei Nikouei N. Development of Novel Stimuli-Responsive Drug Delivery Systems. Doctor of Philosophy thesis; Chapter 3.

## Chapter 5

### **Thermoresponsive PCBCL-PEG-PCBCL triblock copolymer for Cyclosporin A delivery**

The content of this chapter has will be submitted as part of: Safaei Nikouei N, Shyam G, Lavasanifar A. In vitro evaluation of thremo-reversible PCBCL-PEG-PCBCL tri block copolymers for depot cyclosporin A delivery



## 1. Introduction

Cyclosporine A (CyA) is a potent immunosuppressive agent used for the prevention of organs` rejection after transplantation or the treatment of autoimmune diseases like rheumatoid arthritis and psoriasis [1,2]. Moreover, because of its anti-inflammatory effect, it has been used for the treatment of many ophthalmic disorders like dry eye syndrome, uveitis, and peripheral ulcerative keratitis [3]. In such disease conditions, T-cell activation leads to the secretion of cytokines causing inflammation on ocular surface. Inflammation of ocular surface in return decreases the sensitivity of eye surface leading to dysfunction of sensory autonomic neural reflex loop and decrease in tear secretion from lacrimal glands [2].

Emulsion based products are used as eye drops but their use is not ideal for several reasons. First, ocular medications used in form of emulsions suffer from low bioavailability. More than 95% of drug reaches systemic circulation through transnasal or conjunctival absorption [3]. Second, the use of emulsions blurs the vision and is inconvenient for the patient. Sustained release of CyA by transparent gels may be used to address the problem of poor retention and low bioavailability of CyA delivery. For instance, incorporation of CyA in nanostructured poly(2-hydroxyethyl methacrylate) (p-HEMA) hydrogels containing microemulsions or micelles of Brij 97 ( $C_{18}H_{35}(OCH_2CH_2)_{10}$ ) has been tried. The *in vitro* release study showed sustained release of CyA from this delivery system for 20 days (4). Peng et al. studied CyA release from ACUVUE® and extended wear silicone hydrogel (SiH) lenses. Cyclosporine was loaded into contact lenses by soaking lenses in CyA solution. The release studies showed one day and two weeks release from ACUVUE® and SiH lenses respectively [3].

Application of thermo-responsive polymer solutions that form gel in contact with cornea, may increase the bioavailability of CyA through increasing residence time of drug in

the eye [5] improving patient compliance. The transparent nature of the polymer solution is an added advantage which can address the problem of blurred vision.

In previous chapters we have reported on the development of thermo and pH responsive gels based on triblock copolymers of poly( $\alpha$ -carboxyl-co-benzyl carboxylate- $\epsilon$ -caprolactone)-*b*-PEG-*b*-poly( $\alpha$ -carboxyl-co-benzyl-carboxylate- $\epsilon$ -caprolactone) (PCBCL-*b*-PEG-*b*-PCBCL) [6] (Chapter 3 and 4). The main objective of this chapter was to evaluate the capacity of PCBCL-PEG-PCBCL triblock copolymer hydrogel for sustained delivery of CyA for intended potential use as an ocular medication in dry eye syndrome or depot immunosuppressant in other inflammatory as well as auto immune disorders. In this context, the capacity of PCBCL-PEG-PCBCL gel for loading and *in vitro* release of CyA, as well as and r biocompatibility, immunogenicity and cytotoxicity of hydrogel was investigated, *in vitro*.

## **2. Materials and methods**

### **2.1. Materials**

Human umbilical vein (HUV-EC) cells were received as gift from the laboratory of Dr Sandra Davidge, University of Alberta.  $\alpha$ -benzyl carboxylate- $\epsilon$ -caprolactone (BCL) was synthesized by Alberta Research Chemicals Inc (ARCI), Edmonton, Canada. Cyclosporine A was purchased from LC laboratories, USA. Poly(ethylene glycol), and sodium dodecyl sulfate (SDS) was purchased from Sigma-Aldrich. Pluronic® F127 was purchased from BASF. All other chemicals and reagents were analytical grade. Fetal calf serum (FCS) was obtained from Hyclone Laboratories (Logan, UT, USA). Anti-mouse CD16/CD32, CD40, and CD86, MHCII mAbs, and their respective isotype controls were purchased from BD Biosciences (Mississauga, ON, Canada). Recombinant granulocyte-macrophage colony-stimulating factor

(GM-CSF) was purchased from Peprotech (Rocky Hill, NJ, USA). Murine IL-2 ELISA kits were purchased from E-Bioscience (San Diego, CA, USA).

## 2.2. Synthesis and characterization of triblock copolymer

Triblock copolymer was synthesized as previously reported (16). Briefly, poly( $\alpha$ -benzyl carboxylate- $\epsilon$ -caprolactone)-*b*-poly(ethylene glycol)-*b*-poly( $\alpha$ -benzyl carboxylate- $\epsilon$ -caprolactone) (PBCL-PEG-PBCL) was synthesized by ring opening polymerization of BCL by dihydroxyl PEG. The polymerization was completed in 15h at 160°C, after 3 h of preheating at 140 °C. The resultant polymer was then undergone partial debenzoylation process using activated charcoal as catalyst. The time of reaction and amount of catalyst was fixed at 45 min and 5% w/w to produce PCBCL-*b*-PEG-*b*-PCBCL with 50 % COOH substitution on the PCBCL segment. In each step, synthesis product was washed by dichloromethane, and then precipitated in hexane. The washing process was repeated three times. <sup>1</sup>H NMR spectroscopy in CDCl<sub>3</sub> was used to study the composition of copolymer. Briefly degree of benzyl carboxylate substitution on the polymer backbone was estimated by comparing the integration of the peak related to the protons of the PCBCL backbone (-CH<sub>2</sub>O-,  $\delta$ = 4.1 ppm) to the integration of the peak related to the methylene protons of the benzyl carboxylate group (-CH<sub>2</sub>-O-C=O,  $\delta$ =5.15). The temperature responsive sol-gel transition of prepared triblock copolymer at different concentrations (7-15 % w/w) was then characterized using inverse flow method, differential scanning calorimetry, and dynamic mechanical analysis [16].

## 2.3 *In vitro* degradation of the gel

The degradation study was carried out at 37 ° C in distilled water. 5 mL polymeric aqueous solution (4 mg/mL) was placed into different vials. The vials were incubated in

waterbath at 37°C. At pre-determined times (0, 1, 2, 4, 8, 12, 16, 20, 30, 40, 50, and 60 days) one vial was removed. Mean diameter of micelles for each sample was determined by dynamic light scattering (DLS) using Nano-ZS Zetasizer (Malvern Instruments Ltd., UK) at 25°C.

The pH of the medium was measured by Accumet® model 20 pH meter. Samples were dried under vacuum for two days, then washed by tetrahydroforane (THF) and precipitated in ethyl ether. The remained THF and ethyl ether was then evaporated. The samples were then dissolved in CDCl<sub>3</sub> for <sup>1</sup>H NMR. Degree of polymerization for PCBCL blocks in PCBCL-PEG-PCBCL was identified by comparing peak intensity of PEG (-CH<sub>2</sub>CH<sub>2</sub>O-, δ=3.65 ppm) to that of PCBCL backbone (-O-CH<sub>2</sub>-, δ=4.1 ppm).

#### **2.4 *In vitro* cytotoxicity assay**

To assess the biocompatibility of the synthesized polymer, cytotoxicity test was performed by MTT assay following incubation of polymer solutions at different concentrations with human umbilicalvein cells (HUV-EC). Cells were seeded in 96-well plates at 10<sup>4</sup> cells per well in 100 μL of M199 and incubated in 5% CO<sub>2</sub> atmosphere for 24 h. To make the complete growth medium, fetal bovine serum and endothelial cell growth supplement (ECGS) was added to the media to make a final concentration of 15 and 1 %, respectively. Then 100 μL of PCBCL-PEG-PCBCL, Pluronic® F-127 (as negative control), and SDS as( positive control) in M199 was added to the cells at concentrations of 2.5, 1.25, 0.625, and 0.325 mg/mL. After 72 h incubation, 10 μL of MTT (5 mg/mL) was added into each well, followed by incubation at 37 °C for 3 h. The MTT-containing media was then replaced by 200 μL of DMSO. The absorbance of samples was measured by Bio-Tek plate reader. Percent cell viability was measure by comparing the absorbance of each sample to

untreated cells grown under the same conditions. Percent cell viability was then plotted versus log concentration.

## **2.5 Assessing the *in vitro* immunogenicity of polymer by studying the level of DC maturation and cytokine quantification**

The immunogenicity of the gel was assessed *ex vitro* following its incubation with murine bone marrow-derived DCs. Murine bone marrow-derived DCs (BMDCs) were generated from femurs of BALB/c mice as reported previously [7]. BMDCs were treated with 1 µg/mL PCBCL in distilled water. Untreated DCs and DCs treated with 1 µg/mL lipopolysaccharide (LPS) were used as negative and positive controls, respectively. Following 72 h incubation, DCs were harvested and tested for the up-regulation of maturation surface markers (CD40, and CD86) by flow cytometry. Culture supernatants were also collected at the end of the 72 h culture and assayed for the level of IL-12 secretion using by ELISA kits as per manufacturer's recommendation. For flow cytometric studies,  $2.5 \times 10^5$  DCs were suspended in FACS buffer (PBS with 5% FCS, and 0.09% sodium azide) and incubated with anti- mouse CD16/CD32 mAb to block Fc receptors, then stained with appropriate fluorescent-labeled conjugated antibodies. All samples were finally acquired on a Becton-Dickinson FAC Sort and analyzed by CellQuest software [7].

## **2.6 Drug loading**

Cyclosporin A incorporation was accomplished by dissolving 100 mg of polymer and 1.5 mg of drug in acetone followed by drop-wise addition of this solution into 1 mL of distilled water. Acetone was then evaporated under vacuum.

Aqueous solution of 50% reduced block copolymer (10% w/w) loaded with two

different feeding amounts of CyA (3, and 1.5 mg/mL) was diluted two times with BSA. The level of CyA loaded in hydrogel was measured by LC-MS (Waters Micromass ZQTM 4000 spectrometer coupled to a Waters 2795 pump and autosampler, Milford, MA, USA) equipped with electron spray ionization (ESI) source. After extracting the drug, to 100  $\mu$ L of sample containing 30  $\mu$ L of amiodarone as internal standard (62.5  $\mu$ g/mL) 700  $\mu$ L of HPLC water and 80  $\mu$ L of 1 M NaOH was added. The CyA was extracted by adding 4 mL of 95:5 ether/methanol followed by vortex mixing for 60 s. The samples were then centrifuged at  $3000 \times g$  for 5 min. The supernatant organic layer was transferred into clean glass tubes and evaporated to dryness in vacuum for 30 min. The dried samples were then reconstituted with 500  $\mu$ L of HPLC-grade methanol. This solution (10  $\mu$ L) was injected into the LC-MS system [1]. Loading efficiency was calculated from the following equation:

$$\text{Loading efficiency} = \frac{\text{Amount of loaded CyA in mg}}{\text{Amount of added CyA in mg}} \times 100$$

## **2.8 Characterization of thermo-responsive sol-gel transition for CyA loaded PCBCL-PEG-PCBCL**

### *a) Visual observation of sol-gel transition by tube inversion method*

The sol to gel transition of block copolymer solution loaded with different amounts of CyA was first determined by the tube inversion method (8,9). Vials (15x45 mm) containing 1 mL polymer aqueous solution were immersed in a waterbath where the temperature was set at 25°C. The temperature of waterbath was allowed to increase by 1°C every 5 min up to 60°C. Phase transition (flow/no flow) was assessed by inverting the incubated tube vertically to allow a visual assessment of the aqueous polymer sample. The copolymer solution was considered gel when the solution did not flow for 1 minute upon inversion of vial. The

incubation temperature, at which this phenomenon was observed, was recorded as the transition temperature.

#### *b) Modulated Differential Scanning Calorimetry (MDSC)*

Thermal analysis was performed with Q series™ 2000 modulated differential scanning calorimeter in order to measure sol-gel behavior of CyA loaded hydrogel. Aqueous solution of block copolymer loaded with CyA (1.5 mg/mL) were prepared and kept in refrigerator overnight. Each sample (10 mg) was then hermetically sealed in an aluminum pan. The samples were first heated to 50°C, and kept for 5 minute at this temperature to eliminate their thermal history. Heating scans were recorded using modulated mode with amplitude of 0.2°C in 60s and ramping of 0.5°C per minute. Scanning was conducted from 8 to 10°C, followed by holding the sample at 10°C for 15 minute, and then increasing the temperature to 70°C. A pan filled with distilled water was used as reference.

### **2.9 *In vitro* release study**

The release of CyA was measured by placing 1 mL of each sample into dialysis bags (M.wt. cut-off = 14000 g/mol). The dialysis bag was located in BSA solution (4% w/v, 80 mL) while stirring at 37 °C. Samples of 1 mL were taken from the BSA solution at predetermined time interval, and replaced by identical volume of fresh media. Level of released CyA in each sample was measured by LC-mass after drug extraction as described in section 2.6.

### **2.11 Statistical analysis**

The significance of differences between results was assessed using unpaired Student's t test. The level of significance was set at  $\alpha=0.05$ .

### 3. Results and Discussion

#### 3.1 Degradation study

The pH value of the polymeric solution at different standing time in water bath at 37°C. It can be seen from the graph that the pH value of the solution didn't change up on 30 days. However, a decrease in pH value from 6 to 4.5 was observed from day 30 to day 60. The same trend was observed in the mean diameter of micelles; where no significant change in the average diameter of micelles up to 30 days of incubation at 37°C was seen, (from 100.2 nm on day one to 95.7 nm on day 30). However, the average diameter of micelles significantly decreased and reached 75 nm at day 60 ( $p < 0.05$ , unpaired student t test) (Figure 5-1B). The change in the degree of polymerization of PCBCL based on  $^1\text{H}$  NMR shows a decreasing trend within 60 days of incubation in water at 37 °C (Figure 5-2). This observation was in line with the decreasing trend in the pH and size of PCBCL-PEG-PCBCL micelles.

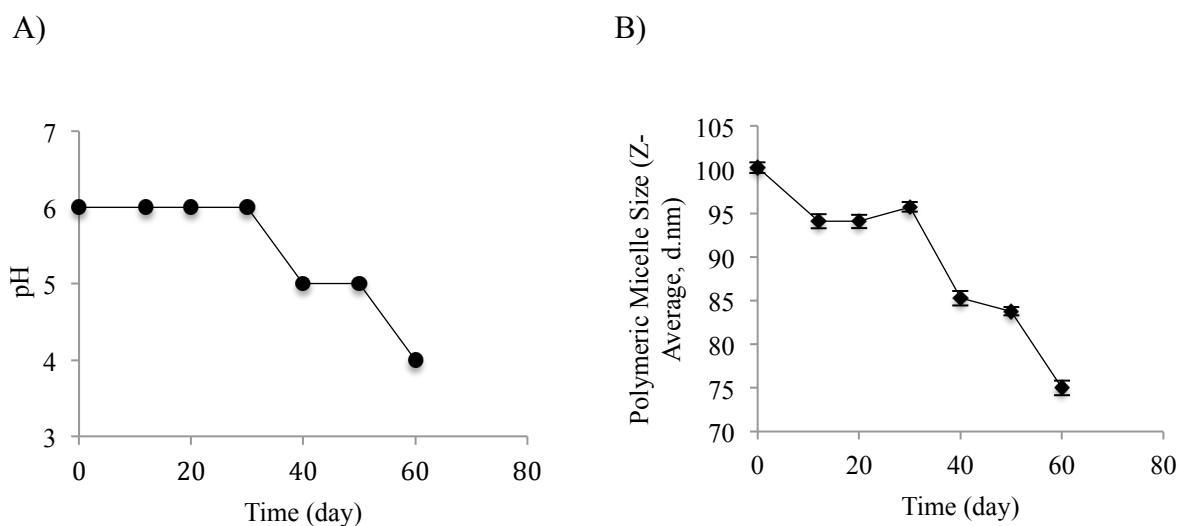


**Figure 5-1** The change in A) medium pH; and B) size of polymeric micelle over time upon incubation in distilled water at 37 °C. Error bar is standard deviation of average size of micelle based on three measurements.



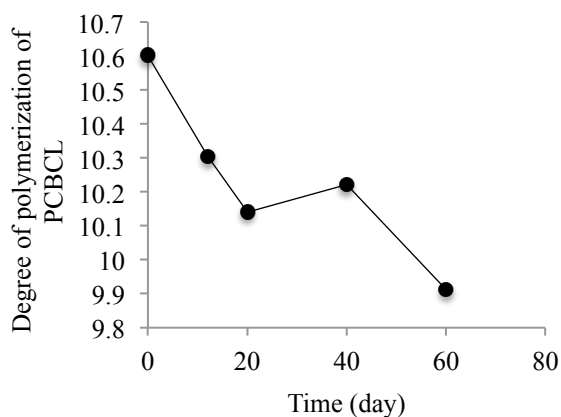


**Figure 5-2** The change in degree of polymerization of PCBCL backbone as measured by  $^1\text{H}$  NMR upon incubation in distilled water at  $37^\circ\text{C}$ .

### **3.2 *In vitro* cytotoxicity assay**

Figure 5-3 exhibits HUV-EC cell viability in the presence of the polymer solution at different concentrations ranging between 0.31 to 2.5 mg/mL using Pluronic® F 127 and SDS as negative and positive controls, respectively. The results demonstrate that cell viability decreased dramatically with increase of SDS concentration (92 and 0.67 % cell viability in the presence of 0.312 and 2.5 mg/mL SDS solution). As shown in Figure 5.3, with an increase in the concentration of PCBCL-PEG-PCBCL block copolymer from 0.312 to 2.5 mg/mL, cell viability only decreased from 98 to 81%. The FDA approved Pluronic® copolymer, showed cell viability of 77.8 and 84.4 % at similar concentrations, respectively.

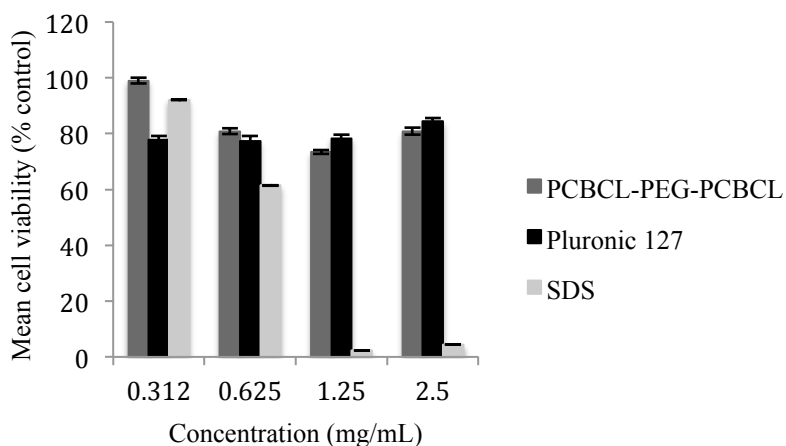
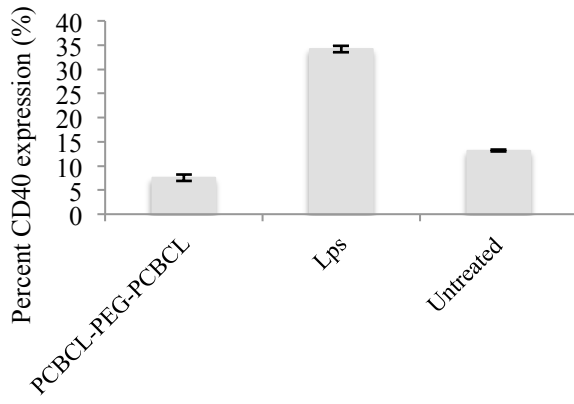


**Figure 5-3 Cytotoxicity of PCBCL-PEG-PCBCL against HUV-EC cell line after 72 h of incubation**

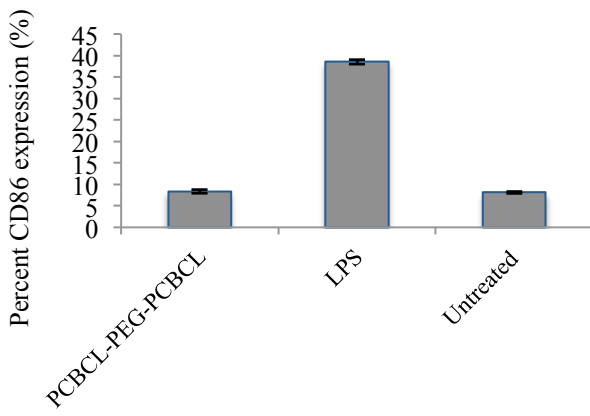
### 3.6 In vitro immunogenicity

Dendritic cells are antigen presenting cells that upon exposure to foreign antigen show maturation, which is characterized by an increase in the expression of MHC class II and co-stimulatory molecules particularly CD86 and CD40 on their surface. Upon maturation, DCs also secrete pro-inflammatory cytokines such as IL-12, TNF $\alpha$  and IL-6 (10). In order to evaluate the immunogenicity of block copolymer under study, level of DC maturation upon exposure to block copolymer was investigated by following the expression levels of CD86 and CD40 (Figure 5.4) and quantification of IL-12 secretion (Figure 5-5). Incubation of DCs with 1  $\mu$ mL of LPS (positive control) led to overexpression of CD86 and CD 40 as well as elevated secretion of IL-12 compared to untreated DCs. Addition of triblock copolymer, did not induce significant changes in the level CD86 and CD40 expression or IL-12 secretion when compared to untreated DCs (negative control) Our results shows non-immunogenicity of PCBCL-PEG-PCBCL block copolymers in terms of DC maturation.

**A)**



**B)**



**C)**

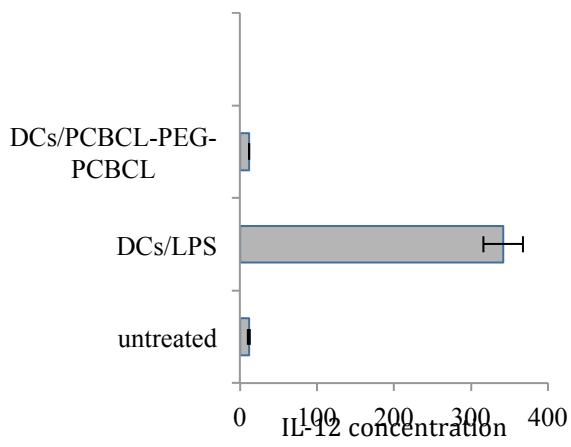


**Figure 5-4** The effect of PCBCL-PEG-PCBCL triblock copolymer on DC maturation measured as expression of of A) CD40; B) CD86 on DCs or C) secretion of IL-12 by DCs in comparison to LPS treated (positive control) or untreated DCs (negative control) (n=3).

### 3.7 Loading CyA into hydrogel

The level of CyA loading into hydrogel was measured using LC-MS. CyA reached a level of 2.7 mg/mL (CyA: polymer weight ratio of 27:1). An increase in the level of added drug led to a significant increase in the level of loaded drug in the hydrogel ( $P < 0.05$ , unpaired Student's t test) keeping the encapsulation efficiency the same upon addition of initial drug levels (Table 5-1).

**Table 5-1 loading efficiency of CyA into hydrogel**

Amount of CyA added (mg)	Loading efficiency (%) $\pm$ SD
1.5	93% $\pm$ 0.10
3.0	90% $\pm$ 0.13

### 3.8 Sol-gel transition of CyA loaded PCBCL-PEG-PCBCL

#### *A) Inverse Flow Method*

Table 5-2 shows sol-gel, and gel-sol transition temperature of block copolymer solution (10% w/w) loaded with different feeding levels of CyA. Increasing the amount of CyA loaded into hydrogel led to a decrease in the sol-gel transition temperature. The upper transition temperature from gel to turbid dispersion did not change.

**Table 5-2 Thermo responsive transition of CyA loaded hydrogel**

Loaded amount of CyA into hydrogel (mg/mL)	Sol-gel Transition Temperature (°C)	Upper Transition Temperature (°C)
1.5	29	45
3	27	45
0	29	47

### *B) MDSC*

Figure 5-6 illustrates the thermographs of aqueous solutions of the block copolymer under study at a concentration of 10% w/w with or without loaded with CyA. The block copolymer showed two endothermic peaks in MDSC. The first peak which appeared at 33.6 °C coincides with the sol to gel transition temperature of aqueous solution of this block copolymer while the second peak at 45.21°C coincides with the second transition. The MDSC analysis of block copolymer solution hydrogel loaded with CyA also showed two transition endothermic peaks, at 32.61 °C and 41.69°C which are close to transition temperatures measured by inverse flow method for CyA loaded gel (Table 5-2). The enthalpy of transitions were 0.31 J/g (at 33.57 °C) and 1.58 J/g (at 45.21 °C) for the unloaded gel. For CyA loaded gel, the enthalpy of transitions were 5.99 J/g (at 32.60 °C ) and 1.58 J/g (at 41.69 °C). The endothermic nature of the peaks and their comparative enthalpy values implies the breaking of hydrogen bonds has been involved in the thermo-responsive transition processes. The first transition may reflect breaking of hydrogen bonds with water or among COOH groups in the PCBCL segments [11] . This can promote the association of micelles through the hydrophobic blocks of the tri block copolymers. The second transition, on the other hand, may reflect the dehydration of PEG and/or a change in micellar conformation leading to

phase separation [12]. The higher value of sol-gel transition enthalpy for the block copolymer solution loaded with CyA may reflect the existence of an interaction between polymer and drug (e.g., hydrogen bonding between amide-NH groups of cyclosporine and COOH group of triblock copolymer).

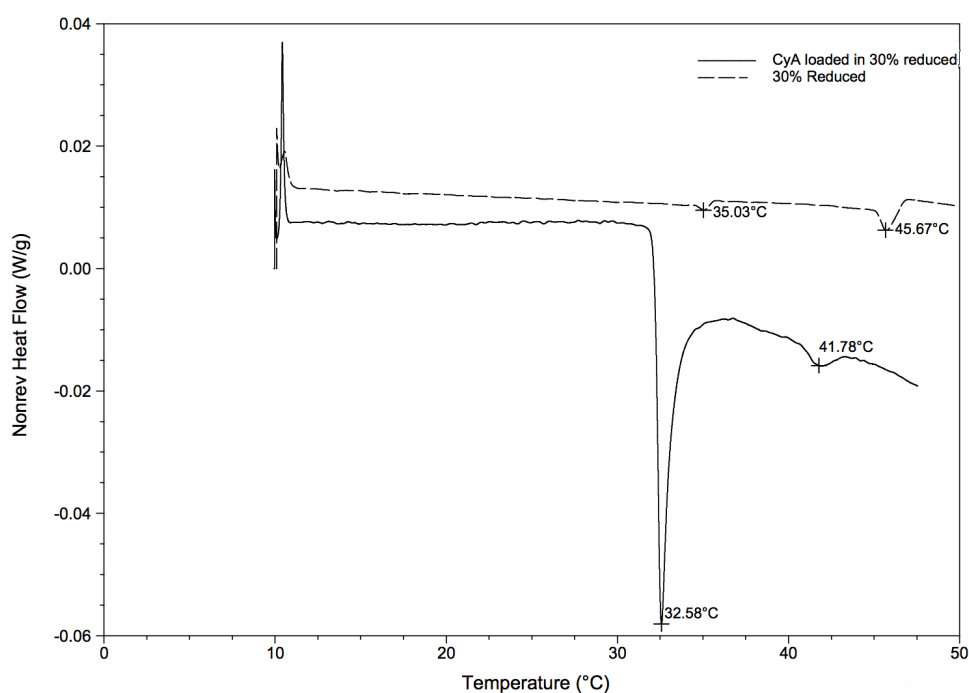


**Figure 5-5 Modulated DSC thermograms of cyA loaded and unloaded block copolymer in distilled water at 10% w/w polymer concentration**

### **3.9 In vitro Release study**

CyA is a cyclic undecapeptide made of eleven amino acids. It is unionized at physiological pH, and its solubility in water at room temperature is 27.67  $\mu\text{g/mL}$  [13,14]. BSA was used as a bio-mimetic recipient phase to maintain sink condition for the release of CyA from hydrogel. Loaded CyA was released to the recipient phase, i.e, BSA solution (4%

w/v, 80 mL), through a Spectra/Por dialysis bag (MWt. cut-off = 12,000– 14,000 g /mol). Transfer of CyA through dialysis membrane to BSA was assumed to take place rapidly, and the release of CyA from hydrogel was assumed to be the rate-limiting step in this process. In fact, 97.1% of unloaded CsA from its ethanolic solution was transferred to BSA within 6 h at 37°C (Figure 5-7). In contrast, the PCBCL-PEG-PCBCL hydrogel only released 7.4% of loaded CyA within the same time frame.

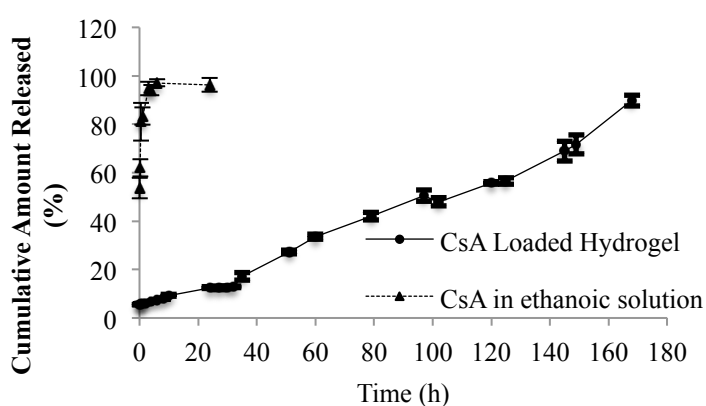


**Figure 5-6 Release profile of CsA from hydrogel or ethanolic solution**

As shown in Figure 5-7, the block copolymer hydrogel under study have sustained the release of CyA over one week. At the end of the release study (168 h), 89.8 % of loaded CyA was released from the hydrogel. This is in contrast to free CsA dissolved in ethanol that has shown 100 percent release within a few hours.

#### 4. Conclusion

The results clearly show a great promise for the developed PCBCL-PEG-PCBCL block copolymer as vehicles for sustained delivery of CyA.

## References:

- (1) Kanduru SV, Somayaji V, Lavasanifar A, Brocks DR. An analytical method for cyclosporine using liquid chromatography–mass spectrometry. *Biomedical Chromatography* 2010;24(2):148-153.
- (2) Perry HD, Donnenfeld ED. Topical 0.05% cyclosporin in the treatment of dry eye. *Expert Opin Pharmacother* 2004;5(10):2099-2107.
- (3) Peng C, Chauhan A. Extended cyclosporine delivery by silicone–hydrogel contact lenses. *J Controlled Release* 2011;154(3):267-274.
- (4) Kapoor Y, Chauhan A. Ophthalmic delivery of Cyclosporine A from Brij-97 microemulsion and surfactant-laden p-HEMA hydrogels. *Int J Pharm* 2008;361(1):222-229.
- (5) Li C, Chauhan A. Modeling ophthalmic drug delivery by soaked contact lenses. *Ind Eng Chem Res* 2006;45(10):3718-3734.
- (6) Safaei Nikouei N, Lavasanifar A. Characterization of the thermo- and pH-responsive assembly of triblock copolymers based on poly(ethylene glycol) and functionalized poly(epsilon-caprolactone). *Acta Biomater* 2011 Oct;7(10):3708-3718.
- (7) Hamdy S, Haddadi A, Shayeganpour A, Alshamsan A, Aliabadi HM, Lavasanifar A. The immunosuppressive activity of polymeric micellar formulation of cyclosporine A: in vitro and in vivo studies. *The AAPS journal* 2011;13(2):159-168.
- (8) Bae SJ, Suh JM, Sohn YS, Bae YH, Kim SW, Jeong B. Thermogelling poly (caprolactone-b-ethylene glycol-b-caprolactone) aqueous solutions. *Macromolecules* 2005;38(12):5260-5265.
- (9) Loh XJ, Li J. Biodegradable thermosensitive copolymer hydrogels for drug delivery. *Expert Opinion* 2007;17:3977-3989.
- (10) Boudier A, Aubert-Pouëssel A, Louis-Plence P, Gérardin C, Jorgensen C, Devoisselle J, et al. The control of dendritic cell maturation by pH-sensitive polyion complex micelles. *Biomaterials* 2009;30(2):233-241.
- (11) Hou Y, Matthews AR, Smitherman AM, Bulick AS, Hahn MS, Hou H, et al. Thermoresponsive nanocomposite hydrogels with cell-releasing behavior. *Biomaterials* 2008;29(22):3175-3184.
- (12) Takeuchi Y, Tsujimoto T, Uyama H. Thermogelation of amphiphilic poly (asparagine) derivatives. *Polym Adv Technol* 2011;22(5):620-626.
- (13) Ran Y, Zhao L, Xu Q, Yalkowsky SH. Solubilization of cyclosporin A. *Aaps Pharmscitech* 2001;2(1):23-26.
- (14) Francis MF, Lavoie L, Winnik FM, Leroux J. Solubilization of cyclosporin A in dextran-*g*-polyethyleneglycolalkyl ether polymeric micelles. *European journal of pharmaceuticals and biopharmaceutics* 2003;56(3):337-346.
- (15) Bezemer J, Radersma R, Grijpma D, Dijkstra P, Feijen J, Van Blitterswijk C. Zero-order release of lysozyme from poly (ethylene glycol)/poly (butylene terephthalate) matrices. *J Controlled Release* 2000;64(1):179-192.
- (16) Safaei Nikouei N, Vakili M, Akbari A, Wu J, Lavasanifar A. Biodegradable Thermo-reversible Hydrogels based on Triblock Copolymers of PEG and Functionalized Poly(ε-caprolactone). *Biomaterials*, submitted (2013)



(17) Costa P, Sousa Lobo J.M. Modeling and comparison of dissolution profiles. *European Journal of Pharmaceutical Sciences* 2011;13: 123-133

## Chapter 6

### **Development of multifunctional polymeric micelles for targeting of cisplatin to EGFR overexpressing tumors**

## 1. Introduction

Cisplatin is used for the treatment of different kinds of cancers including testicular, ovarian, bladder, head and neck, and lung cancers. Clinical benefit of cisplatin has been restricted due to emergence of drug resistance and/or systemic dose limiting toxicity by the drug. The most common systemic side effects associated with cisplatin administration are nephrotoxicity, neurotoxicity, and ototoxicity. Resistance to cisplatin mostly happens through following mechanisms: increased drug efflux; increased cisplatin detoxification through elevated glutathione or thiol level in cells; development of tolerance to DNA damage, and prevention of apoptosis cascade [1].

Properly designed drug delivery systems can change the biological disposition of cisplatin taking it away from site of drug toxicity thus reducing drug side effects. Nano delivery systems can also enhance the accumulation of cisplatin in solid tumors through enhanced permeability and retention (EPR) effect [2]. However, mere passive targeting of cisplatin may not provide the required therapeutic outcome in terms of cisplatin anticancer activity without efficient release of cisplatin from the carrier within the tumor microenvironment or tumor cells. Tumor tissue have lower pH compared to normal tissue (6.5-7), therefore, nano-carriers with the ability to release drug at lower pH can be used to provide increased release of cisplatin in tumors. Moreover, targeting a receptor on tumor cells can help in internalization of nano-carrier, and release cisplatin inside cancer cells or cell organelles like lysosome (pH=4.5-5.5).

NC-6004 is one of the representative polymeric micelle carriers for cisplatin in phase II clinical trial [3]. NC-6004 is composed of a block copolymer of PEG and poly(glutamic acid) (PGlu) which has formed a complex with cisplatin. The *in vitro* release study on this

formulation has shown 19.6 and 47.8 % cisplatin release after 24 and 96 h incubation, respectively. Lipoplatin® is a liposomal formulation of cisplatin in phase III clinical trial, made of dipalmitoyl phosphatidyl glycerol (DPPG), soy phosphatidylcholine, and methoxypoly(ethylene glycol) distearoylphosphatidylethanolamine. A phase II clinical study on twenty-seven patients with pretreated advanced malignant tumors, has shows no nephrotoxicity for this formulation [3,4].

The objective of this chapter was to develop a multifunctional polymeric micellar formulation for cisplatin. For this purpose the surface of polymeric micelles were modified with targeting ligand, GE11 peptide, interacting with EGFR receptor overexpressed on cancer cells. Micellar core, on the other hand, was composed of poly( $\alpha$ -benzyl carboxylate- $\epsilon$ -caprolactone) (PCCL), that can provide acid sensitive drug release properties The potential of this delivery system for physical targeting of cisplatin was then evaluated. GE11 is a synthetic peptide ligand, which can compete with EGF, the natural ligand of EGFR. EGFR positive signaling is responsible for cell proliferation stimulation, prevention of apoptosis, and induction of angiogenesis [5,6]. Therefore, EGF is not a proper targeting ligand for EGFR. GE11 modified PEO-PCCL micellar complexes of cisplatin are expected to enhance the interaction of polymeric micelles with EGFR positive cells and provide enhanced cisplatin release in the acidic environment of extracellular space in tumor or within acidic organelles inside EGFR positive tumor cells (following endocytosis) leading to a better anti-cancer activity for the encapsulated cisplatin. The potential of GE11 modified polymeric micelles for physical targeting of cisplatin was investigated here.

## 2. Materials & Methods

### 2.1 Materials

*Cis*-Dichlorodiammineplatinum (II) (CDDP) was purchased from AK Scientific, Inc. Methoxy-poly(ethylene glycol) (PEG) ( $M_w = 5000$ ), sodium (in kerosin), and palladium-coated charcoal were purchased from Sigma, St. Louis, MO. Tin (II) Chloride ( $\text{SnCl}_2$ ) was purchased from Sigma-Aldrich.  $\alpha$ -benzyl carboxylate- $\epsilon$ -caprolactone (BCL) was synthesized by Alberta Research Chemicals Inc (ARCI), Edmonton, Canada. All other chemicals and reagents were analytical grade. Ethylene oxide and potassium naphthalene and diethoxy propanol was purchased from Sigma. GE11 was a gift from Laboratory of Dr. Kuar.

### 2.2 Synthesis of PEO-b-poly( $\alpha$ -carboxy- $\epsilon$ -caprolactone) ( PEO-b-PCCL)

The synthesis of PEO-b-PCCL was accomplished in two steps as described before(7): i) ring opening polymerization of BCL using methoxy PEO as initiator and stannous octoate as catalyst at 140°C for 4 hours leading to the formation of methoxyPEO-b-poly( $\alpha$ -benzyl carboxylate- $\epsilon$ -caprolactone) (PEO-b-PBCL); and ii) complete debenylation of diblock copolymer using palladium 10% on activated charcoal as catalyst leading to the preparation of PEO-b-PCCL.

### 2.3 Synthesis of acetal-PEO-b-PCCL

Acetal-PEO-b-PCCL was synthesized as described before (8,9) Briefly, in a double neck rounded bottom flask 25 mL dry THF was added to the initiator, i.e., 3,3 diethoxy propanol (0.15 mL, 1 mmol) and argon gas was applied on the solution. Then 4.4 mL (1 mmol) potassium naphthalene (catalyst) was added dropwise until a deep green color was obtained. The temperature was increased during the addition of catalyst up to 30°C. The

reaction was left for half an hour before adding the ethylene oxide. The temperature of solution decreased, and the color of the mixture turned to yellowish green within this time. Dry ice was added to reduce the temperature of reaction just before the addition of ethylene oxide. The needle for transferring the ethylene oxide was left inside the dry ice for at least 5-10 minute. The ethylene oxide was added (7 mL) to the flask while in dry ice to reduce the temperature. After addition of ethylene oxide, the reaction was removed from the dry ice and left at room temperature for 48 h under argon gas.

Diblock copolymers composed of acetal poly(ethylene oxide)-b-poly( $\alpha$ -carboxyl- $\epsilon$ -caprolactone) (acetal-PEo-PCCL) were synthesized through ring opening polymerization of  $\alpha$ -benzyl carboxylate- $\epsilon$ -caprolactone by acetal-PEO using stannous octoate as catalyst. Further debenylation of synthesized copolymer was conducted by removal of the benzyl groups of acetal-PEO-b-PBCL in the presence of hydrogen gas. For this purpose, acetal-PEO-b-PBCL (1 g) was dissolved in 25 mL of THF and placed into a 100 mL round bottom flask. Then, charcoal-coated with palladium (300 mg) was dispersed in this solution and hydrogen gas was introduced to the reaction flask. After stirring for 24 h in the presence of hydrogen gas, the reaction mixture was centrifuged at 3,000 rpm to remove the catalyst. The supernatant was collected, condensed under reduced pressure, precipitated in diethyl ether and washed repeatedly to remove impurities. The final product was dried under vacuum at room temperature for 48 h [9].

## **2.4 Characterization of prepared copolymer**

$^1\text{H}$  NMR spectroscopy in  $\text{CDCl}_3$  was used to study the composition of copolymers. The degree of polymerization for the PCCL blocks in block copolymer was identified by

comparing peak intensity of PEO (-CH<sub>2</sub>CH<sub>2</sub>O-,  $\delta$ =3.65 ppm) to that of PCCL (-O-CH<sub>2</sub>-,  $\delta$ =4.1 ppm).

## 2.5 Conjugation of GE11 to polymeric micelles

Conjugation of the peptide into the acetal terminus of acetal-PEO-*b*-PCCL was performed through thiazolidine ring formation using Cystein terminated GE11 peptide. In a typical process, acetal-PEO-*b*-PCCL (50 mg) was added to GE11 (5 mg) in 0.2 M AcOH buffer (pH 4.0, 5 mL) and stirred at room temperature for 5 days. Peptide conjugated polymeric micelles were purified by dialysis against 1000 mL distilled water and lyophilized to obtain GE11-PEO-*b*-PCCL [10]. The amount of conjugated peptide was calculated using Micro BCA Protein Assay using manufacturer's protocol.

## 2.6 Preparation of cisplatin loaded micelles

Cisplatin loaded micelles were prepared through addition of a weak base to GE11-PEO-PCCL or PEO-*b*-PCCL to induce ionization of free carboxyl groups on PCCL. In a typical process, GE11-PEO-*b*-PCCL (68 mg) or PEO-*b*-PCCL (33 mg) was dissolved in 60 mL THF. Sodium bicarbonate solution (1.4 % w/v) in water was added to this solution. The resultant solution was then inserted into waterbath at 37°C for 2 hours. The THF was evaporated and the solution was freeze dried. Freeze-dried polymer (1.2. mg/mL) was then reconstituted in water and cisplatin (1.25 w/w polymer) was added to this solution.

The amount of unloaded cisplatin was determined using Tin (II) chloride following dialysis of the prepared micelles (4 mL) against 175 mL distilled water using dialysis membrane (MWCO, 3500 g.mol<sup>-1</sup>). After 15 h of dialysis, 3 mL solution from outside of the dialysis bag was diluted with 2 mL of 0.2 M Tin (II) chloride solution in 2 N HCL. The

cisplatin content in the solution was determined by Beckman coulter ® UV-Vis based on the absorbance of cisplatin complex with Tin (II) chloride at 403 nm. Free cisplatin content in the dialysis medium was measured. The amount of complexed cisplatin was calculated by subtracting the amount of free cisplatin from initial cisplatin added to the encapsulation process [11]. Encapsulation efficiency was then calculated using the following equations:

$$\text{Encapsulation Efficiency (\%)} = \frac{\text{Amount of cisplatin encapsulated in mg}}{\text{Amount of cisplatin initially added in mg}} \times 100$$

### **2.7 *In vitro* release study**

Release of cisplatin from PEO-b-PCCL micelles was evaluated in the presence of sodium salt at pH 5.0 and 7.4 at 37 °C. Briefly, 4 mL of micelle solution loaded with cisplatin was placed into a dialysis bag (M.wt. cut-off = 3500 g/mol) and then immersed into 200 mL of phosphate buffer saline (PBS, pH 7.4) at 37°C. At defined time intervals, 3 mL of the solution outside of dialysis bag was sampled and mixed with 2 mL SnCl<sub>2</sub> solution in 4N HCL (0.4 mg/mL of SnCl<sub>2</sub>) to determine the amount of released cisplatin spectrophotometrically, as described above. In a separate set of experiments, release media was prepared at pH 5.0 by adding few drops of 0.5 N HCL and the release of free cisplatin from dialysis bag was measure at this pH following the same procedure as explained for pH 7.4. Cumulative release percentage of cisplatin was then calculated and plotted versus time.

### **2.8 *In vitro* cytotoxicity study**

Human SK-BR-3 cancer cell line was a gift from the laboratory of Dr Allen, University of Alberta. and the cells were maintained in DMEM supplemented with 10% fetal bovine serum. Cytotoxicity of cisplatin-loaded polymer micelles was assessed by a standard MTT assay. Briefly, 96-well micro titer plates were seeded with 10,000 cells per well and allowed

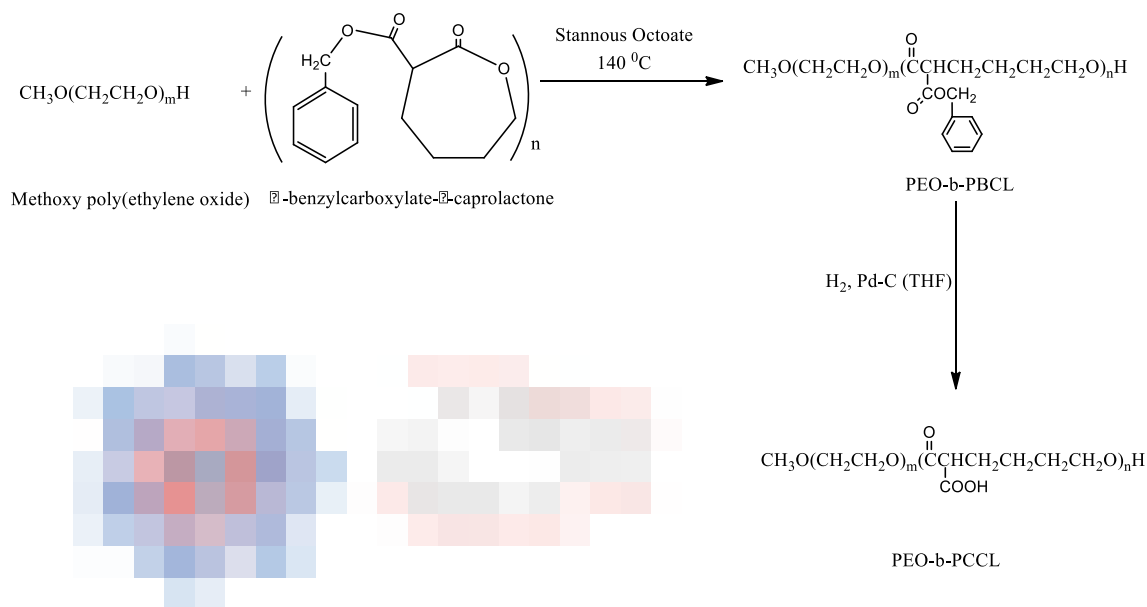


to adhere for 24 h prior to the assay. Cells were exposed to various doses (0.97-2000  $\mu\text{g}/\text{mL}$  on cisplatin basis) of free drug, polymeric micelles alone, or cisplatin-loaded polymeric micelles for 48 and 72 h at 37° C. 20  $\mu\text{L}$  of MTT indicator dye (5 mg/mL) was added to each well and the cells were incubated for 3 h at 37° C. Medium with the indicator was then removed and 100  $\mu\text{L}$  DMSO was added to each well. Absorption as measured at 550 nm in a microplate reader. Obtained values were used to calculate the percentage of viable cells in test groups compared to the control cells to which no drugs were added. The graph of cell viability percentage versus log concentration was plotted and  $\text{IC}_{50}$  was calculated from the linear section of the sigmoidal cell viability plot.

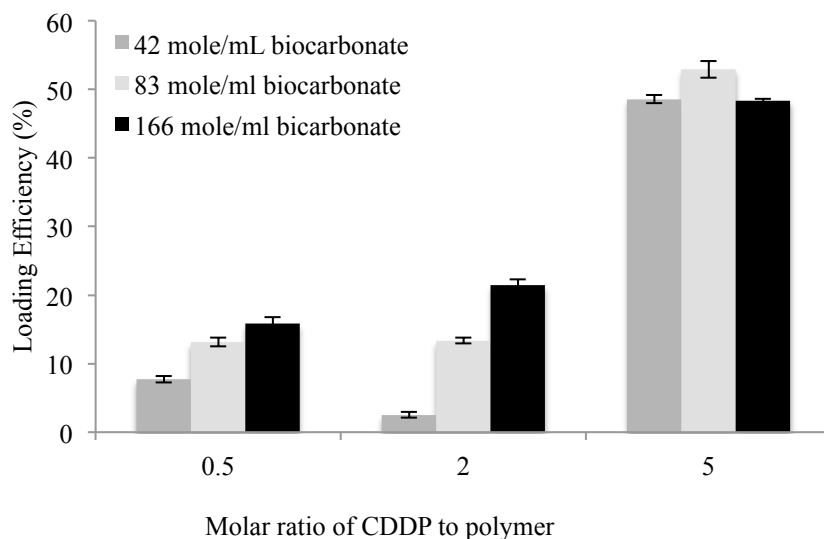
### 3. Results and Discussion

Figure 6-1 shows the scheme for the preparation of methoxyPEO-b-PCCL micelles containing cisplatin through metal-ion complex formation between cisplatin and the carboxyl ion of the PCCL block followed by self-assembly of PEO-b-PCCL/cisplatin polyion complexes to polymeric micelles. This structure is similar to the structure of NC-6004 micellar formulation of cisplatin which is in clinical trials phased II at the moment (3) . The advantage of the current formulation is the possibility for the hydrolytic and acid catalyzed degradability of the micellar core in PEO-b-PCCL micelles, which may not be achieved as easily by the poly(glutamic acid) core of NC-6004.

Complexation of cisplatin with poly(glutamic acid) core of NC-6004 occurs in the presence of a strong base NaOH, by converting the free COOH group to  $\text{COO}^-$ . Addition of NaOH; however, led to the degradation of the PCCL core. We used a weak base (sodium bicarbonate), to improve the complexation of cisplatin by PEO-b-PCCL micelles here (data not shown).



**Figure 0-1 Scheme for the preparation of cisplatin loaded PEO-b-PCCL micelles**



**Figure 0-2 Effect of concentration of sodium bicarbonate/or molar ratio of cisplatin to polymer on loading efficiency**

Figure 6-2 shows the effect of molar ratio of cisplatin to polymer and concentration of sodium bicarbonate in loading content of cisplatin in to the micelles. It can be seen that the

highest loading content was achieved when cisplatin to polymer molar ratio of 5:1 was used. At this level, changing concentration of sodium bicarbonate did not affect the loading efficiency of cisplatin. At lower cisplatin to polymer molar ratios of 2:1, increasing the level of sodium bicarbonate from 42 to 83 and 166 mol/mL enhanced loading efficiency of cisplatin in polymeric micelles ( $P < 0.05$ , paired student's t test). At a cisplatin to polymer molar ratio of 0.5:1, an increasing trend in loading efficiency as a result of an increase in bicarbonate concentration was seen but it was not statistically significant ( $P > 0.05$ , paired student's t test).

Under optimum conditions (cisplatin;polymer ratio of 5:1 and 166 mole/mL of bicarbonate sodium) encapsulation efficiency of 36.5 and 35.5% for cisplatin in PEO-b-PCCL and GE11-PEO-b-PCCL micelles was achieved, respectively. This corresponds to 18 % (mol/mol) of conjugated peptide to the polymer for GE11-PEO-b-PCCL. The conformation of cisplatin within the micellar core is not clear in this case and can consist of a mixture of single or double bond between cisplatin and free carboxyl groups on a single polymer chain or between two adjacent polymer chains. Nevertheless, the complexation of cisplatin is expected to increase the stability of PEO-b-PCCL micelles against dissociation.

Figure 6-3 shows the cumulative release of cisplatin from PEO-b-PCCL micelles at two different pHs (pH 5.0 and 7.4). It can be seen that the release of cisplatin was affected by the pH of media . Significantly ( $p < 0.05$ , unpaired Student's t test) higher release was seen at lower pH 5.0 compared to pH 7.4 after 24 h. At 48h, 16.7 % cisplatin was released at pH 5.0 compared to 12.5% at pH 7.4. The accelerated release of cisplatin at acidic pH may be due to the protonation of carboxyl ions substituted on the caprolactone backbone that will weaken the cisplatin/polymer complexation. It may also reflect the acid induced cleavage of the PCCL backbone within the micellar core leading to better release of cisplatin or cisplatin

derivatives from the polymeric micelles. Further studies are required to account for the relative contribution of each mechanism in the overall release profile of cisplatin from PCCL core. The acid triggered release of cisplatin from PEO-b-PCCL micelles is expected to be advantageous in targeted delivery of cisplatin by its nano-carrier. In this case, premature release of cisplatin in the blood circulation (pH 7.4) is prevented by the PEO-PCCL micelles, while accelerated cisplatin release is achieved in the extracellular space in tumour tissue upon micellar accumulation or inside endosomal compartment of cancer cells upon micellar cell uptake.

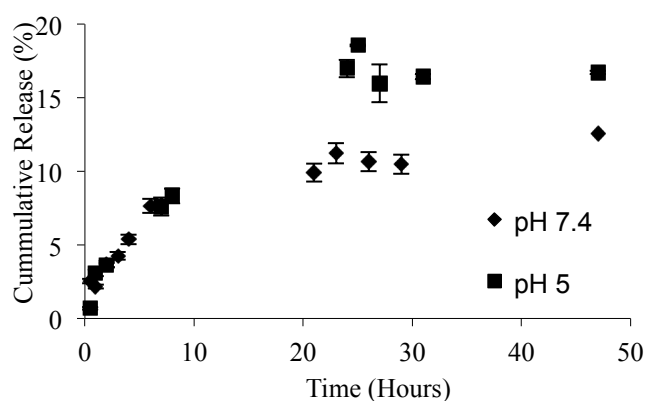


**Figure 0-3 Release profile of cisplatin from PEO-PCCL micelle at two different pHs.**

We then developed multifunctional polymeric micelle formulations of cisplatin through conjugation of GE11 peptide ligand on the PEO terminus of acetal-PEO-b-PCCL. Based on BCA assay, 62% of used peptide was conjugated into copolymer. The GE11-PEO-PCCL micellar formulations of cisplatin is an example of a multifunctional micelles that may provide better association of the micellar carrier with EGFR expressing cells due to its GE11 ligand on the shell, and at the same time provide enhanced release of the incorporated drug at target cells due to its acid triggered drug release properties. Figure 6.4 compares the IC<sub>50</sub> of

methoxy and GE11 modified polymeric micellar formulations of cisplatin in SKBR3 cells that overexpress EGFR. The results indicates that cytotoxicity of encapsulated cisplatin was increased when micelles were modified with GE11. This can be attributed to an enhanced uptake of GE11 modified cisplatin loaded polymeric micelles compared to unmodified ones leading to better exposure of the cisplatin to its intracellular site of action.

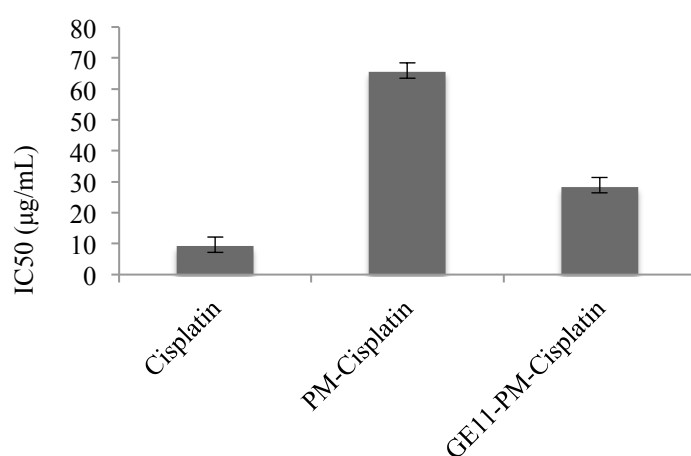


**Figure 0-4 IC<sub>50</sub> obtained by MTT Assay using SKBR3 cell line after 72 h incubation**

#### **4. Conclusions**

Novel polymeric micelles developed here may prove to be excellent candidates for cisplatin therapy of solid tumors for several reasons including stability in physiological condition mimicking that of blood circulation; acidic pH triggered drug release and enhanced association with EGFR expressing tumor cells. Such characteristics warrant further investigations on *in vivo* performance of the PEO-PCCL and GE11-modified PEO-PCCL micellar formulation of cisplatin.

## References:

- (1) Perez R. Cellular and molecular determinants of cisplatin resistance. *Eur J Cancer* 1998;34(10):1535-1542.
- (2) Fang J, Nakamura H, Maeda H. The EPR effect: Unique features of tumor blood vessels for drug delivery, factors involved, and limitations and augmentation of the effect. *Adv Drug Deliv Rev* 2011;63(3):136-151.
- (3) Wang X, Guo Z. Targeting and delivery of platinum-based anticancer drugs. *Chem Soc Rev* 2013;42(1):202-224.
- (4) Stathopoulos GP, Boulikas T, Vougiouka M, Deliconstantinos G, Rigatos S, Darli E, et al. Pharmacokinetics and adverse reactions of a new liposomal cisplatin (Lipoplatin): phase I study. *Oncol Rep* 2005;13(4):589-596.
- (5) Agrawal SK, Sanabria-DeLong N, Coburn JM, Tew GN, Bhatia SR. Novel drug release profiles from micellar solutions of PLA-PEO-PLA triblock copolymers. *J Controlled Release* 2006;112(1):64-71.
- (6) Li Z, Zhao R, Wu X, Sun Y, Yao M, Li J, et al. Identification and characterization of a novel peptide ligand of epidermal growth factor receptor for targeted delivery of therapeutics. *The FASEB journal* 2005;19(14):1978-1985.
- (7) Mahmud A, Xiong X, Lavasanifar A. Novel Self-Associating Poly (ethylene oxide)-b lock-poly ( $\epsilon$ -caprolactone) Block Copolymers with Functional Side Groups on the Polyester Block for Drug Delivery. *Macromolecules* 2006;39(26):9419-9428.
- (8) Xiong X, Ma Z, Lai R, Lavasanifar A. The therapeutic response to multifunctional polymeric nano-conjugates in the targeted cellular and subcellular delivery of doxorubicin. *Biomaterials* 2010;31(4):757-768.
- (9) Xiong X, Mahmud A, Uludağ H, Lavasanifar A. Multifunctional polymeric micelles for enhanced intracellular delivery of doxorubicin to metastatic cancer cells. *Pharm Res* 2008;25(11):2555-2566.
- (10) Oba M, Fukushima S, Kanayama N, Aoyagi K, Nishiyama N, Koyama H, et al. Cyclic RGD peptide-conjugated polyplex micelles as a targetable gene delivery system directed to cells possessing  $\alpha\beta 3$  and  $\alpha\beta 5$  integrins. *Bioconjug Chem* 2007;18(5):1415-1423.
- (11) Nishiyama N, Yokoyama M, Aoyagi T, Okano T, Sakurai Y, Kataoka K. Preparation and characterization of self-assembled polymer-metal complex micelle from cis-dichlorodiammineplatinum (II) and poly (ethylene glycol)-poly ( $\alpha$ ,  $\beta$ -aspartic acid) block copolymer in an aqueous medium. *Langmuir* 1999;15(2):377-383.

## Chapter 7

### **General Discussion and Conclusion**

## **1. Introduction**

The development of advanced drug delivery systems that are able to release drug molecules in specific sites or the incorporated molecule according to a specific physiological need creates an opportunity to cure diseases more efficiently. Stimulus responsive polymers are designed as “smart” materials, with potential for numerous medical and pharmaceutical applications such as drug delivery systems, diagnostic agents, tissue engineering scaffolds, and biosensors. Thermo-responsive polymers that exhibit an inverse sol-gel transition in response to changes in temperature can deliver drug molecules to the site of action by a simple injection of a polymer and drug solution in a less invasive way. Upon being injected into the body, the solution becomes a gel, and releases its incorporated drug molecules in a controlled manner. Moreover, because the resultant hydrogel contains a significant amount of water, it is biocompatible with human tissue. Thermo-responsive hydrogels are excellent vehicles for biological cells as well, as cells can be simply suspended into polymeric solutions and injected to the site of action. The cells are then trapped in the three-dimensional network of the in situ hydrogel, and grow in a three-dimensional way. Growing in three dimensions can make a huge difference in gene expression as compared to two-dimensional growth [1]. Stimulus responsive polymers can also be designed to release the incorporated drug in response to acidic or basic pHs. Such materials may be applied for targeted drug delivery at specific sites within the body.



## 2. General Discussion

The long-term objective of our research is to design and develop delivery systems that can enhance the performance of existing and emerging therapeutics in different disease states. In this thesis, we have developed novel stimulus responsive delivery systems based on amphiphilic block copolymers and showed the efficacy of these new excipients in the controlled delivery of macromolecular and small molecular drugs like cyclosporine A and cisplatin. In this context, I have synthesized di and triblock copolymers based on poly(ethylene glycol) (PEG) and  $\alpha$ -carbon functionalized poly( $\epsilon$ -caprolactone), and investigated the potential of these materials in formation of thermo and/or pH responsive hydrogels and micelles for depot and targeted drug delivery applications. In Chapter 2 a series of novel tri block copolymers composed of PEG and poly( $\epsilon$ -caprolactone)-bearing benzyl carboxylate on the  $\alpha$ -carbon of  $\epsilon$ -caprolactone were synthesized through the ring opening polymerization of  $\alpha$ -benzyl carboxylate- $\epsilon$ -caprolactone by dihydroxylated PEG. The debenzilation of the synthesized copolymer, i.e., poly( $\alpha$ -benzyl carboxylate- $\epsilon$ -caprolactone)-*b*-PEG-*b*-poly( $\alpha$ -benzyl-carboxylate- $\epsilon$ -caprolactone) (PBCL-*b*-PEG-*b*-PBCL), in the presence of hydrogen gas using different levels of catalyst, was carried out to achieve copolymers with various degrees of free  $\alpha$ -carboxyl to  $\alpha$ -benzyl- $\epsilon$ -carboxylate groups on the hydrophobic block. Because PBCL was not completely reduced, poly( $\alpha$ -carboxyl-co-benzyl caboxylate- $\epsilon$ -caprolactone) PCBCL formed in the lateral blocks at 27, 50 and 75 % carboxyl group substitution. Synthesized copolymers formed stable micelles at low concentrations [Critical Micellar Concentrations (CMC) of 0.34-12.5  $\mu\text{g/mL}$ ]. The CMC of polymers containing carboxyl groups in their structure was dependent on pH. In contrast, the CMC in polymers without the carboxyl group was independent of pH (0.55  $\mu\text{g/mL}$ ). In this series of block copolymers, micellar size was shown to change as a function of temperature, and the

direction of this change depended on the level of free carboxyl groups on PCBCL. Polymers with 27% of pendent COOH on PCBCL illustrated a rise in micelle size as the temperature was increased above 29°C, while polymers with 50% COOH showed a decrease in micelle size, when the temperature increase. A similar trend was observed in pHs 4.5, 7.0 and 9.0 for polymers containing carboxyl groups on their hydrophobic block. The temperature for the onset of size change was found to depend on the pH of the medium and the polymer concentration. The results pointed to the temperature and pH responsive self-association of prepared tri block copolymers and implied a potential for the developed materials to be used to form the temperature and pH responsive gels [2].

We then optimized the synthetic procedure to production the above-mentioned triblock copolymers and characterized the thermo-responsive sol-gel transition of PCBCL-PEG-PCBCL block copolymers that have varying levels of pendent COOH groups on their PCBCL block (Chapter 3). Our results showed a concentration-dependent sol to gel transition as a result of a rise in temperature above ~ 30 °C for partially COOH-substituted (30 and 50 %) PBCL-PEG-PBCL triblock copolymers as defined by three different methods: the inverse flow method, dynamic mechanical analysis and DSC. Overall, we observed a good agreement between different methods of measurement in defining the transition temperature of block copolymers under study. The viscoelastic properties of the gels above their transition temperature depended on the level of the carboxyl group substitution. Triblock copolymers with 50% COOH group substitution formed more stable bonds, as their viscoelastic properties did not change as a function of increasing temperature within a broad temperature range [9]. The transition temperature of PCBCL-PEG-PCBCL tri block copolymers was found to be ideal for their application as injectable implants for depot or regional drug delivery. This transition temperature was comparable to what found for PNIPAm ReGel®

and Pluronic® [11,12,13,14]. The current polymer; however, may prove to be advantageous over those products because of its better stability profile, stronger gel characteristics and existence of functional groups in the polymer structure.

In the next step, we characterized the effects of aqueous media and pH on the gelation of a solution of PCBCL-PEG-PCBCL with 30 % COOH groups on PCBCL (Chapter 4). When a Tris buffer was used as the media, gels were formed at a lower temperature and had better viscoelastic properties (as evidenced by DMA). Gel formation of PCBCL-PEG-PCBCL block copolymers was also found to depend on the pH of the media. At pH 3.0, the polymer solution did not form a gel in response to a rise in temperature. At pH 5.0 and above, the PCBCL-PEG-PCBCL solution formed a gel in a temperature-dependent manner; however. We also investigated temperature and pH responsive delivery of a model macromolecule drug, TMR-D, from the gel. Hydrogels loaded with TMR-D underwent sol-gel transition at temperatures similar or lower to that without TMR-D loading. The in vitro release of TMR-D was sustained by the thermo-responsive gel at 37° C and the cumulative release rate of TMR-D was affected by the size of the TMR-D molecule. With an increase in the size of TMR-D, the rate of drug release dropped. Moreover, the amount of TMR-D released from the hydrogel was significantly influenced by the pH and the temperature of the release media. Increasing the temperature of the release media to 50°C or decreasing it to 25 °C, or decreasing the pH to 5.0, caused a significant increase in the amount of TMR-D release. The results pointed to a potential of triblock copolymers of PCBCL-*b*-PEG-*b*-PCBCL for depot delivery of macromolecules at physiological temperature/pH. It also showed the potential of developed hydrogel in temperature- and/or acidic pH-triggered release of high molecular weight drugs.

In Chapter 5, we investigated the potential of prepared hydrogels for the depot delivery of a small molecule peptide drug, cyclosporin A (CyA), for a potential application for dry eye syndrome. The high loading efficiency of CyA in the hydrogel indicated a potential for the prepared triblock copolymer in the solubilization of poorly water soluble CyA. We envision formation of hydrogen bonds between CyA (a peptide drug with several hydrogen bond forming groups in its structure) and free COOH groups in the triblock copolymer structure to be a reason for this observation. The *in vitro* release experiments on CyA loaded hydrogel in the BSA medium demonstrated a slow release of loaded CyA from the gel within a 7 day period. Moreover, cytotoxicity and biocompatibility studies highlighted the potential of developed triblock copolymer to serve as an efficient and safe vehicle to deliver CyA in dry eye syndrome. The materials developed here are expected to be superior to the commercial formulation of CyA for this indication, Restasis®. Unlike Restasis®, the block copolymer solution and gel produced here are transparent and do not blur vision. Additionally, forming a gel at physiological temperature and pH may assist the retention of CyA on the cornea and reduce the need for frequent use of eye drops by the patient.

Finally, in Chapter 6, we assessed the potential of multi-functional polymeric micelles formed from GE11-modified PEG (as the shell) and carboxyl-substituted PCL (as the core) for the physical targeting of cisplatin. A di block copolymer composed of acetal poly(ethylene glycol)-b-poly( $\alpha$ -carboxyl- $\epsilon$ -caprolactone) (acetal-PEG-PCCL) was synthesized through a ring-opening polymerization of  $\alpha$ -benzyl carboxylate- $\epsilon$ -caprolactone by acetal-PEG and further debenzylation of a synthesized copolymer in the presence of hydrogen gas. Acetal-PEG-*b*-PCCL/Na<sup>+</sup> was then prepared by adding sodium bicarbonate into the polymer solution in THF. The peptide was conjugated into the PEG terminus of PEG-*b*-PCCL/Na<sup>+</sup> was performed through thiazolidine-ring formation using a cysteine-modified

G11 peptide. PEG-*b*-PCCL/Na<sup>+</sup> and GE11-PEG-*b*-PCCL/Na<sup>+</sup> were used to form complexes with cisplatin. The encapsulation efficiency of cisplatin into the polymeric micelle was around 35%. The peptide was conjugated into peptide successfully with 62% conjugation efficiency. The in vitro release study showed similarly slow release rates of cisplatin from PEG-PCCL micelles with higher amounts released at an acidic pH (12.5, and 16.7 % within 47 h, respectively). The introduction of the peptide improved the cytotoxicity of the cisplatin-loaded polymeric micelle against EGFR expressing SK-BR3 cells. The IC<sub>50</sub> for the peptide-decorated polymeric micelles was 28.35 μM compared to 65.52 μM for the unmodified micelles. The results point to a potential of peptide-conjugated block copolymers of GE11-PEG-*b*-PCCL/Na<sup>+</sup> as actively targeted nano-carriers of cisplatin for EGFR-expressing cells. The GE11-PEO-PCCL formulation of cisplatin is expected to be superior to other nano-cisplatin formulations currently under clinical trials for three major functional features: degradability of the PCCL core which can be promoted in acidic conditions, acidic pH-triggered drug release, and the possibility for active targeting of EGFR-expressing tumor cells. Current nano-cisplatin delivery systems in clinics are shown to be effective in reducing the nephrotoxic and hematological side effects of cisplatin, but do not provide any benefit in therapeutic measures. This might be due to the restricted release of cisplatin from its carrier even within the tumor. A combination of active drug targeting via the GE11 ligand and acid-triggered drug release in the current formulation is expected to enhance the therapeutic effects of cisplatin against tumor cells while minimizing its side effects and toxicity by providing a physical barrier limiting cisplatin access to normal tissues, such as the kidney [15].

### 3. Future Direction

In this study, we synthesized tri- and diblock copolymers based on PEG and  $\alpha$ -carbon functionalized poly( $\epsilon$ -caprolacton) and assessed the potential of these ABCs in formation thermo- and/or pH-responsive hydrogels and micelles. Future studies on the development of these materials towards production of effective drugs and drug delivery systems may proceed through several different avenues.

First a systematic study on the characteristics of developed materials as gel forming delivery systems with pH and temperature responsive properties in the delivery of large and small molecule drugs should be conducted. For instance, in chapter 5 we accessed the release of a hydrophobic molecule, i.e., CyA, from a 54% reduced-block copolymer gel. It will be useful to assess the incorporation, release and characteristics of produced gel for a formulation of CyA in 30 % reduced PCBCL-PEG-PCBCL gel. Such studies can assist in identifying the role of COOH group level and hydrogen bonding in drug loading, release and gelation behaviors of developed material. In addition, loading and release of other model drugs with various log P, molecular weights, charge and ionization capability in the gel may be pursued [10]. The effect of pH and electrolytes on the loading and release of such compounds from the hydrogel can also be investigated. In addition, the effect of pH on the mechanical strength of hydrogels would allow us to properly optimize the sol-gel behavior of hydrogels for different delivery applications.

We conducted an *in vitro* degradation study following incubation of the gel in water on the 54% reduced triblock copolymer in Chapter 5. However, degradation study in the presence of relevant enzymes, such as lipase, has to be done in order to predict the biodegradation kinetic of block copolymers under *in vivo* condition. Moreover, the

biodegradation study can be conducted on copolymers with different percentage of reduction, to determine how the polymer structure affects the kinetics of degradation. Finally, systematic studies on the biocompatibility and protein adsorption on the developed block copolymer gels and micelles having different levels of COOH substitution on the hydrophobic block, and their drug-loaded counterparts should be performed. Structure activity relationships should be developed with respect to properties described here and the level of COOH substitution on the block copolymer.

The effect of PEG and PCBCL backbone molecular weight on the thermo-responsive gelation and other characteristics of developed delivery system might be investigated.

Another future development could involve *in vivo* assessment of pharmacokinetics and pharmacodynamics of the hydrogel and micelle formulations of CyA and cisplatin, respectively [3,4]. For CyA, loaded hydrogel animal studies can be designed to investigate eye irritation, and distribution of CyA into the cornea, tear ducts, and conjunctiva (5). As for cisplatin, loaded micelles *in vivo* studies can be designed to investigate tissue distribution of cisplatin in order to access the accumulation of cisplatin in EGFR + versus EGFR - tumors. Moreover, *in vivo* antitumor activity in terms of tumor size in mice-bearing EGFR + versus EGFR - tumors should be conducted [6,7]. We showed in Chapter 3 that the tri block aqueous solutions have a viscoelastic nature; therefore they are able to hold cells while circulating nutrition and clearing by-products easily through hydrogel pores and water-filled regions. Therefore, another area for future development is studying the incorporation of biological cells into hydrogels for tissue engineering applications [5].

#### 4. Conclusions

In this thesis, we have developed novel stimulus responsive and biodegradable materials with great potential for application in drug and protein delivery. The developed materials were based on block copolymers of PEG and functionalized PCL bearing benzyl carboxylate and/or carboxyl groups on their structure. The introduction of free COOH pendant substituents on functionalized PCL introduced temperature- and pH- responsive properties to the developed block copolymers. The aqueous solutions of these block copolymers underwent sol-to-gel transition in the temperature range of 29-35 °C, which is an important physiological temperature range. Gel formation was perhaps triggered through conformational changes to the structure of prepared block copolymers leading to micellar aggregation through hydrophobic interaction at elevated temperatures. The transition temperature of the developed block copolymer was found to be dependent on the concentration of the polymer and the level of COOH substitution on the polymeric backbone. The visco-elastic properties of the gel were also affected by the concentration of the polymer and the level of COOH substitution on the polymeric backbone where mechanically more stable gels were formed from block copolymers with 50 % COOH substitution compared to those with 30 % COOH. The results of our studies also showed a pH dependent gelation for the developed polymers. At 37 °C, gel was only formed at pHs  $\geq 5.0$ . Although the sol-gel transition temperature of the polymer solution was independent of the pH of the media at pH  $\geq 5.0$ . Our results showed great potential of developed materials in formation of in situ hydrogels for use as injectable implants for the delivery of low and large molecular weight drugs. The temperature-responsive behavior of prepared tri block copolymers allowed design and development of delivery systems for depot delivery of large molecular weight water soluble model materials (i.e., TMR-D) and a poorly water soluble low molecular weight



peptide, i.e., CyA. Diblock copolymers developed based on PEG and functionalized PCL, on the other hand, were used to develop tumor-targeted delivery systems with acid-sensitive drug release properties for cisplatin. Both formulations are currently going through in vivo assessments in relevant animal models in our research group.

## Reference:

- (1) Moon HJ, Park MH, Joo MK, Jeong B. Temperature-responsive compounds as in situ gelling biomedical materials. *Chem Soc Rev* 2012;41(14):4860-4883.
- (2) Safaei Nikouei N, Lavasanifar A. Characterization of the thermo- and pH-responsive assembly of triblock copolymers based on poly(ethylene glycol) and functionalized poly(epsilon-caprolactone). *Acta Biomater* 2011 Oct;7(10):3708-3718.
- (3) Lin C, Metters AT. Hydrogels in controlled release formulations: network design and mathematical modeling. *Adv Drug Deliv Rev* 2006;58(12):1379-1408.
- (4) Bezemer J, Radersma R, Grijpma D, Dijkstra P, Feijen J, Van Blitterswijk C. Zero-order release of lysozyme from poly (ethylene glycol)/poly (butylene terephthalate) matrices. *J Controlled Release* 2000;64(1):179-192.
- (5) Wu Y, Yao J, Zhou J, Dahmani FZ. Enhanced and sustained topical ocular delivery of cyclosporine A in thermosensitive hyaluronic acid-based in situ forming microgels. *International journal of nanomedicine* 2013;8:3587.
- (6) Nishiyama N, Okazaki S, Cabral H, Miyamoto M, Kato Y, Sugiyama Y, et al. Novel cisplatin-incorporated polymeric micelles can eradicate solid tumors in mice. *Cancer Res* 2003;63(24):8977-8983.
- (7) Uchino H, Matsumura Y, Negishi T, Koizumi F, Hayashi T, Honda T, et al. Cisplatin-incorporating polymeric micelles (NC-6004) can reduce nephrotoxicity and neurotoxicity of cisplatin in rats. *Br J Cancer* 2005;93(6):678-687.
- (8) Tan H, Ramirez CM, Miljkovic N, Li H, Rubin JP, Marra KG. Thermosensitive injectable hyaluronic acid hydrogel for adipose tissue engineering. *Biomaterials* 2009;30(36):6844-6853.
- (9) Safaei Nikouei N, Vakili M, Akbari A, Wu J, Lavasanifar A. Biodegradable Thermo-reversible Hydrogels based on Triblock Copolymers of PEG and Functionalized Poly(epsilon-caprolactone). *Biomaterials*, submitted (2013)
- (10) Xiong X, Mahmud A, Uludağ H, Lavasanifar A. Multifunctional polymeric micelles for enhanced intracellular delivery of doxorubicin to metastatic cancer cells. *Pharm Res* 2008;25(11):2555-2566.
- (11) Ruel-Gariépy E, Leroux J. In situ-forming hydrogels — review of temperature-sensitive systems. *European Journal of Pharmaceutics and Biopharmaceutics* 2004;58(2):409-426.
- (12) Ross-Murphy SB. Rheology of biopolymer solutions and gels. *The Scientific World Journal* 2003;3:105-121.
- (13) Loh XJ, Li J. Biodegradable thermosensitive copolymer hydrogels for drug delivery. *Expert Opinion* 2007;17:3977-3989.
- (14) Loh XJ, Li J. Biodegradable thermosensitive copolymer hydrogels for drug delivery. 2007.
- (15) Uchino H, Matsumura Y, Negishi T, Koizumi F, Hayashi T, Honda T, et al. Cisplatin-incorporating polymeric micelles (NC-6004) can reduce nephrotoxicity and neurotoxicity of cisplatin in rats. *Br J Cancer* 2005;93(6):678-687.

